In vitro phospholipid biosynthesis for growing and dividing minimal cells

Scott, Andrew

DOI
10.4233/uuid:25cfdc64-409c-4a5f-a571-8c643d87820d

Publication date
2016

Document Version
Final published version

Citation (APA)
Scott, A. (2016). *In vitro phospholipid biosynthesis for growing and dividing minimal cells*. [Dissertation (TU Delft), Delft University of Technology]. https://doi.org/10.4233/uuid:25cfdc64-409c-4a5f-a571-8c643d87820d

IN VITRO PHOSPHOLIPID BIOSYNTHESIS FOR GROWING AND DIVIDING MINIMAL CELLS

IN VITRO PHOSPHOLIPID BIOSYNTHESIS FOR GROWING AND DIVIDING MINIMAL CELLS

Proefschrift

ter verkrijging van de graad van doctor
aan de Technische Universiteit Delft,
op gezag van de Rector Magnificus prof. ir. K.C.A.M. Luyben,
voorzitter van het College voor Promoties,
in het openbaar te verdedigen op maandag 4 April 2016 om 10:00 uur

door

Andrew SCOTT

s geboren te Saint John, Canada.

Dit proefschrift is goedgekeurd door de

promotor: prof. dr. M. Dogterom
copromotor: dr. C.J.A. Danelon

Samenstelling promotiecommissie:

Rector Magnificus,	voorzitter
Prof. dr. M. Dogterom,	Technische Universiteit Delft
Dr. C.J.A Danelon,	Technische Universiteit Delft

Onafhankelijke leden:

Prof. dr. J. H. van Esch	Technische Universiteit Delft
Prof. dr. B. Poolman	Universiteit Groningen
Prof. dr. D. Baigl	University Pierre and Marie Curie
Dr. G. Bokinsky	Technische Universiteit Delft
Prof. dr. A. Engel	Technische Universiteit Delft

Keywords: minimal cell, liposome growth, liposome division, in vitro, lipid synthesis

Printed by: Gildeprint

Front & Back: Cover art by Christine Scott

ISBN 978-90-8593-251-2

An electronic version of this dissertation is available at
http://repository.tudelft.nl/.

To my nieces and nephew,
may this work someday benefit you.

April 2016

CONTENTS

1

INTRODUCTION

1.1. CONCEIVING OF THE MINIMAL CELL

Natural life is extraordinarily complex, which by definition means that it has many interconnected and functioning parts. The goal of synthetic biology is to engineer living systems, though due to their very complexity they remain recalcitrant to engineering [1]. What if it were possible to reduce the complexity to a finite amount of parts that are well understood and therefore possible to manipulate. That is the motivation for constructing a so called minimal cell.

How complex, and what functions should something have to be considered alive? A definition that we find fundamental is an entity, that can take chemicals from its environment and be able to maintain itself, in spite of the fact that globally entropy is increasing. The key process required is self reproduction, i.e. the manufacture of the components comprising the system [2]. That central process is accompanied by degradation, recycling and repair of decaying components, where feasible. Together the living system thus maintains itself in a process called homeostasis. However, those processes cannot happen indefinitely due to the increase of energetic costs of replacing, recycling and repairing components as the age of the system increases and more components decay. It is therefore natural to start over by replicating the entire entity. To produce its parts, a living system needs a program that encodes the parts and that itself must be replicated. The above extends the necessary requirements of life to self maintenance and self replication. If in replicating itself, the living thing can alter the copy to give it an advantage in performing the first two tasks, it is more likely to continue to exist. That is to say it will evolve and the ability to do so can be considered a third requirement for life. Another way of stating all of the above is that a living entity must be able to metabolize, have a container which specifies a boundary that can grow and be replicated, have genes which encode the above functions, and the genes themselves should be able to be replicated with the possibility for mutation, which is necessary for evolution.

What is meant by minimal? A simple way of quantifying the complexity of an organ-

1

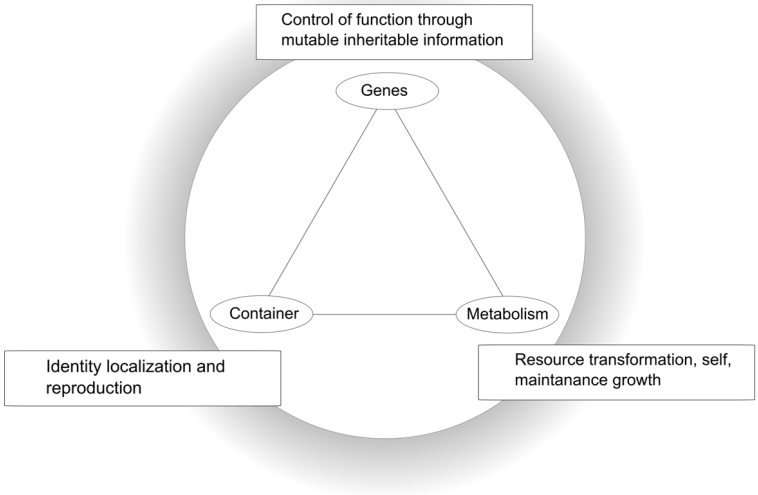

Figure 1.1: The requirements for a molecular assembly to be considered living can be summarized as having a metabolism, for resource transformation, self maintenance and growth, a container for identity localization and reproduction, and genes for controlling those functions through mutable inheritable information.

ism is by simply counting the number of genes it has [1], this implies that the organism is based on DNA, which is read by an RNA polymerase. It also implies that at least some of the RNA is translated into protein. Note however that some origins of life researchers envision an early version of life without proteins, called the RNA world, [3]. If we accept the number of genes as a metric of complexity for an organism, then we can approach finding the minimal genome in two ways: the top down and bottom up approaches.

In the top-down approach, as many genes as possible are deleted from existing organisms while they still maintain their functions [4]. An example of this approach involved the bacteria *Mycoplasma genitalium*, which is the organism with the smallest known genome that can survive in pure culture. Its genome was reduced from the original 482 genes to only 385 genes [5]. On the other hand, in the bottom-up approach, cellular functions are reconstituted from purified components with an emphasis on the process being under controlled conditions [6], [7] [8]. In this approach the predicted number of genes from biochemical considerations is approximately 150 [9]. In both these instances it should be noted that the reduced complexity of the organism requires a corresponding increased complexity of the environment. Some bacterial symbionts survive inside other organisms such as *Candidatus Tremblaya Princeps* which survives only inside of *Moranella Endobia* [10] and has a genome of only 121 genes. Likewise it is clear that a bottom up minimal cell that has the ability to synthesize amino acids must be more complex than a minimal cell which has amino acids in its culture medium. As such their can be a continuum of minimal cells with varying degrees of complexity.

[1] this is not necessarily a good measure of biological complexity, because the expression level of the genes as well as modifications of RNA and proteins after transcription and translation can alter the number of interacting elements in the cell and therefore the complexity of the organism.

The approach that we have been describing of creating a minimal cell based on DNA, RNA and protein is the so called semi-synthetic cell. There are also researchers attempting to make truly synthetic protocells, [11], [12], [13] though we will not touch upon them here.

What do we hope to learn and gain by building a minimal cell? Firstly a goal is to identify the design principles of life, i.e. what chemical and biophysical processes are necessary for life to sustain itself. We also stand to learn a great deal about the individual components which may provide opportunities for the development of new biotechnologies. It will also be possible to design and develop new kinds of sensing technologies, smart medicine, and eventually allow the production of chemicals with a specialized and therefore efficient artificial cell.

1.2. IMPLEMENTING THE MINIMAL CELL

We have highlighted the functions of a minimal cell as self maintenance, self reproduction and the encoding of these functions through mutable inheritable information. Those functions must be implemented in an entity able to metabolize, have a container which specifies a boundary that can grow and be replicated, and have genes which encode those processes and which themselves can be replicated with the possibility for mutation so that evolution may occur. In our lab we aim to achieve these functions in our own minimal cell project. As we are implementing these functions in a semi-synthetic manner, it means that DNA, RNA and protein are the core functioning elements. To get from DNA to RNA, a process known as transcription is necessary and from RNA to protein, a process known as translation must take place. As discussed below, to perform these core functions we make use of the PURE system [14]. The PURE system's main function is to metabolize RNA and proteins from small molecules, though it also has the ability to regenerate some of its chemical components and degrade others. Encapsulation of purified proteins into cellular units is also necessary for making a minimal cell and for reasons discussed below this is done with glycerophospholipids [15] [16] [17]. *Furthermore we aim to grow and divide those compartments, which is the main focus of this thesis.* Other projects in our lab aim to replicate the contents of the compartments, to date this involves DNA replication but in the future will include the contents of the PURE system itself including the ribosomes. And finally the lab investigates genetic circuits to control and time the functions of the minimal cell.

Transcription and translation can be implemented outside of cells, in so called cell extracts. In these systems cellular extracts derived from cytoplasmic parts of *E. coli* are able to transcribe and translate DNA constructs [18]. There are advantages to this approach including high yield of protein expression [19], reduced cost [8] and the possibility to use the diverse σ factors of *E. coli* bacterial RNA polymerases which impart transcriptional specificity [20]. However, these systems are poorly defined, containing many components whose precise activity is unknown. In contrast, the PURE (Protein synthesis Using Recombinant Elements) system developed by Takuya Ueda (Tokyo University) [21] [14] is a minimal set of purified enzymes and co-factors (36 proteins), which reconstitute the functions of transcription, translation, amino-acylation, energy regeneration and pyrophosphate hydrolysis. The main advantage of this system is that because the enzymes are individually purified its total contents are known and thus modules im-

plemented within it will not have interference from other unknown processes. In this thesis we use mainly the PURE*frex* (GeneFrontier), and in a few experiments we use the PURExpress® (New England Biolabs), whose composition has been modified from the original PURE system [21]. By including various DNA templates in the PURE system, which encode for proteins performing cellular functions, we expand the functionality of our minimal cell.

The second important aspect of the minimal cell is the boundary. The first reason for that is fairly intuitive, to be an individual, and to be able to replicate and therefore evolve, a entity must have a boundary which defines it as separate from the rest of existence. The more subtle reasoning for needing a boundary and individuality has to do with the so-called error catastrophe. That is to say, during the process of evolution errors in the replication will be made which without compartmentalization and selection will overrun the system. In an experiment, genes encoding a polymerase underwent cycles of self replication. In a series of parallel reactions, when PCR amplified polymerase genes of initially one genotype per reaction were expressed *in vitro*, allowed to replicate their own template, then diluted so that only a single copy per reaction was passed to a next generation for PCR amplification and finally the cycle repeated, the process lasted many (10) generations [22]. In another series of parallel experiments, where, after the initial PCR amplification, *in vitro* expression and self replication steps, a pool of 100 molecules from each reaction were passed to the next generation (starting with the new PCR amplification step) and the ability of the polymerases to self replicate was lost after three generations. That is due to the fact that templates that erroneously replicated during the self replication step pollute the population of good replicators, and cause non functional enzymes to be expressed, eventually taking over the population due to the greater number of possible non functional enzymes as functional ones [22]. The contrasting of the two ways of passing genes to the next generation shows that strict compartmentalization (passing one gene to the PCR amplification step), prevents the erroneous sequences from taking over a population and preventing replication, which does occur when loose compartmentalization (passing pools of sequences to the PCR amplification step) is used. For the survival of the minimal cell over many generations it is therefore important that it be compartmentalized, ideally passing only a few copies of its genome to future generations. To encapsulate the PURE system, we and others make use of glycerophospholipids [17] [23] that form so called lipid vesicles. Glycerophospholipids form stable bilayers, are the main component of natural cell boundaries and are not precipitated by the magnesium present as cofactor in the PURE system, as are, for instance, fatty acids [24]. In this thesis we will focus on the growth of these lipid compartments in chapters 2-5 with a preview into methods of division in chapters 6.

The other functions of replication of DNA and of the PURE system itself as well as division of the compartment are also to be performed with proteins and mRNA expressed in the PURE system, and we speculate on tools for doing so in chapter 6.

1.3. THESIS OUTLINE

In chapter 2, we implemented lipid biosynthesis by PURE system synthesized proteins. Using glycerophospholipid liposomes as scaffolds, we synthesized the *E. coli* proteins GPAT and LPAAT, responsible for the synthesis of lysophosphatidic acid and phospha-

tidic acid, respectively. First, by synthesizing the proteins from outside of liposomes and then purifying the liposomes we showed that the proteins are associated with liposomal membranes. Second, we developed a liquid chromatography mass spectrometry (LC-MS) method for the detection of enzyme products. We then used the LC-MS method to study the activity of GPAT (*plsB* gene) and LPAAT (*plsC* gene) from proteins expressed outside of liposomes. Our findings include that proteins are active in various buffers, even when the proteins were co-expressed with the activity step. Next we found that it was crucial to have liposome supports to have efficient protein activity. We further observed that it was possible to use at least two types of fatty acyl CoA substrates and that the composition of the liposomal supports can be at least slightly varied. We also showed that at least some of the synthesized lipids are incorporated into liposomal membranes, i.e the liposomes are growing. Finally we found that it was possible to express the proteins and perform lipid synthesis from inside liposomes, which is an important step in making a minimal cell.

In chapter 3 we present findings supporting those of chapter 2, as well as general laboratory techniques. In particular we show experimental details of how the gene constructs for *plsB* (GPAT protein) and *plsC* (LPAAT protein) were obtained and a brief study of the optimal type of template to use in the PURE system. We provide details of the liquid chromatography and mass spectrometry principles and methods employed in this thesis. We also present information obtained regarding improvement of LC-MS sensitivity by including EDTA in the sample. Furthermore we present data suggesting that glycerol-3-phosphate (G3P) contamination existed either in the lipids used, or in the PURE system. We also present data on the effect of preparing PURE system additives G3P and β-mercaptoethanol freshly, or from stored stock solutions. In addition we study the effect of the concentration of palmitoyl CoA in synthesis reactions. Finally, for future experimenters in our lab, we provide a simple guide to the handling of the lipids used.

In chapter 4 we continued the study of lipid biosynthesis in the PURE system by expressing six phospholipid headgroup-modifying enzymes. We expressed the *E. coli* proteins phosphatidate cytidylyltransferase (cdsA gene), phosphatidylserine synthase (pssA gene), phosphatidylserine decarboxylase (psd gene), which are responsible for converting phosphatidic acid to diacyl-phosphatidylethanolamine. We also expressed phosphatidylglycerophosphate synthase (pgsA gene), and 2 phosphatidylglycerolphosphatases (pgpA gene, and pgpC gene) which along with phosphatidate cytidylyltransferase (cdsA gene) are responsible for converting phosphatidic acid to diacylphosphatidylglycerol. By adapting the LC-MS method of chapters 2 and 3, we were able to detect the end products of the two enzymatic pathways indicating that all enzymes were active. We also report on how we formed the DNA constructs for the proteins studied.

In chapter 5 we further studied the activity of the GPAT and LPAAT enzymes using light. We found that it was possible to detect the by-product of the GPAT and LPAAT reactions, co-enzyme A, with a proprietary fluorogenic assay from Enzo Life Sciences. To use the assay we developed multiple methods for removing DTT from the samples, which would otherwise interfere with the fluorescence signal. We studied the enzymes under various conditions using the CoA assay and found that it is, in particular, useful for studying LPAAT, which appeared to be active in the non-reducing conditions required for the assay. We also developed methods to study GPAT and LPAAT based upon

an NBD (nitrobenzoxadiazole)-labeled fatty acyl CoA, which increases its fluorescence when moved from a polar to a non polar environment. We studied this molecule with and without the presence of enzymes, by spectrofluorometry, mass spectrometry and microscopy. We found that it was particularly useful for studying LPAAT, and the combination of GPAT and LPAAT, which gave a signal in the NBD assays over their respective controls.

In chapter 6 we examine areas of research that we initiated but did not yet bring to full fruition. We begin by delving into the meaning of evolution. We then focus on *in vitro* implementations of evolution as a bridge to a minimal cell, examining ways that genome replication and screening of large numbers of genes can be applied to the minimal cell project. We then discuss division, in particular how lipid biosynthesis and the biophysical properties of membranes may provide a route to division of liposomes. Finally we present a few results from a project to build chambers and microchambers to compartmentalize reactions.

REFERENCES

[1] R. Kwok, "Five hard truths for synthetic biology." *Nature*, vol. 463, no. 7279, p. 288, 2010.

[2] A. Pross, *What is Life?: How chemistry becomes biology*. Oxford University Press, 2012.

[3] P. G. Higgs and N. Lehman, "The rna world: molecular cooperation at the origins of life," *Nature Reviews Genetics*, 2014.

[4] A. Moya, R. Gil, A. Latorre, J. Peretó, M. P. Garcillán-Barcia, and F. De La Cruz, "Toward minimal bacterial cells: evolution vs. design," *FEMS microbiology reviews*, vol. 33, no. 1, pp. 225–235, 2009.

[5] J. I. Glass, N. Assad-Garcia, N. Alperovich, S. Yooseph, M. R. Lewis, M. Maruf, C. A. Hutchison, H. O. Smith, and J. C. Venter, "Essential genes of a minimal bacterium," *Proceedings of the National Academy of Sciences of the United States of America*, vol. 103, no. 2, pp. 425–430, 2006.

[6] P. L. Luisi, F. Ferri, and P. Stano, "Approaches to semi-synthetic minimal cells: a review," *Naturwissenschaften*, vol. 93, no. 1, pp. 1–13, 2006.

[7] P. Schwille, "Bottom-up synthetic biology: engineering in a tinkerer's world," *Science*, vol. 333, no. 6047, pp. 1252–1254, 2011.

[8] M. C. Jewett and A. C. Forster, "Update on designing and building minimal cells," *Current opinion in biotechnology*, vol. 21, no. 5, pp. 697–703, 2010.

[9] A. C. Forster and G. M. Church, "Towards synthesis of a minimal cell," *Molecular systems biology*, vol. 2, no. 1, p. 45, 2006.

[10] J. P. McCutcheon and N. A. Moran, "Extreme genome reduction in symbiotic bacteria," *Nature Reviews Microbiology*, vol. 10, no. 1, pp. 13–26, 2012.

[11] H. J. Morowitz, B. Heinz, and D. W. Deamer, "The chemical logic of a minimum protocell," *Origins of Life and Evolution of the Biosphere*, vol. 18, no. 3, pp. 281–287, 1988.

[12] J. W. Szostak, D. P. Bartel, and P. L. Luisi, "Synthesizing life," *Nature*, vol. 409, no. 6818, pp. 387–390, 2001.

[13] D. Loakes and P. Holliger, "Darwinian chemistry: towards the synthesis of a simple cell," *Molecular BioSystems*, vol. 5, no. 7, pp. 686–694, 2009.

[14] Y. Shimizu, T. Kanamori, and T. Ueda, "Protein synthesis by pure translation systems," *Methods*, vol. 36, no. 3, pp. 299–304, 2005.

[15] S.-i. M. Nomura, K. Tsumoto, T. Hamada, K. Akiyoshi, Y. Nakatani, and K. Yoshikawa, "Gene expression within cell-sized lipid vesicles," *ChemBioChem*, vol. 4, no. 11, pp. 1172–1175, 2003.

[16] V. Noireaux and A. Libchaber, "A vesicle bioreactor as a step toward an artificial cell assembly," *Proceedings of the national academy of sciences of the United States of America*, vol. 101, no. 51, pp. 17 669–17 674, 2004.

[17] Z. Nourian, W. Roelofsen, and C. Danelon, "Triggered gene expression in fed-vesicle microreactors with a multifunctional membrane," *Angewandte Chemie*, vol. 124, no. 13, pp. 3168–3172, 2012.

[18] E. D. Carlson, R. Gan, C. E. Hodgman, and M. C. Jewett, "Cell-free protein synthesis: applications come of age," *Biotechnology advances*, vol. 30, no. 5, pp. 1185–1194, 2012.

[19] F. Caschera and V. Noireaux, "Synthesis of 2.3 mg/ml of protein with an all escherichia coli cell-free transcription–translation system," *Biochimie*, vol. 99, pp. 162–168, 2014.

[20] J. Shin and V. Noireaux, "Research study of messenger rna inactivation and protein degradation in an escherichia coli cell-free expression system," *J Biol Eng*, vol. 4, pp. 1–9, 2010.

[21] Y. Shimizu, A. Inoue, Y. Tomari, T. Suzuki, T. Yokogawa, K. Nishikawa, and T. Ueda, "Cell-free translation reconstituted with purified components," *Nature biotechnology*, vol. 19, no. 8, pp. 751–755, 2001.

[22] T. Matsuura, M. Yamaguchi, E. P. Ko-Mitamura, Y. Shima, I. Urabe, and T. Yomo, "Importance of compartment formation for a self-encoding system," *Proceedings of the National Academy of Sciences*, vol. 99, no. 11, pp. 7514–7517, 2002.

[23] T. Sunami, K. Sato, T. Matsuura, K. Tsukada, I. Urabe, and T. Yomo, "Femtoliter compartment in liposomes for in vitro selection of proteins," *Analytical Biochemistry*, vol. 357, pp. 128–136, 2006.

[24] F. Anella and C. Danelon, "Reconciling ligase ribozyme activity with fatty acid vesicle stability," *Life*, vol. 4, no. 4, pp. 929–943, 2014.

2

LIPID SYNTHESIS WITH *in vitro* SYNTHESIZED GPAT AND LPAAT

The goal of bottom-up synthetic biology culminates to the assembly of an entire cell from separate biological building blocks. One major challenge resides in the in vitro production and implementation of genetic and metabolic pathways that can support essential cellular functions. Here, we show that phosphatidic acid synthesis, a two step process involved in cell membrane homeostasis, can be reconstituted starting from the genes encoding for necessary proteins. Two E. coli enzymes for acyl transfer reactions were produced in a cell-free gene expression system and were co-translationally reconstituted in liposomes. Acyl-coenzyme A and glycerol-3-phosphate were used as precursors to generate lysophosphatidic acid and phosphatidic acid. Moreover, this study demonstrates that two-step acyl transfer can occur from enzymes synthesized inside vesicles. Besides clear implications for growth and potentially division of a synthetic cell, we postulate that gene-based lipid biosynthesis can become instrumental for ex vivo and protein purification-free production of natural and non-natural lipids.

2.1. INTRODUCTION

Life as we know it is compartmentalized: a continuous membrane encloses the cytoplasm protecting it from the environment and specifying a unit of evolutionary selection. This cellular envelop is primarily made of phospholipids that, together with specific proteins, control shape transformation and regulate the ionic and molecular exchanges with the external medium. Several laboratories are now attempting to construct a minimal, albeit sufficient, cell starting from purified components derived from existing organisms [1] [2] [3] [4] [5] [6]. Given the central roles played by the cellular membrane, an important milestone in the road map for creating an elementary cell that can grow and divide is the *de novo* synthesis of membrane constituents from internally produced enzymes.

An attractive metabolic pathway for lipid biosynthesis is through diacyl-phosphatidic acid (PA), the universal precursor of glycerophospholipids in bacteria [7]. The pathway for PA synthesis in *E. coli* entails two acyltransferase enzymes: the glycerol-3-phosphate (G3P) acyltransferase (GPAT) and the lysophosphatidic acid (LPA) acyltransferase (LPAAT) [8] [9]. The enzyme GPAT is an integral membrane protein that uses G3P and either acyl-CoA (CoA, coenzyme A) or acyl-ACP (ACP, acyl carrier protein) substrates to generate 1-acyl-sn-glycerol 3-phosphate (LPA) products. In a subsequent enzymatic reaction the LPA and another acyl-CoA/acyl-ACP are converted into 1,2-diacyl-sn-glycerol 3-phosphate (PA) by the membrane-bound enzyme LPAAT. In the cellular context of *E. coli*, the GPAT and LPAAT enzymes are then complemented by a few others to modify the lipid headgroup and produce (PG) phosphatidylglycerol, a bilayer-forming anionic lipid, and (PE) phosphatidylethanolamine, a zwitterionic lipid, together representing the largest fraction of the *E. coli* inner membrane lipidome [10].

To date several attempts have been made to stimulate compartment growth in phospholipid vesicles by using purified acyltransferase enzymes [11] [12] [13]. More recently, the activity of the GPAT and LPAAT enzymes synthesized from a reconstituted *in vitro* transcription-translation (IVTT) system has been demonstrated in separate reactions [14]. However, these two enzymes failed to work in the same environment and conflicting oxidative-reductive conditions for proper enzymatic activities were invoked [14]. Moreover, gene expression was not integrated with lipid synthesis and no kinetics data were available.

Hereby, we report on the cell-free production and functional liposome reconstitution of multiple lipid-synthesizing enzymes in the PURE system, a well-defined IVTT system, starting from acyltransferase genes and the phospholipid precursors G3P and acyl-CoA. We validated the use of liquid chromatography mass spectrometry (LC-MS) as a powerful analytical technique to quantify the amount of synthesized lipids. Focusing on the two-step acyl transfer reaction, we first demonstrated that the co-expressed GPAT and LPAAT enzymes enabled the synthesis of the membrane constituent 1,2-diacyl-sn-glycerol 3-phosphate in a single-pot reaction, including when compartmentalized inside liposomes. Capitalizing on the *de novo* synthesis of PA, in chapter 4 we then reconstituted the entire *E. coli* metabolic pathways to convert PA into PE and PG lipids. Our work provides a new experimental framework to build up a genetically controlled synthetic cell where the compartment is produced *in situ* from simple biochemical precursors.

2.2. RESULTS

2.2.1. *In vitro* SYNTHESIS AND LIPOSOME RECONSTITUTION OF THE GPAT AND LPAAT ENZYMES

We first verified that cell-free expression of the *plsB* and *plsC* genes, respectively encoding for the GPAT and LPAAT proteins, in the PURE system led to full-length proteins. The *E. coli* GPAT and LPAAT enzymes were separately synthesized from their respective DNA templates and the translation products were analyzed by SDS-PAGE and fluorescence gel imaging. A fraction of tRNA pre-loaded with a fluorescently labeled lysine was supplemented in the IVTT reaction to facilitate detection of the synthesized protein over the PURE system background. The *in vitro* produced GPAT and LPAAT proteins were visualized as distinct bands at around 83 kDa [15] and 27 kDa [16], as previously reported.

It is known that GPAT is an integral membrane protein [17] and LPAAT is thought to be a membrane-anchored protein [16]. We thus examined the ability of the synthesized enzymes to associate to the liposome membrane. Preformed small unilamellar vesicles (SUVs) composed of DOPC/DOPE/DOPG/cardiolipin were supplemented in the IVTT reaction carrying out the expression of the *plsB* and/or *plsC* genes, whose encoded proteins inserted into the SUV membranes in an inside-out configuration. The proteoliposomes were purified from the bulk fraction by ultracentrifugation and the protein content associated to the liposome membrane was analyzed by SDS-PAGE (figure 2.1 b). The PURE system proteins could efficiently be eliminated, whereas both GPAT and LPAAT enzymes co-purified with the liposomes, suggesting that these two *in vitro* synthesized proteins have the correct properties for stable co-translational insertion or anchoring to the membrane. The process of membrane incorporation is passive, in that it does not require a translocation machinery.

2.2.2. BOTH SYNTHESIZED GPAT AND LPAAT ENZYMES ARE ACTIVE WHEN CO-INSERTED IN LIPOSOMES

Having established that the full-length GPAT and LPAAT proteins can be synthesized in the PURE system and incorporated in the membrane of liposomes we then explored the potential of mass spectrometry (MS) combined with liquid chromatography (LC) to detect the products of the GPAT and LPAAT enzymatic reactions in a background of liposomes also composed of lipids and to quantify the amounts of all of the above. Initially the method was developed for 16:0 LPA and 16:0/16:0 phosphatidic acid (DPPA) in a cardiolipin/DOPX (where PX = PC, PE, PG headgroups) lipid matrix and it was later expanded to include 18:1 LPA and 18:1/18:1 phosphatidic acid (DOPA), as well as 16:0/16:0 phosphatidylethanolamine (DPPE) and 16:0/16:0 phosphatidylglycerol (DPPG) (chapter 4). A typical chromatogram, where one can clearly distinguish the enzymatic products LPA and DPPA from the matrix lipids, is shown in figure 2.1 c. The detection sensitivity of the combined LC-MS was estimated to 0.25 pmol for 16:0 LPA and DPPA (figure 2.8), which is better than usually reported via radioactive elements separated by thin layer chromatography.

Next, we sought to assay the activity of the two enzymes. Gene expression and lipid synthesis were first examined sequentially. The enzymes GPAT and LPAAT were individually assayed in specific buffer conditions known to support their activity [14]. GPAT cat-

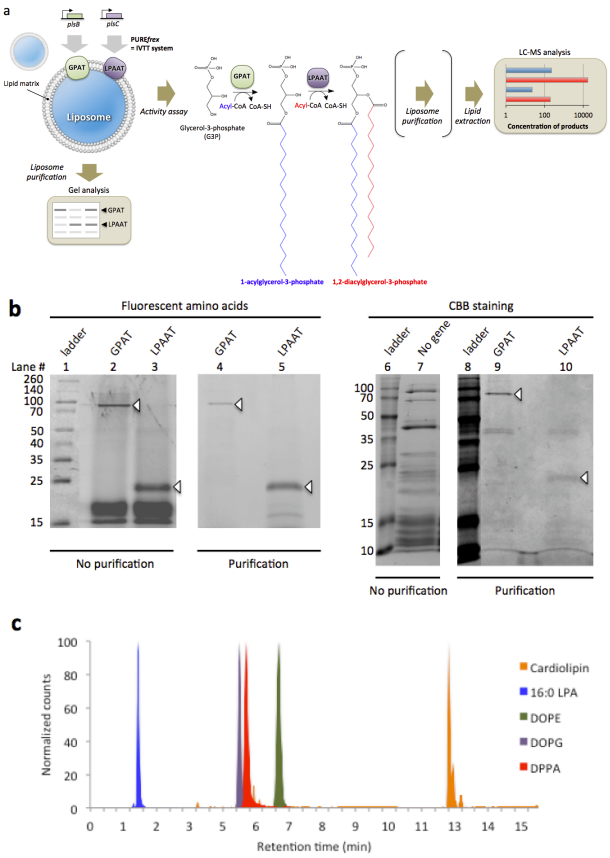

Figure 2.1: | Overview of methods for cell-free transcription-translation of acyltransferase enzymes. (a) The genes *plsB* and *plsC* coding for the GPAT and LPAAT enzymes, respectively, were expressed by *in vitro* transcription translation (IVTT) in the presence of SUVs. Spontaneously assembled proteoliposomes containing synthesized GPAT and LPAAT proteins were isolated by ultracentrifugation (flotation method) and the protein content was analyzed by SDS-PAGE. Activity assays were performed by adding the phospholipid precursors G3P and acyl-CoA (shown in the reaction scheme is palmitoyl-CoA, p-CoA) either before or subsequent to IVTT reaction. Biosynthesis of 1,2-diacylglycerol-3-phosphate (here DPPA) occurs in a two-step acyl transfer reaction catalyzed by the GPAT and LPAAT enzymes. The intermediate product 1-acylglycerol-3-phosphate (here 16:0 LPA) and two free CoA molecules are also formed. After reaction the lipid fraction was extracted and assayed by LC-MS. To quantify the enrichment of vesicles with synthesized lipids, liposomes were purified by immobilization on beads before the lipid extraction step. (b) Cell-free expression of either the *plsB* or *plsC* gene (no gene as negative control) occurred for 3 h at 37 °C in the presence of 100-nm SUVs and of Green$_{Lys}$ reagent (tRNA-loaded fluorescent amino acid) for fluorescence labeling of translation products. Reconstituted proteoliposomes were purified and membrane-integrated proteins separated by SDS-PAGE were visualized with coomassie brilliant blue (CBB) staining and fluorescence scanning. As shown with CBB staining the PURE system background proteins (lane 7) can efficiently be eliminated by purification, while the GPAT and LPAAT protein bands were co-purified with the SUVs (lanes 9,10). Isolation of acyltransferase enzymes is also visible on the fluorescence scan (lanes 4,5). The lower bands on lanes 2,3 correspond to background signal from the GreenLys reagent. (c) Normalized chromatogram of lipids as measured by LC-MS operating in multiple reaction monitoring (MRM) mode with negative polarity. In this example, 16:0 LPA, DOPG, DPPA, DOPE and cardiolipin were clearly resolved. DOPC is not well detected in the negative mode. It was also possible to detect 18:1 LPA, DOPA.

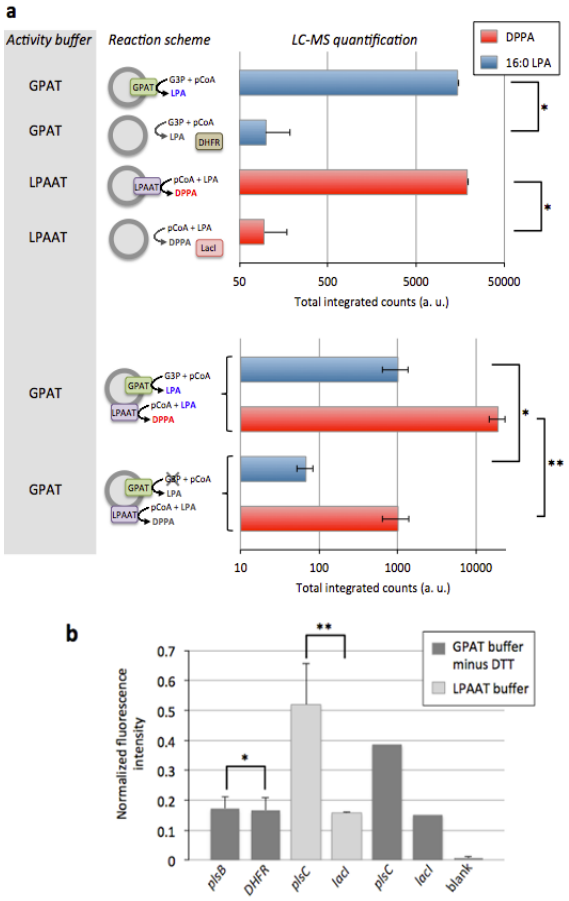

Figure 2.2: | Two-step acyl transfer reaction mediated by cell-free synthesized GPAT and LPAAT enzymes. (a) LC-MS analysis of the GPAT and LPAAT reaction products. The lipid precursors G3P and palmitoyl-CoA (p-CoA), or p-CoA and 16:0 LPA (66.6 μM each, except in two-enzyme cascade experiments, where p-CoA concentration was 133.3 μM) were added after the IVTT reactions performed in the presence of SUVs. The two enzymes were assayed separately in their respective activity buffer or together in the reducing buffer known to support GPAT activity. Negative controls in GPAT and LPAAT activity buffers were performed using the DHFR and LacI genes respectively. For combined GPAT and LPAAT reactions, controls were conducted without G3P. Error bars in single-enzyme experiments are s.e.m. from multiple measurements of one sample. In the GPAT and LPAAT co-expression experiments data are mean and s.e.m. across four independent samples; for each repeat the sample was injected multiple times, the average value of the different injections was calculated and data are reported as the mean and standard error of independent trials. Student t-test analysis: * GPAT vs DHFR, LPA $P < 0.0128$, * LPAAT vs LacI, DPPA $P < 0.0146$, * GPAT/LPAAT LPA $P < 0.0797$, ** GPAT/LPAAT, DPPA $P < 0.0245$. (b) Acyltransferase activity as measured using a fluorescence - based assay in which released CoA reacts with a fluorogenic substrate. Negative controls for GPAT and LPAAT activity were performed using the DHFR and LacI genes, respectively. DTT was dialyzed out after the IVTT reaction to create the non reducing conditions compatible with the assay. Blank was measured from the buffer included in the fluorescence-based CoA assay kit. Data are mean values and s.e.m. of two independent experiments. Student t-test analysis: * Difference statistically not significant, **$P < 0.23$.

alyzed the formation of 16:0 LPA starting from G3P and palmitoyl-CoA substrates, while LPAAT converted palmitoyl-CoA and LPA into DPPA. The formation of enzymatic products and precursor consumption were quantitatively detected by LC-MS (figure 2.2 a). In addition, we used a fluorescence-based acyltransferase activity assay to monitor the accumulation of released CoA molecules through enzymatic reaction of the GPAT and LPAAT proteins. As anticipated GPAT activity could not be observed since the reducing agent DTT had to be removed before triggering the reactions (Methods). However, a clear increase of fluorescence signal was detected when LPAAT proteoliposomes were incubated with p-CoA and LPA substrates in LPAAT-specific buffer and, interestingly, in the GPAT-specific buffer too (figure 2.2 b).

The two-enzyme cascade reaction was analyzed using inside-out proteoliposomes containing both synthesized GPAT and LPAAT proteins. The proteoliposomes were supplied with G3P and palmitoyl-CoA and incubated in the GPAT activity buffer. In contrast to what has previously been reported [14], we found that the output lipid, DPPA, was successfully produced, demonstrating that LPAAT can also be active in a reducing environment (figure 2.2 a). Because the LPA produced by the GPAT enzyme is subsequently used as a substrate by LPAAT in the cascade reaction, it does not accumulate and its end-point concentration is less than that in a GPAT-only reaction (figure 2.2 a).

2.2.3. COMBINED GENE EXPRESSION AND ENZYME-CATALYZED LIPID BIOSYNTHESIS IN A ONE-POT REACTION

In light of this new result, we tested whether the GPAT and LPAAT enzymes could be synthesized from their DNA, insert into the membrane of preformed vesicles and generate lipid products, all in a single-pot reaction. Both 16:0 LPA and DPPA products were measured, showing that gene expression and lipid biosynthesis can successfully be integrated in the PURE system. In a cascade reaction with both GPAT and LPAAT in the same reaction, about 10% of LPA was measured relative to the amount detected with GPAT-only proteoliposomes. This can be explained by the rapid conversion of LPA into DPPA by the LPAAT enzyme when both proteins are present. To determine if the lipid products were generated from enzymes co-localizing in the vesicle membrane after co-translational incorporation, or instead, from synthesized enzymes that fail to insert into the lipid bilayer, we carried out experiments where liposomes were omitted during gene expression. When GPAT and LPAAT enzymes were separately assayed in the absence of liposomes, measurable amounts of LPA and DPPA were observed respectively. However, the amounts of 16:0 LPA and DPPA formed in one- or two-enzyme reactions were consistently higher in the presence of vesicles (figure 2.3), indicating that co-translational incorporation of the proteins into a lipid matrix greatly enhances enzymatic activity.

We next investigated the kinetics of 16:0 LPA and DPPA formation in combined gene expression and lipid biosynthesis experiments. To the best of our knowledge only the kinetics of *E. coli* GPAT has been studied to date[18]. Inside-out proteoliposomes containing either the GPAT or LPAAT protein were produced in the presence of their respective substrates and the enzyme kinetics were monitored (figure 2.4 a,c). The amount of detected 16:0 LPA gradually increased for 4 h at a rate of 2.5 μM/h and subsequently rose abruptly to plateau after about 6 h (figure 2.4 a). This result suggests that GPAT protein folding and membrane insertion could be rate-limiting steps for product formation in

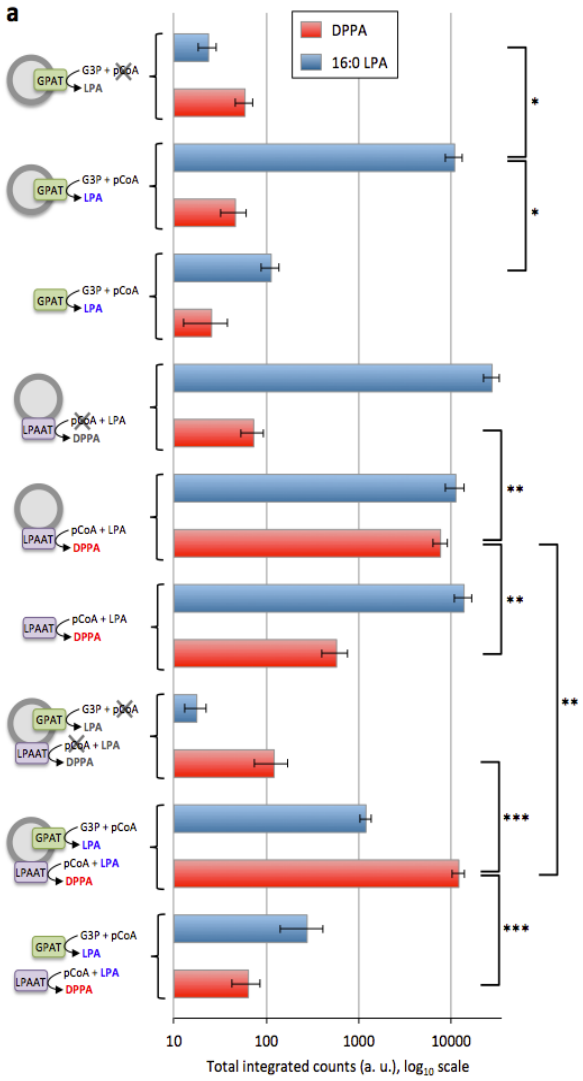

Figure 2.3: | Co-expression of enzymes and activity and the requirement of liposomes for full enzyme activity. The GPAT and LPAAT enzymes were either produced separately or concurrently in the presence of G3P and p-CoA substrates. The generated lipid products 16:0 LPA and DPPA were detected by LC-MS. (a) End-point measurements of 16:0 LPA and DPPA synthesized under various experimental conditions. Substrate concentrations were 500 μM G3P, 100 μM p-CoA and 100 μM 16:0 LPA. Individual and combined enzymatic reactions were carried out with (inside-out configuration) or without 400-nm liposomes during overnight incubation at 37 °C. Samples with liposomes and without p-CoA served as a negative control. Both acyltransferase enzymes showed reduced activity in the absence of SUVs. Higher yield of DPPA is obtained by two-step acyl transfer catalyzed by GPAT and LPAAT enzymes co-reconstituted in proteoliposomes. Data represent mean and s.e.m. of three independent experiments. For each repeat the mean of multiple sample injections was calculated and data are reported as the mean and standard error of three independent trials. Student t-test analysis: *P<0.1, **P<0.12, ***P<0.012.

the initial phase of the reaction. The final 42-μM concentration of synthesized LPA corresponds to a consumption of 45 % of palmitoyl-CoA substrate (G3P being present in excess), which we suspect is due to enzyme inhibition by free CoA product [18], protein inactivation or spontaneous cleavage of the p-CoA thioesther bond. Moreover, the final amount of 16:0 LPA produced represents around 8% of total lipids forming the vesicles. The LPAAT enzyme converted 16:0 LPA and palmitoyl-CoA into DPPA at an initial rate of 5 μM/h and a maximum concentration of ~21 μM was reached after 15 h (figure 2.4 c). This final concentration corresponds to ~4% increase in the total amount of phospholipids. The reaction consumed ~42% of the 50 μM of substrates, again suggesting possible reaction inhibition, enzyme inactivation or substrate depletion. The time profiles of LPA and DPPA levels were also analyzed by co-expressing both GPAT and LPAAT enzymes in the presence of liposomes along with the G3P and palmitoyl-CoA precursors. After a lag phase of approximately 4 h, the concentration of LPA peaked to 2.3 μM at 8

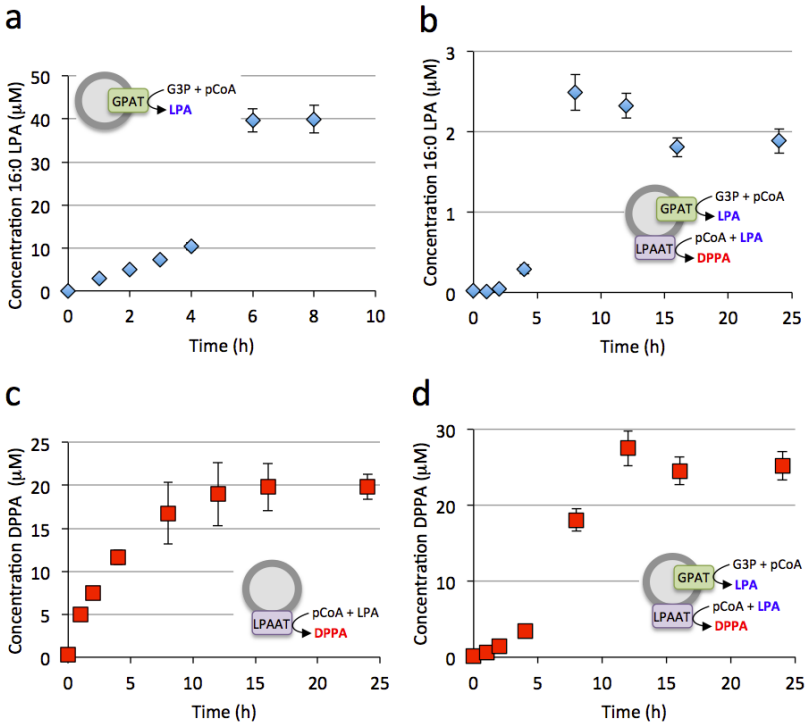

Figure 2.4: | Reaction kinetics of GPAT and LPAAT separate and combined.
(a-d) Kinetic of acyltransferase activity in single-enzyme and two-enzyme modes. Substrate concentrations were all: 500 μM G3P, GPAT: 100 μM P-CoA, LPAAT: 50 μM PcoA, 50 μ LPA, GPAT/LPAAT 100 μM PcoA. Produced 16:0 LPA does not accumulate beyond 3 μM (c) since it is consumed in the second enzymatic reaction. When GPAT and LPAAT are co-expressed, production of DPPA is initially limited by GPAT activity but then it reaches higher concentration (e) than with LPAAT only starting from purified LPA and p-CoA precursors (d). Each data points are mean and s.e.m. of two separate sample preparations. For each replicate the mean of two sample injections was calculated and data are reported as the mean and standard error of independent trials.

h and subsequently decreased to equilibrate around 1.5 μM at 16 h (figure 2.4, b). The amount of accumulated LPA is more than one order of magnitude lower than that with GPAT-only proteoliposomes, which can be attributed to its concurrent consumption by the LPAAT enzyme. The kinetics of DPPA production by LPAAT is initially limited by the rate of LPA formation (figure 2.4 d). The final concentration of DPPA, ~26 μM, represents a consumption of 52% of palmitoyl-CoA that was initially present at a concentration of 100 μM (two palmitoyl-CoA molecules are consumed to generate one DPPA molecule). This corresponds to ~5 % increase in the total amount of phospholipids. Moreover, it is approximately 5 μM more than with LPAAT-only proteoliposomes despite the fact that the IVTT resources and machineries are shared when the two genes are co-expressed. This result suggests enhanced activity when the GPAT and LPAAT proteins work in tandem [19], underlying the role of the lipid membrane as a functional scaffold. In such a chain reaction the spatial proximity of the enzymes in the lipid matrix may facilitate the transfer of intermediate products from one catalytic site to the other [19]. Alternatively, direct interaction between the GPAT and LPAAT proteins may act as allosteric regulation that enhances mutual activity. Further investigations are needed to validate these hypotheses.

2.2.4. ENRICHMENT OF LIPOSOME WITH SYNTHESIZED DPPA INDICATES MEMBRANE GROWTH

With the ultimate goal to stimulate vesicle growth through phospholipid biosynthesis in mind, we examined where the enzymatically produced DPPA lipid localized. Both GPAT and LPAAT enzymes were co-expressed to form hybrid proteoliposomes and the IVTT system was supplemented with palmitoyl-CoA and G3P precursors to initiate lipid synthesis concurrent to protein production. Liposomes were purified using streptavidin-coated magnetic beads via biotinylated lipids added in the initial membrane composition (figure 2.7). The vesicle content in DOPG (internal standard), LPA, and DPPA was quantified before and after purification, and the fraction of synthesized lipids that co-purified with the vesicles was calculated (figure 2.5). The low number of counts for LPA detected post purification indicates that it does not stably insert into the membrane (figure 2.5 b). Therefore, it was not possible to accurately determine the LPA membrane fraction after correcting for the loss of lipids during purification and filtering. However, we found that 28 % of *in situ* synthesized DPPA lipids co-purified with liposomes (figure 2.5 d). This corresponds to a concentration of 7 μM, which represents an increase of 1% of the total vesicle surface area.

2.2.5. *In vesiculo* ENZYME PRODUCTION AND SYNTHESIS OF THE MEMBRANE PRECURSOR DOPA

As a next step towards self-producing phospholipid vesicles [20], we used oleoyl-CoA as a substrate to enzymatically produce DOPA (18:1/18:1) lipids whose acyl moieties match that of pre-existing DOPX vesicles. Here, DOPC was removed from the membrane composition to simulate more closely the native *E. coli* lipid mixture. Using liposomes consisting of DOPG/DOPE/cardiolipin along with G3P and oleoyl-CoA as substrates, we demonstrated that DOPA, the direct precursor of the vesicle lipids, could be produced by the GPAT and LPAAT enzymes in combined IVTT and acyltransferase activity assays

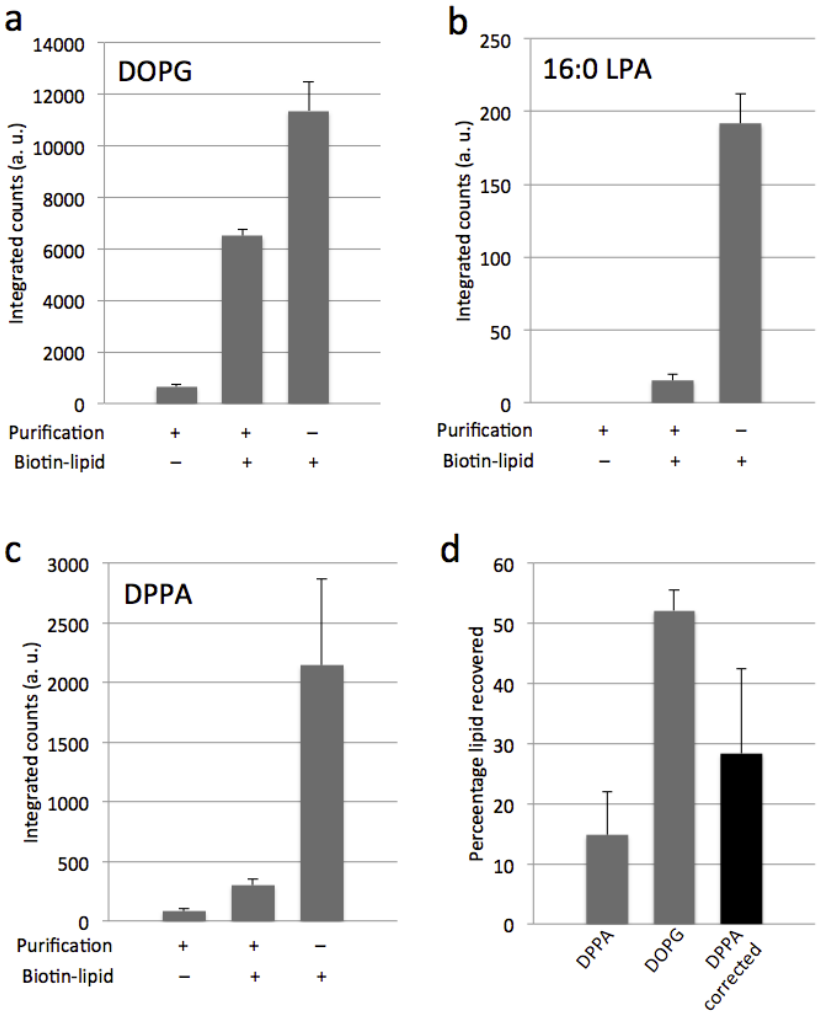

Figure 2.5: | Inside-out acyltransferase proteoliposomes are enriched with synthesized DPPA lipid.
(a-c) LC-MS analysis of synthesized 16:0 LPA and DPPA lipids with or without liposome purification. Lipid DOPG present in the initial composition of the 400 nm vesicles was used as an internal standard to correct for the loss of lipids during purification. Lipid biosynthesis occurred in a one-pot IVTT and acyl transfer reaction starting from 500 μM G3P and 100 μM p-CoA substrates. In some samples SUV membranes were doped with a biotinylated lipid for immobilization of liposomes on streptavidin-coated magnetic beads. Inspection of the amounts of lipids detected for the different experimental conditions allowed us to discriminate between liposome-integrated and free DPPA. Data are mean and s.e.m. of three independent experiments. For each replicate the same sample was injected 2x times in the MS, their averaged value was calculated and data are reported as the mean and standard error across the three trials. (d) Calculation of the percentage of synthesized DPPA co-localizing with liposome membrane. The use of DOPG as an internal standard enabled to quantify the fraction of non-immobilized or disrupted vesicles that were washed away during the purification step. Percentage values of recovered DPPA and DOPG were calculated as [counts(purif+|biotin+) – counts(purif+|biotin–)] / [counts(purif–|biotin+)] x 100. Then, the obtained value for DPPA was divided by that for DOPG to correct for the loss of lipids during purification (figure 2.7), resulting in a value of 28% ± 14% as an estimation of synthesized DPPA that effectively localized in liposomes.

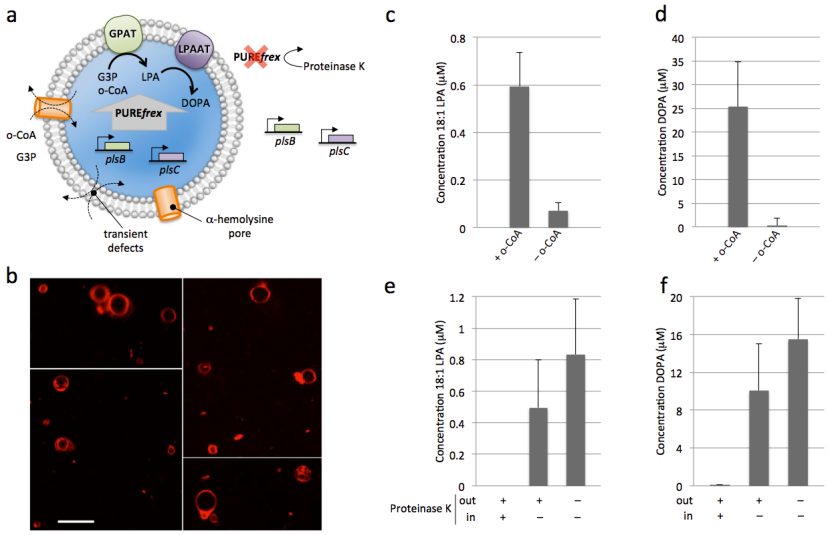

Figure 2.6: | Synthesis of 18:1 LPA and DOPA from GPAT and LPAAT enzymes produced inside and outside liposomes.
(a) Schematic of vesicle-confined experiments. PURE*frex* supplemented with the *plsB* and *plsC* genes and with 500 μM G3P was encapsulated inside liposomes using gentle rehydration of a lipid film covering submillimetre glass beads. Lipid composition consisted of DOPC, DOPE, DOPG, cardiolipin, TexasRed-DHPE and DSPE-PEG-biotin (Table 2.1). Liposome swelling occurred at 4 °C to prevent initiation of PURE system reaction. Gene expression outside liposomes was inhibited by protein digestion. Lipid biosynthesis was triggered by external supply of 100 μM oleoyl-CoA (o-CoA). (b) Confocal microscopy images of liposomes after swelling. Vesicles were labeled with a membrane dye (Texas-Red). Scale bar is 5 μm. (c,d) Concentration of 18:1 LPA (c) and DOPA (d) synthesized in a one-pot reaction by GPAT and LPAAT enzymes produced outside liposomes composed of DOPG, DOPE and cardiolipin (Table 2.1). Lipid precursors were 500 μM G3P and 100 μM o-CoA (except in negative control). Error bars indicate s.e.m. of two injections of the same sample. (e,f) Concentration of 18:1 LPA (e) and DOPA (f) produced by GPAT and LPAAT enzymes generated inside liposomes. Three experimental configurations corresponding to different localizations of protein digestion were tested. As expected, addition of Proteinase K both inside and outside liposomes totally inhibited lipid synthesis. In the absence of Proteinase K 18:1 LPA and DOPA accumulated as a result of both internal and external acyltransferase production. Liposome-confined IVTT and lipid synthesis was demonstrated by supplementing Proteinase K outside vesicles according to the reaction scheme illustrated in (a). Data are mean and s.e.m. of three independent experiments. For each replicate the same sample was injected two times in the MS, their averaged value was calculated and data are reported as the mean and standard error across the three trials.

(figure 2.6 d). Production of the 18:1 LPA intermediate was also detected (figure 2.6 c), though in lower amount than DOPA due to its subsequent consumption by the LPAAT enzyme. Around 25 μM of DOPA was produced, a concentration similar to that of DPPA when starting from palmitoyl-CoA instead of oleoyl-CoA.

Further, to mimic the cellularization of gene expression, the PURE system together with the *plsB* and *plsC* genes were compartmentalized inside cell-sized liposomes as shown in figure 2.6 a/b. These *in vesiculo* experiments aim to recapitulate some essential features specific to the native cellular context, such as confinement and entropy effects, and exposure to lipidic boundaries. Additionally, they may simulate the cytoplasm-like crowding environment in the lumen of the vesicle, as remarkably high concentrations

of proteins can be entrapped upon liposome formation [21]. The method to prepare gene expressing-vesicles is based on gentle lipid film swelling (Methods) and it generates a heterogeneous population of uni- and multilamellar liposomes with sizes ranging from < 0.5 μM to several micrometers in diameter, as visualized on a fluorescence confocal microscope (figure 2.6 b). Compared to our previously described protocol [22], the complete PURE*frex* system – comprising the transcription-translation machineries, the tRNAs and the feeding solution – supplemented with G3P and β-mercaptoethanol, was encapsulated inside liposomes. The average number of DNA molecules per 5-μm diameter vesicle is 30 and 140 for *plsB* and *plsC* genes, respectively; the DNA copy number per liposome is not a limiting factor [23]. To prevent the reactions from starting prematurely, lipid film swelling was performed at 4 °C, which is still above the phase transition temperature of the bilayer. Non-encapsulated proteins were digested by external addition of proteinase K and intravesicular gene expression was simultaneously initiated all at 37 °C. In control experiments, proteinase K was added in the swelling medium such that digestion of proteins occurred both inside and outside vesicles. The liposome membrane was equipped with the pore-forming protein α-hemolysin to facilitate the uptake of G3P, amino acids and nucleoside triphosphates present in the external environment, while providing a path for side products removal. After 3 h gene expression, lipid synthesis was triggered by adding the co-substrate oleoyl-CoA from the outside of the vesicles and the solution was incubated overnight at 37 °C.

Liposome-confined production of 18:1 LPA and DOPA could clearly be demonstrated (Figure 2.6. e/f). As expected, addition of proteinase K completely impedes gene expression and thus lipid synthesis. In the absence of active protein degradation, bulk production of lipids seems to be inefficient since the total amount of DOPA is not largely reduced upon addition of proteinase K. This result suggests that at least one of the key reaction steps, i.e. gene expression, co-translational membrane insertion, or lipid biosynthesis, is enhanced when compartmentalized inside liposomes. One hypothesis is that *in vesiculo* co-production of GPAT and LPAAT enzymes will give rise to a higher density of the two enzymes in the vesicle membrane, which may favor molecular transfer during the cascade reaction. How the oleoyl-CoA substrate supplied outside reaches the GPAT and LPAAT catalytic sites needs clarification, but it likely involves transient membrane defects due to lipid chain mismatch and osmotic pressure [22]. Compared to inside-out proteoliposome experiments, a larger enrichment of the vesicle membrane with DOPA is expected (i.e. > 27 %) when both gene expression and lipid biosynthesis occur inside liposomes.

2.2.6. DISCUSSION

Cell-free synthesis of membrane proteins has become instrumental for structural and functional studies of this important class of proteins [24]. Tens of different membrane proteins have already been co-translationally reconstituted into liposomes, including the GPAT and LPAAT enzymes studied here [5], [6], [24], [14], [25]. However, the co-reconstitution of even simple enzymatic cascades has remained a challenge. Using the *E. coli*-based minimal PURE system as a protein factory and liposomes as functional scaffolds, we have shown here that two enzymes GPAT and LPAAT could be active after *in vitro* synthesis. We demonstrated that LC-MS is a powerful experimental tool to

gain quantitative insights into the enzymatic processes by detecting the amounts of reaction substrates and products as a function of time or initial conditions. In particular, we provided a quantitative analysis of the two-step acyltransferase reaction that converts non bilayer forming substrates into PA lipids, the universal precursor of all other glycerophospholipids. Examination of the role of the liposome membrane and of cooperative functioning of the two acyltransferases suggests that the integration of both enzymes in the same bilayer matrix leads to a gain of function, as measured by a higher yield of end product compared to that when the second enzyme is assayed separately. Further investigations are necessary to obtain detailed mechanistic insights about substrate selectivity, the transfer of compounds from one enzymatic active site to the next, allosteric regulations and spontaneous protein insertion into the membrane.

Our liposome-based cell-free platform is highly versatile in terms of the lipidic composition of the vesicular membrane and orthogonal control of multiple biochemical parameters. Compared to *E. coli* extracts, the PURE system benefits from remarkably reduced contamination by RNase and lipids. Besides, in cell extract systems the synthesized proteins are not insulated from endogenous components, which may influence the performance of the reconstituted functions. Because of the reconstituted nature of PURE system with specialized enzymes for gene expression, interference between the host protein machinery and the newly synthesized components/functions is limited. At least regarding the membrane proteins studied here, no active membrane translocation complexes are required for insertion into the membrane.

Besides, various precursors (including acyl-ACP) and additional enzymes (besides those presented here and in chapter 4), can be used to generate a larger repertoire of lipids that may act as topological activators for membrane deformation, as cofactors to assist some protein reactions or as signaling molecules. We also envision the possibility to synthesize novel artificial lipids that would be difficult to generate chemically or *in vivo*. Our findings also resonate in the experimental framework of the construction of a minimal cell based on IVTT compartmentalized inside liposomes. Despite significant advances to endow gene expressing-vesicles with cell-like functionalities [6], many challenging obstacles limit the synthesis and quantitative analysis of a large repertoire of proteins, in particular membrane proteins, which precludes the achievement of elaborate functions, such as compartment growth and division. In this chapter, we demonstrate how 2 essential enzymes in phospholipid biosynthesis, a process essential for cellular growth could be produced *in vitro* from genomic DNA. In chapter 4, we extend that by 6 additional phospholipid modifying enzymes. Additionally, a protocol was established to compartmentalize gene expression and lipid synthesis inside cell-sized liposomes. These experiments are foundational to future investigations aiming at reconstituting complete lipid biosynthesis pathways embedded inside the membrane of growing vesicles. Such a constructive biology approach, in which the building blocks and processes are directly inspired from those existing in modern organisms, will complement chemical routes using artificial membrane components [26],[27], [28] for repetitive growth and fission of liposomal structures. Besides volume expansion, we postulate that *in vesiculo* lipid biosynthesis could be exploited to change the equilibrium state of the membrane and trigger asymmetric division. First, in light of the recently unveiled mechanism of L form cell reproduction [29], we predict that internal synthesis of phospholipids could

be sufficient to induce shape deformation as a manifestation of the excess surface area of membrane. The resulting unbalanced surface-to-volume ratio will eventually be released by division through budding. Second, the synthesis of topologically active lipids (e.g. PE, chapter 4) coupled to temperature cycling to cross the bilayer phase transition might stimulate shape transformation and complete fission of vesicles.

2.3. MATERIAL AND METHODS

2.3.1. MATERIALS

Palmitoyl coenzyme A (p-coA), oleoyl coenzyme A (o-CoA), palmitoyl lysophosphatidic acid (16:0 LPA), oleoyl lysophosphatidic acid (18:1 LPA), 1,2-dipalmitoyl-sn-glycero-3-phosphate (DPPA), 1,2-dioleoyl-sn-glycero-3-phosphate (DOPA), 1,2-dioleoyl-sn-glycero-3-phosphocholine (DOPC), 1,2-dioleoyl-sn-glycero-3-phosphoethanolamine (DOPE), 1,2-dioleoyl-sn-glycero-3-phospho-(1'-rac-glycerol) (DOPG), 1',3'-bis[1,2-dioleoyl-sn-glycero-3-phospho]-sn-glycerol (cardiolipin), and 1,2-distearoyl-sn-glycero-3- phosphoethanolamine-N-[biotinyl(polyethylene glycol)-2000] (DSPE-PEG-biotin) were purchased from Avanti Polar Lipids. N-(6-tetramethylrhodaminethiocarbamoyl)-1,2-dihexadecanoyl-sn-glycero-3-phosphoethanolamine (TRITC-DHPE) was from Invitrogen. Texas Red 1,2-dihexadecanoyl-sn-glycero-3-phosphoethanolamine, triethylammonium salt (Texas Red DHPE), 212 μm -300 μm acid washed glass beads, chloroform, methanol, acetylacetone, glycerol-3-phosphate (G3P), β-mercaptoethanol, and L-serine were from Sigma-Aldrich. Formic acid, ammonium formate and ULC grade organic solvents for mobile phases were from Biosolve. Cytidine triphosphate (CTP) was from Promega.

2.3.2. BUFFERS

Buffer A (GPAT buffer, 150 mM Tris-HCl, 400 mM NaCl, 3 mM MgCl2, 5 mM β-mercaptoethanol, 1 mg/mL BSA, pH 8.4), buffer B (LPAAT buffer, 100 mM Tris-HCl, 200 mM NaCl, 0.5 mM MgCl2, 1 mg/mL BSA, pH 9.0), buffer C (50 mM HEPES, 100 mM potassium glutamate, 13 mM magnesium acetate, pH 7.6), buffer D (20 mM HEPES, 180 mM potassium glutamate, 14 mM magnesium acetate, pH 7.6), buffer E (GPAT dialysis buffer, 150 mM Tris-HCl, 400 mM NaCl, 3 mM MgCl2, pH 8.4), buffer F (LPAAT dialysis buffer, 100 mM Tris-HCl, 200 mM NaCl, 0.5 mM MgCl2, pH 9.0), buffer G (150 mM Tris-HCl, 400 mM NaCl, 3 mM MgCl2, 1mg/ml BSA, 66.6 μM G3P, pH 8.4).

2.3.3. PREPARATION OF DNA CONSTRUCTS

The genes *plsB* and *plsC* were kindly provided by Dr. Yutetsu Kuruma [14] in the form of circular plasmids. The plasmids carrying an ampicillin selection marker were amplified in *E. coli* (TOP10) cells and purified with a PureYield™ plasmid miniprep (Promega). Linear DNA templates were generated by PCR using the primers:
plsB fwd: 5'-CATTCGCCATTCAGACTACG-3'
plsB rev: 5'-GACTATGATTACGCCGGTAC-3'
plsC fwd: 5'-TCGACTCTAGAGGATCTCG-3'
plsC rev: 5'-CCTCAAGACCCGTTTAGAG-3'.

Experiments	Figures	Lipid compositions
Regular	2.2,2.3,2.4	DOPC, DOPE, DOPG, cardiolipin, 50.8:35.6:11.5:2.1 in mol. %
Biotinylated liposomes for purification with Dynabeads®	2.5	Regular supplemented with DSPE-PEG-biotin 0.1% (weight percent)
Proteoliposome purification by flotation	2.1b	Regular supplemented with DHPE-TRITC 0.5% and DSPE-PEG-biotin 0.5%, both in weight percent
Production DOPA	2.6c,d	DOPG, DOPE, cardiolipin 54.4:35.6:10 in mol. %
In vesiculo assay	2.6b,e,f	Regular supplemented with TexasRed-DHPE 0.5 % and DSPE-PEG-biotin 1 %, both in weight percent

Table 2.1: Various lipid compositions used in experiments in this chapter.

2.3.4. PREPARATION OF SMALL UNILAMELLAR VESICLES (SUVS)

Lipids dissolved in chloroform were transferred to a 2 ml glass vial. Unless indicated, the regular lipid composition was DOPC, DOPE, DOPG, cardiolipin, 50.8:35.6:11.5:2.1 in mol. %. An overview of the different lipid mixtures used is provided in table 2.1. The chloroform was evaporated under gentle argon flow. Traces of chloroform were removed by placing the lipid film-containing vial in a vacuum desiccator for 1 h. The lipid film was then hydrated with buffer D (Figures 2.2a, 2.3, 2.4, 2.5, and 2.6c/d) or buffer C (Figures 2.1b and 2.2b). The sample was vortexed to re-suspend the lipids in aqueous solution and the produced multilamellar liposomes were subjected to five freeze-thaw cycles in liquid nitrogen (figures 2.2a, 2.3, 2.4, 2.5, and 2.6c/d) except in proteoliposome purification by flotation (figures 2.1b) and CoA assay experiments (Figure 2.2b), where this step was omitted. Next, the liposomes were extruded 20 times through a polycarbonate membrane with 0.4 μm (Figures 2.2a, 2.3, 2.4, 2.5, and 2.6c/d) or 0.1 μm (Figures 2.1b and 2.2b) pores using an Avanti mini-extruder (Avanti Polar Lipids). Finally, the SUV samples were aliquoted, snap-frozen in liquid nitrogen (figures 2.2a, 2.3, 2.4, 2.5, and 2.6c/d) or simply frozen (figures 2.1b and 2.1b), and stored at – 20 °C until use.

2.3.5. CELL-FREE PROTEIN SYNTHESIS

In vitro transcription-translation (IVTT) reactions were performed in the PURE*frex* kit (GeneFrontier, Japan; local supplier Eurogentec). PURE*frex* is composed of three different solutions: the enzyme mixture (T7 RNA polymerase, translation factors, energy recycling system, etc.), the *E. coli* ribosomes, and the feeding mixture (amino acids, NTPs, tRNAs, creatine phosphate). All solutions were aliquoted in small volumes and stored at –80 °C. For bulk experiments, in which IVTT occurred outside or in the absence of liposome, the PURE*frex* reaction solution was assembled on ice by mixing 1 part of enzyme mix, 1 part of ribosome, 10 part of feeding mix, the DNA template(s) (final concentration typically between 1.7 nM and 16.9 nM), and the total volume was adjusted to 20 parts

with nuclease-free water. When indicated, Superase RNase inhibitor (Thermo Fisher), β-mercaptoethanol, lipid precursors and SUVs were supplemented to IVTT reactions. For SDS-PAGE analysis of the translation products, ~5% v/v of BODIPY-Lys-tRNA (FluoroTect™ GreenLys, Promega), a fluorescence-based *in vitro* translation labeling system, was included to the reaction. Gene expression reactions were carried out at 37 °C for 3 h unless coupled with *in situ* lipid biosynthesis.

2.3.6. ACYL TRANSFER REACTIONS FOLLOWING CELL-FREE PROTEIN SYNTHESIS

Enzyme-containing proteoliposomes were prepared by performing PURE*frex* reactions using 10 ng/μl of *plsB* and/or *plsC* DNA templates, 0.4 U/μl of RNase inhibitor and 400 nm SUVs (2 g/l lipid). The DHFR-encoding expression plasmid provided in the PURE*frex* kit (5.78 ng/μl final) was used in control experiments for GPAT activity. A linear DNA coding for the LacI protein (20.8 ng/μl final) was employed in control experiments for LPAAT activity. Lipid substrate palmitoyl-CoA was dissolved in a solvent mixture chloroform:methanol:water with vol. % 80:20:2 and 16:0 LPA was dissolved in chloroform:methanol:water with vol. % 65:35:8. The solutions were transferred to a 1.5-ml glass vial and the solvent was evaporated at room temperature and ambient pressure under a chemical hood. The dried lipid substrates were then resuspended in a pre-ran proteoliposome-containing IVTT solution that was diluted ten times either in buffer A (GPAT buffer) or buffer B (LPAAT buffer). The final concentration of palmitoyl-CoA was either 133.3 μM when both GPAT and LPAAT enzymes were co-assayed or 66.6 μM for single-enzyme assays. In addition, reactions with only the LPAAT (or LacI) enzyme included 66.6 μM LPA. All reactions with the GPAT (or DHFR) protein contained 66.6 μM G3P. Negative controls for reactions with both GPAT and LPAAT proteins were performed without G3P. The samples were incubated overnight at 22 °C and assayed by LC-MS.

2.3.7. ACYL TRANSFER FLUORESCENCE ASSAY

Using acyl-CoA as the acyl donor substrate for GPAT and LPAAT leads to the release of CoA. Accumulation of free CoA was measured by using an acyltransferase activity kit (Enzo Life Sciences), in which CoA reacts with a fluorogenic substrate to form a fluorescent thiol adduct. The acyl transfer activity of the GPAT and LPAAT enzymes was assayed subsequently to protein synthesis and liposome inclusion in PURE*frex*. Conditions for IVTT reactions were as described above with the following modifications: 100 nm SUVs were used at a concentration of 2 g/L and the RNase inhibitor was absent. The DHFR-encoding plasmid (5.78 ng/μl final) provided as a positive expression template in the PURE*frex* kit and a linear DNA coding for the LacI protein (20.8 ng/μl final) were used as DNA templates in negative control experiments for GPAT and LPAAT activity, respectively. Because the CoA-sensitive assay is not compatible with the presence of reducing agents, the DTT contained in PUREfrex was dialyzed out overnight at 4 °C using a floating dialysis membrane (V-Series from Millipore) with 25 nm pore size on 100 ml of buffer E (GPAT dialysis buffer) or buffer F (LPAAT Dialysis Buffer). The 10 μl of dialyzed samples were diluted to 100 μl to have final composition buffer G to assay GPAT activity or to have final composition of buffer B to assay LPAAT activity. The solutions were then used to resuspend the lipid substrates dried into glass vials. Final concentrations were 66.6 μM of

palmitoyl-CoA for GPAT activity assay, and 33.3 μM of palmitoyl-CoA along with 33.3 μM of LPA for LPAAT activity assay. The samples were incubated for 2 h at room temperature and assayed according to the instructions of the supplier. Briefly, 25 μl of sample was mixed with 25 μl of proprietary buffer ("Transferase Assay Buffer"). The samples were further mixed with 50 μl of ice-cold isopropanol, then with 100 μl of detection solution and incubated 10 min. Fluorescence signal was measured with a BMG Clariostar or Agilent Eclipse plate reader (results combined by normalizing to positive control) at 486 nm excitation and 540 nm emission.

2.3.8. COMBINED IVTT AND ACYL TRANSFER REACTIONS

PURE*frex* solutions were assembled using 3.4 nM *plsB* and 16.9 nM *plsC* DNA templates supplemented with 0.4 g/l of 400-nm SUVs, 0.4 U/l of RNase inhibitor, 5 mM β-mercaptoethanol and 500 μM G3P. Lipid precursors palmitoyl-CoA and oleoyl-CoA were separately dissolved in a solvent mixture chloroform:methanol:water with vol. 80:20:2 and 16:0 LPA in chloroform:methanol:water with vol. % 65:35:8. The solutions were transferred to a 0.2-ml Eppendorf PCR tube and the solvent was evaporated at room temperature and ambient pressure under a chemical hood. The dried lipid substrates were then resuspended in the PURE*frex* mix leading to the final concentrations of 100 μM palmitoyl-CoA or oleoyl-CoA, and 100 μM 16:0 LPA when LPAAT alone was measured and with the exception of the kinetics experiments (Fig. 3b-e), where 50 μM palmitoyl-CoA and 50 μM 16:0 LPA were used with LPAAT-only. The samples were incubated at 37 °C overnight or shorter when indicated, and the lipid content was assayed by LC-MS.

2.3.9. PURFICATION OF LIPOSOMES BY FLOTATION

A 20-μl IVTT reaction was run with 12.5 ng/μL of the *plsB* and/or *plsC* constructs and 1.66 g/l of 100 nm SUVs. The reaction solution was further supplemented with 0.8 μl of BODIPY-Lys-tRNA. The *in vitro* synthesized acyltransferase GPAT and LPAAT enzymes successfully reconstituted in proteoliposomes were separated from bulk proteins, including all PURE*frex* components, by liposome flotation technique. First, the pre-ran IVTT reaction solution was mixed with 1 μl of RQ1 DNase and 1 μl of RNase I, and held at 37 °C for 1 h. The sample was then diluted two times in buffer C, layered on top of 40 μl of a 7.5 % w/v sucrose solution in a 230-μl ultracentrifugation tube (Beckmann Coulter). The sample was spun at 40,000 rpm (203,000 g) for 4 h using a 42.2 Ti rotor in a Ultima L-90K centrifuge (Beckmann Coulter). The floating liposomes, which were labelled with the DHPE-TRITC membrane dye for easy visualization, were then harvested with a cut pipette tip from the surface and the co-purified proteins were analysed by SDS-PAGE.

2.3.10. SDS-PAGE ANALYSIS

For SDS-PAGE analysis of protein synthesis, samples containing the Green$_{Lys}$-labeled translation products were denatured for 2 min at 65 °C, loaded on a 12% SDS-PAGE gel (figure 2.1) with 37.5:1 ratio of acrylamide:bis acrylamide and analyzed using a fluorescence gel imager (Typhoon, Amersham Biosciences). Ladder was either prestained or stained with coomassie blue and appended to the images to scale with GIMP image editor.

2.3.11. DYNABEADS® PURIFICATION OF LIPOSOMES.

For the experiments of LC-MS analysis of liposome enrichment with synthesized lipids, PURE*frex* solutions were assembled with 10 ng/μl of *plsB* and *plsC* templates, 0.5 U/μl RNase inhibitor, 5 mM β-mercaptoethanol, 500 μM G3P and 2 μg/μl 400 nm SUVs with (two samples pooled) or without (one sample) biotinylated lipids. The two PURE*frex* solutions were added separately to 100 μM of dried palmitoyl-CoA and reacted overnight at 37 °C. Two samples, one from the biotinylated liposomes reaction and the other from the non-biotinylated liposomes, were subject to purification using streptavidin-coated magnetic beads. A third sample from the biotynalated pool did not undergo purification. The overall sample purification workflow is illustrated in figure 2.7. 30 μl of M-270 Dynabeads® were washed three times with 200 μl of buffer D. The beads were resuspended in 100 μl of buffer D and 12.5 μl of the proteoliposome-containing solutions were added to separate tubes. The samples were then incubated at room temperature in a rotator for 80 min. The beads were then washed five times with 200 μl of buffer D and the sample volume was adjusted to 12.5 μl. The three 12.5-μl samples (two undertook purification, one did not) were mixed with 387.5 μl methanol and then sonicated for 10 min. The samples were then supplemented with 1.6 ml methanol (final volume 2 ml) and filtered using a 0.2-μm Acrodisc® (Pall) syringe filter to remove the magnetic beads (procedure was also done for the non purified sample). The volume of the solution was finally reduced to approximately 112.5 μl with an Eppendorf Concentrator Plus and 12.5 μl of MilliQ was added along with 1.25 μl of 500 mM EDTA and 1.25 μl of 200 mM acetylacetone. The samples were then assayed by LC-MS.

2.3.12. *In vesiculo* GENE EXPRESSION AND ACYL TRANSFER EXPERIMENTS

Liposomes were formed by natural swelling of a lipid film coated onto 212–300-μm glass beads according to our previously reported protocol [22], with some modifications. Five milligrams of lipids dissolved in chloroform were mixed in a round-bottom glass flask. Lipid composition was DOPC, DOPE, DOPG and cardiolipin at 50.8:35.6:11.5:2.1 mol. %. The mixture was supplemented with TexasRed-DHPE 0.5 % and DSPE PEG-biotin 1 %, both in mass percent. To improve lipid film swelling at low temperature, 63.5 μmol. of rhamnose (from a 100-mM stock solution in methanol) was added to the lipid mixture [30]. Finally, 1.5 g of glass beads was added and the organic solvent was rotary evaporated at 200 mbar at room temperature. The dried lipid-coated beads were transferred to a 2-mL polypropylene tube and put in a vacuum desiccator overnight to remove traces of solvent. The beads were then stored under argon at –20 °C and were re-dessicated for 30 min before use. The IVTT reaction solution to be internalized inside liposomes was prepared by pooling the three PUREfrex reagents in a ratio feeding/ribosome/enzymes of 10:1:1 supplemented with 7.4 ng/μl of *plsB* and *plsC* DNA templates (final concentrations 2.5 nM and 12.5 nM, respectively), 0.74 U/μl RNase inhibitor, 7.4 mM β-mercaptoethanol and 740 μM G3P. The solution was split into three samples of 13.5 μl each. To one sample 1 μl of 100 μg/ml proteinase K (from Promega, stock solution in MilliQ water) was added, while in the other two samples 1 μl of MilliQ was injected. The IVTT mixture was then added to lipid-coated glass beads to form liposomes. Lipid film swelling was performed for 2 h at 4 °C to prevent gene expression from starting, while maintaining the bilayer in the liquid disordered phase. After swelling

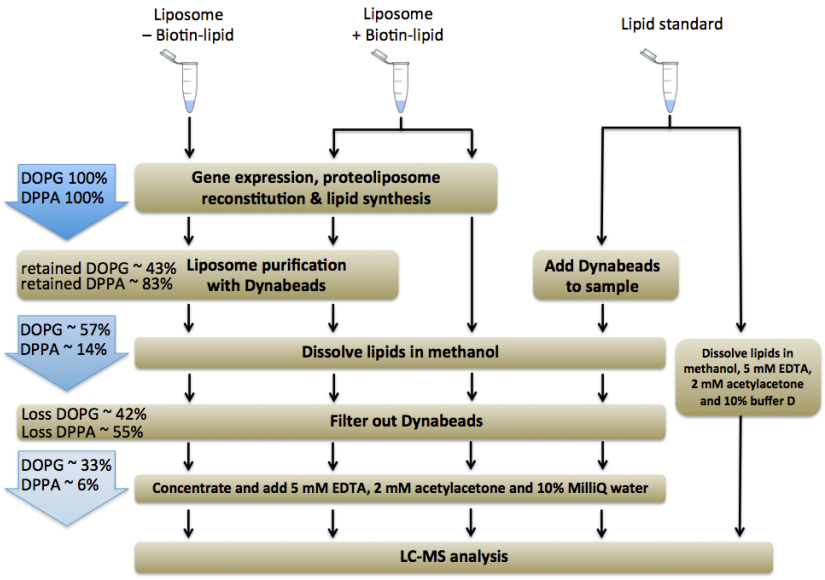

Figure 2.7: | Experimental workflow for assessing the fraction of synthesized DPPA localized in the liposome membrane.
The loss of lipids during the filtration step was determined by measuring the number of counts of lipid standards (DPPA and DOPG, three concentrations each) treated with or without filtration. Linearity over the used concentration range was validated for both lipids and both treatments (not shown). For each lipid the loss introduced by filtering was calculated as: Loss % = slope filtered / slope unfiltered x 100. Values of 42% and 55% were obtained for DOPG and DPPA, respectively. The fraction of DOPG and DPPA lipid retained during purification was assessed using biotin-labeled vesicles and subjecting, or not, samples to purification with Dynabeads. Recovered lipid values correspond to 57% and 14% for DOPG and DPPA, respectively. The sample devoid of biotinylated lipid served to infer the loss of DPPA due to nonspecific adsorption to the magnetic beads or to the tube during purification. The corresponding count number was subtracted from that of the biotin-labeled vesicle sample to determine the actual fraction of DPPA that was retained through liposome immobilization. In Fig. 4, we estimated this fraction to represent 15% of the total DPPA synthesized, which after correcting for the fact that only 52% of internal standard DOPG is recovered leads to 30%.

the samples were subjected to four freeze-thaw cycles (alternating exposure to 4 °C and liquid nitrogen) to break multilamellar structures. From each reaction 4.35 μl of supernatant was harvested, mixed with 1.35 μl of 4.44 M α-hemolysin (Sigma-Aldrich) and incubated at room temperature for 10 min. To one of the samples that had not received proteinase K, 0.3 μL of the protease stock solution was added to digest all proteins outside liposomes, while 0.3 μl of MilliQ was added in the other two samples. All three samples were then incubated at 37 °C for 3 h. The 6-μl samples were transferred into new 0.2-ml PCR tubes, where dried oleoyl-CoA had been deposited, leading to a final concentration of lipid precursor of 100 μM. The samples were further incubated at 37 °C overnight and their lipid contents were assayed by LCMS.

2.3.13. LIQUID CHROMATOGRAPHY-MASS SPECTROMETRY (LC-MS) FOR LIPID DETECTION

The lipid fraction was extracted by first diluting the samples ten times with methanol containing 2 mM acetylacetone. For *in vesiculo* experiments (figure 2.6) 5 mM of EDTA was also included in the organic solvent to improve the stability of the LC-MS method (chapter 3). The samples were then sonicated for 10 min in a bath sonicator, spun down at 16,100 rcf in an Eppendorf 5415R centrifuge to remove protein and nucleic acid precipitates, and the supernatant was harvested for LC-MS analysis. The LC-MS method for lipid analysis was adapted from previous studies [31] [32]. In all experiments, 5 μl samples were injected into an LC system (Agilent 1260) equipped with a XSELECT HSS T3 2.5 μm analytical column. Lipids elute sequentially (a typical chromatogram is shown in figure 2.1 c) providing a pre-separation step before entering the MS system. The mobile phase A consisted of (all % given in vol./vol.) 60% acetonitrile, 40% deionized water, 7 mM ammonium formate, 0.0114% formic acid and 2 mM acetylacetone. Formic acid and ammonium formate were used to set the pH to 4.0. The mobile phase B was 90% isopropanol, 10% acetonitrile, 0.0378% formic acid and 2 mM acetylacetone. Acetylacetone was used to chelate metal ions, which reduced peak tailing of LPA and DPPA [33]. The output from the analytical column was connected to an MS instrument (Agilent 6460 Triple Quad MS) that was operated according to the parameters reported in chapter 3, tables 3.3, 3.4 and 3.5, where the values in non-calibrated data represent the integrated peak area. We analyzed multiple reaction monitoring transitions, i.e. the lipids were ionized, selected by mass in a first ion filter, fragmented by collisions with nitrogen gas in a collision cell and then the fragment masses were monitored in another ion filter.

2.3.14. PREPARATION OF LIPID STANDARDS AND CALIBRATION CURVES FOR ABSOLUTE QUANTITATION OF SYNTHESIZED LIPID CONCENTRATIONS

Calibration measurements were performed to determine the absolute concentration of 16:0 LPA, 18:1 LPA, DPPA and DOPA produced in some experiments (figure 2.4 and 2.6). Standard samples were prepared by serial dilution of stock concentrations of lipids in their respective organic solvent mixture used for storage. For 16:0 LPA and DPPA standard solutions, 2 μl of each samples was added to 3 μl of PURE*frex* system (containing 10ng/μL of *plsB* and *plsC* DNA) with 0.4 mg/ml SUVs of regular composition, 5 mM β-mercaptoethanol, 500 μM G3P and and 0.4 U/μl RNase inhibitor in order to reproduce the same lipid background than that in the measured IVTT reaction samples. Samples were further diluted with 25 μl methanol containing 2 mM acetylacetone to a final concentration of 5 μM. The standard solutions were then centrifuged at 16,100 rcf (Eppendorf 5415R) and 5 μl of the supernatants were injected in the LC-MS system. For experiments with oleoyl lipids in the inside-out proteoliposome configuration, 18:1 LPA and DOPA stock solutions in chloroform were diluted in methanol with 2 mM acetylacetone. For *in vesiculo* experiments, standards were prepared by mixing SUVs, 18:1 LPA and DOPA in 90% methanol with 2 mM acetylacetone and 5 mM EDTA (see section on EDTA), 10% buffer D (20 mM HEPES, 14 mM magnesium acetate, 180 mM potassium glutamate, pH 7.6) to final concentrations of 2.1 mg/ml liposome and 5 μM 18:1 LPA and DOPA. The standards were finally diluted with a solution of methanol with 2 mM acetylacetone and 5 mM EDTA. Calibration curves for the different lipid standards

were obtained by plotting the number of integrated counts against concentration and a linear fit of the data was performed using IGOR Pro 17 (WaveMetrics) (Figure 2.8). The concentration of synthesized lipids in reaction samples was determined by reporting the calculated peak integrated counts on the calibration curve and correcting for the 10-time dilution of the samples.

In order to correct for variations in pipetting, the amount of DOPG was used as an internal standard. The counts measured for each data point was normalized by the number of DOPG counts:

$$Ct_{norm} = \frac{Ct}{C_{DOPG}} \tag{2.1}$$

The standard deviation and average for the normalized counts for each time point were calculated. The concentrations were then calculated by multiplying the normalized counts by the average concentration of DOPG and solving the line equation for concentration

$$Conc = \frac{Ct_{norm} \cdot \overline{DOPG}}{b} \tag{2.2}$$

To calculate the errors of the concentration we used variance formula

$$\sigma_{conc} = \sqrt{\left(\frac{\overline{DOPG}}{b}\right)^2 \sigma^2_{Ctnorm} + \left(\frac{\overline{Ctnorm}}{b}\right)^2 \sigma^2_{\overline{DOPG}} + \left(\frac{Ctnorm \cdot \overline{DOPG}}{b^2}\right)^2 \sigma^2_b} \tag{2.3}$$

An alternative method was used to convert MS counts into lipid concentrations. First, a linear regression of the count ratios DPPA/DOPG to the known concentrations of DPPA was made:

$$\frac{DPPA_c}{DOPG_c} = b[DPPA] \tag{2.4}$$

The slope b and its error σ_b were extracted. We then calculated the actual value of the concentrations in a sample as:

$$[DPPA] = \frac{\frac{DPPA_c}{DOPG_c}}{b}. \tag{2.5}$$

The error of DPPA/DOPG counts was calculated as:

$$\sigma_{DPPA} = \sqrt{\left(\frac{1}{b}\right)^2 \sigma^2_{\frac{DPPA_c}{DOPG_c}} + \left(\frac{\frac{DPPA_c}{DOPG_c}}{b^2}\right)^2 \sigma^2_b} \tag{2.6}$$

Similar results were obtained as with the first method.

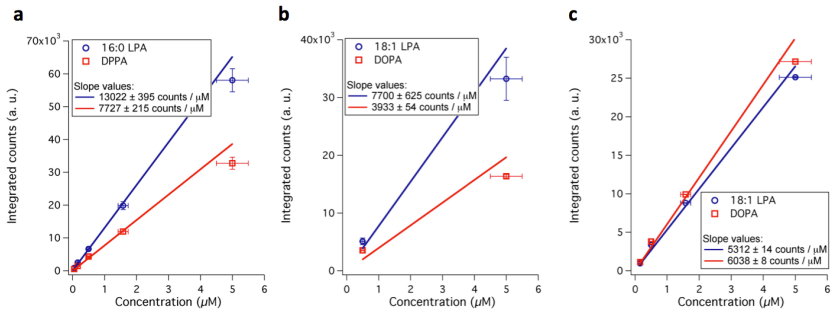

Figure 2.8: | Calibration curves for quantifying absolute lipid concentrations.
The number of counts for lipid standard samples of known concentrations was plotted against the concentration and a linear fit of the data was performed. For each sample, the concentration error was estimated to be 10% based on the fact that lipids obtained from Avanti Polar Lipids are overpacked by as much as 10% and that standard stocks may experience degradation. The counts error was calculated directly from multiple measurements of lipid standards. Alternatively the error percentage was calculated from multiple injections of synthesized lipids-containing samples as an estimate of the MS data variability on a given day. The concentration to counts conversion factors are calculated from the slopes divided by ten to account for the ten-fold dilution of samples before injection to the MS. (a) Calibration plots for the kinetics measurements presented in figure 2.4 a-d. Values of conversion factors are 1302 cts/μM for LPA and 778 cts/μM for DPPA. (b) Calibration plots for the oleoyl-CoA bulk experiments presented in figure 2.6 c,d. Values of conversion factors are 770 cts/μM for 18:1 LPA and 393 cts/μM for DOPA. (c) Calibration plots for the oleoyl-CoA *in vesiculo* experiments presented in figure 2.6 e,f. Values of conversion factors are 531 cts/μM for 18:1 LPA and 604 cts/μM for DOPA. Calibration curves were performed on the same day as measurements on stored samples to minimize differences observed when experiments were made on different days. This, together with contribution from the fact that preparation of lipid standards was different for the three sets of experiments (2.3.14), explains the different conversion factor values obtained in b) and c).

2.3.15. CALCULATION OF GROWTH OF VESICLES

Calculation of increase surface area of liposomes upon incorporation of synthesized DPPA. To estimate the vesicle growth through synthesis and membrane incorporation of DPPA lipids, the following calculation was made. First the initial surface area, A, of a 400-nm-sized vesicle was calculated:

$$A = 4 \cdot \pi \cdot (200 \cdot 1e-9)^2. \tag{2.7}$$

Then the total number of lipids per vesicles, $N_{lip}./$ves., was calculated taking into account the two leaflets of the membrane. A cross-sectional area of 72.1 Å^2 corresponding to that of a DOPC molecule was assumed.

$$N_{lip}./ves. = 2 \cdot A/(72.1 \cdot (1e-10)^2). \tag{2.8}$$

The concentration of vesicles is derived from the initial concentration of lipids, $C_{lip}.$ = 508 μM, and the number of lipids per liposome as:

$$C_{ves}. = C_{lip}./(N_{lip}./ves.) \tag{2.9}$$

The concentration of synthesized DPPA was determined by kinetics experiments with both GPAT and LPAAT enzymes and a value of 26 μM was found (figure 2.4 d). Given that

about 28% of total synthesized DPPA integrated in liposome membrane (figure 2.5 d), the concentration of membrane inserted DPPA, C_{PA}, is ~7 μM. Therefore, assuming homogenous partitioning of DPPA lipids between vesicles, the number of DPPA molecules per liposome is:

$$N_{PA}/ves. = C_{PA}/C_{ves}. \tag{2.10}$$

Using a cross-sectional area per DPPA lipid of 50 Å^2 it is possible to calculate the total additional surface area as:

$$A_{PA}/ves. = 50 \cdot (1e-10)^2 \cdot (N_{PA}/ves.)/2. \tag{2.11}$$

The percentage area increase was calculated as $(A_{PA}/ves.)/A \cdot 100$ and a value of ~1% was found.

2.3.16. STATISTICAL ANALYSIS OF DATA

Whenever indicated, a two-sample t-test (unequal variances) was performed using MATLAB (MathWorks), with the hypothesis that the population means are unequal.

2.3.17. FLUORESCENCE CONFOCAL MICROSCOPY

The lipid mixture used to prepare liposomes for the *in vesiculo* experiments (figure 2.6) was supplemented with TexasRed-DHPE 0.5 % and DSPE-PEG-biotin 1 % in mass. Lipid film formation and rehydration was performed according to a similar protocol used for vesicle-confined reactions. 13.5 μl of PURE system was added to beads. 4 μl of supernatant was harvested and 2 μl of MQ was added to it. A 6-μl-solution droplet was deposited into a homemade silicon chamber mounted onto a #1.5 glass coverslip. The sample was imaged using a fluorescence confocal microscope (A1+ from Nikon) equipped with a 100x oil immersion objective and a 561-nm laser line with appropriate dichroic mirror and emission filter.

REFERENCES

[1] P. L. Luisi, "Toward the engineering of minimal living cells," *The Anatomical Record*, vol. 268, no. 3, pp. 208–214, 2002.

[2] P. L. Luisi, F. Ferri, and P. Stano, "Approaches to semi-synthetic minimal cells: a review," *Naturwissenschaften*, vol. 93, no. 1, pp. 1–13, 2006.

[3] A. C. Forster and G. M. Church, "Towards synthesis of a minimal cell," *Molecular systems biology*, vol. 2, no. 1, p. 45, 2006.

[4] V. Noireaux, Y. T. Maeda, and A. Libchaber, "Development of an artificial cell, from self-organization to computation and self-reproduction," *Proceedings of the National Academy of Sciences*, vol. 108, no. 9, pp. 3473–3480, 2011.

[5] P. Schwille, "Bottom-up synthetic biology: engineering in a tinkerer's world," *Science*, vol. 333, no. 6047, pp. 1252–1254, 2011.

[6] F. Caschera and V. Noireaux, "Integration of biological parts toward the synthesis of a minimal cell," *Current opinion in chemical biology*, vol. 22, pp. 85–91, 2014.

[7] J. E. Cronan, "Bacterial membrane lipids: where do we stand?" *Annual reviews in microbiology*, vol. 57, no. 1, pp. 203–224, 2003.

[8] J. Yao and C. O. Rock, "Phosphatidic acid synthesis in bacteria," *Biochimica et Biophysica Acta (BBA)-Molecular and Cell Biology of Lipids*, vol. 1831, no. 3, pp. 495–502, 2013.

[9] A. Röttig and A. Steinbüchel, "Acyltransferases in bacteria," *Microbiology and Molecular Biology Reviews*, vol. 77, no. 2, pp. 277–321, 2013.

[10] C. Sohlenkamp and O. Geiger, "Bacterial membrane lipids: diversity in structures and pathways," *FEMS microbiology reviews*, p. fuv008, 2015.

[11] D. W. Deamer and V. Gavino, "Lysophosphatidylcholine acyltransferase: purification and applications in membrane studies," *Annals of the New York Academy of Sciences*, vol. 414, no. 1, pp. 90–96, 1983.

[12] P. K. Schmidli, P. Schurtenberger, and P. L. Luisi, "Liposome-mediated enzymatic synthesis of phosphatidylcholine as an approach to self-replicating liposomes," *Journal of the American Chemical Society*, vol. 113, no. 21, pp. 8127–8130, 1991.

[13] R. Wick and P. L. Luisi, "Enzyme-containing liposomes can endogenously produce membrane-constituting lipids," *Chemistry & biology*, vol. 3, no. 4, pp. 277–285, 1996.

[14] Y. Kuruma, P. Stano, T. Ueda, and P. L. Luisi, "A synthetic biology approach to the construction of membrane proteins in a semi-synthetic minimal cells," *Biochimica et Biophysica Acta*, vol. 1788, pp. 567–574, 2009.

[15] T. J. Larson, V. A. Lightner, P. R. Green, P. Modrich, and R. M. Bell, "Membrane phospholipid synthesis in escherichia coli. identification of the sn-glycerol-3-phosphate acyltransferase polypeptide as the plsb gene product." *Journal of Biological Chemistry*, vol. 255, no. 19, pp. 9421–9426, 1980.

[16] J. Coleman, "Characterization of the escherichia coli gene for 1-acyl-sn-glycerol-3-phosphate acyltransferase (pisc)," *Molecular and General Genetics MGG*, vol. 232, no. 2, pp. 295–303, 1992.

[17] W. O. Wilkison, J. P. Walsh, J. M. Corless, and R. M. Bell, "Crystalline arrays of the escherichia coli sn-glycerol-3-phosphate acyltransferase, an integral membrane protein," *The Journal of Biological Chemistry*, vol. 251, no. 21, pp. 9951–9968, 1986.

[18] P. R. Green, A. H. Merril, and R. M. Bell, "Membrane phospholipid synthesis in escherichia coli purification, reconstitution, and characterization of sn-glycerol-3-phosphate acyltransferase," *The Journal of Biological Chemistry*, vol. 256, no. 21, pp. 11 151–11 159, 1981.

[19] J. Kessels, H. Ousen, and H. Van den Bosch, "Facilitated utilization of endogenously synthesized lysophosphatidic acid by 1-acylglycerophosphate acyltransferase from escherichia coli," *Biochimica et Biophysica Acta (BBA)-Lipids and Lipid Metabolism*, vol. 753, no. 2, pp. 227–235, 1983.

[20] F. Varela, H. Maturana, and R. Uribe, "Autopoiesis: The organization of living systems, its characterization and a model," *Biosystmes*, vol. 5, pp. 187–196, 1974.

[21] T. P. de Souza, P. Stano, F. Steiniger, E. D'Aguanno, E. Altamura, A. Fahr, and P. L. Luisi, "Encapsulation of ferritin, ribosomes, and ribo-peptidic complexes inside liposomes: insights into the origin of metabolism," *Origins of Life and Evolution of Biospheres*, vol. 42, no. 5, pp. 421–428, 2012.

[22] Z. Nourian, W. Roelofsen, and C. Danelon, "Triggered gene expression in fed-vesicle microreactors with a multifunctional membrane," *Angewandte Chemie*, vol. 124, no. 13, pp. 3168–3172, 2012.

[23] Z. Nourian and C. Danelon, "Linking genotype and phenotype in protein synthesizing liposomes with external supply of resources," *ACS synthetic biology*, vol. 2, no. 4, pp. 186–193, 2013.

[24] F. Junge, S. Haberstock, C. Roos, S. Stefer, D. Proverbio, V. Dötsch, and F. Bernhard, "Advances in cell-free protein synthesis for the functional and structural analysis of membrane proteins," *New biotechnology*, vol. 28, no. 3, pp. 262–271, 2011.

[25] H. Matsubayashi, Y. Kuruma, and T. Ueda, "In vitro synthesis of the e. coli sec translocon from dna," *Angewandte Chemie International Edition*, vol. 53, no. 29, pp. 7535–7538, 2014.

[26] R. J. Brea, C. M. Cole, and N. K. Devaraj, "In situ vesicle formation by native chemical ligation," *Angewandte Chemie*, vol. 126, no. 51, pp. 14 326–14 329, 2014.

[27] M. D. Hardy, J. Yang, J. Selimkhanov, C. M. Cole, L. S. Tsimring, and N. K. Devaraj, "Self-reproducing catalyst drives repeated phospholipid synthesis and membrane growth," *Proceedings of the National Academy of Sciences*, vol. 112, no. 27, pp. 8187–8192, 2015.

[28] K. Kurihara, Y. Okura, M. Matsuo, T. Toyota, K. Suzuki, and T. Sugawara, "A recursive vesicle-based model protocell with a primitive model cell cycle," *Nature communications*, vol. 6, 2015.

[29] R. Mercier, Y. Kawai, and J. Errington, "Excess membrane synthesis drives a primitive mode of cell proliferation," *Cell*, vol. 152, no. 5, pp. 997–1007, 2013.

[30] K. Tsumoto, H. Matsuo, M. Tomita, and T. Yoshimura, "Efficient formation of giant liposomes through the gentle hydration of phosphatidylcholine films doped with sugar," *Colloids and Surfaces B: Biointerfaces*, vol. 68, no. 1, pp. 98–105, 2009.

[31] G. Astarita, J. H. McKenzie, B. Wang, K. Strassburg, A. Doneanu, J. Johnson, A. Baker, T. Hankemeier, J. Murphy, R. J. Vreeken *et al.*, "A protective lipidomic biosignature associated with a balanced omega-6/omega-3 ratio in fat-1 transgenic mice," *PloS one*, vol. 9, no. 4, p. e96221, 2014.

[32] V. Gonzalez-Covarrubias, M. Beekman, H.-W. Uh, A. Dane, J. Troost, I. Paliukhovich, F. M. Kloet, J. Houwing-Duistermaat, R. J. Vreeken, T. Hankemeier *et al.*, "Lipidomics of familial longevity," *Aging Cell*, vol. 12, no. 3, pp. 426–434, 2013.

[33] D. Siegel, H. Permentier, and R. Bischoff, "Controlling detrimental effects of metal cations in the quantification of energy metabolites via ultrahigh pressure-liquid chromatography–electrospray-tandem mass spectrometry by employing acetylacetone as a volatile eluent modifier," *Journal of Chromatography A*, vol. 1294, pp. 87–97, 2013.

3

FURTHER STUDIES RELATED TO GPAT AND LPAAT

In addition to the published results of chapter 2 we performed several complementary experiments and employed other techniques related to the study of E. Coli GPAT and LPAAT synthesized in the PUREfrex. In this chapter we present some of the important results. We examined the effect of various concentrations of palmitoyl CoA in co-expression and activity reactions, which is a relevant quantity if one wants to improve the magnitude of growth of liposomes. We also examined the effect of β-mercaptoethanol on the co-expression and activity reactions, and found that its presence indeed enhances enzyme activity. We further experimented with the effect of storage of glycerol-3-phosphate (G3P) and β-mercaptoethanol in aqueous solution at -20 °C before use in reactions and found that at least one of the compounds experiences some form of degradation under those conditions. In chapter 2 we showed GPAT and LPAAT proteins are incorporated upon synthesis into liposomes forming proteoliposomes. Here, we show the same with an alternate method, i.e. the use of Dynabeads® to purify liposomes from background proteins. GPAT has been shown in the literature to form filaments observable by transmission electron microscopy [1]. Here we show that we were also able to form filaments with PUREfrex synthesized GPAT albeit of a different diameter. We further present results of the optimization of expression of the plsB and plsC genes at the protein and mRNA levels. We found that plsB was best used in its plasmid form, while plsC was effective as a linear PCR product. Finally we found that during liquid chromatography mass spectrometry (LC-MS) signal of phosphatidic acid was improved with the addition of EDTA to the sample preparation. In addition to these experiments, we also present a special section on laboratory techniques that were developed by the author along with other members of the lab, that may not be recorded elsewhere. It is intended as a brief guide to communicate important techniques that were developed during the studies. I.e the preparation of LC-MS samples, the liquid chromatography method, the details of the mass spectrometry method as well as techniques for handling the various lipids used in the lab.

3.1. RESULTS

3.1.1. CONCENTRATION OF PALMITOYL COA

We were interested to discover what amount of palmitoyl CoA to use in co-expression and activity reactions. We assembled co-expression and activity of GPAT and LPAAT reactions with various concentrations of palmitoyl CoA. We observed by eye that above 100 μM palmitoyl CoA there appeared to be precipitate in the sample which corresponds well with experiments in the literature [2].

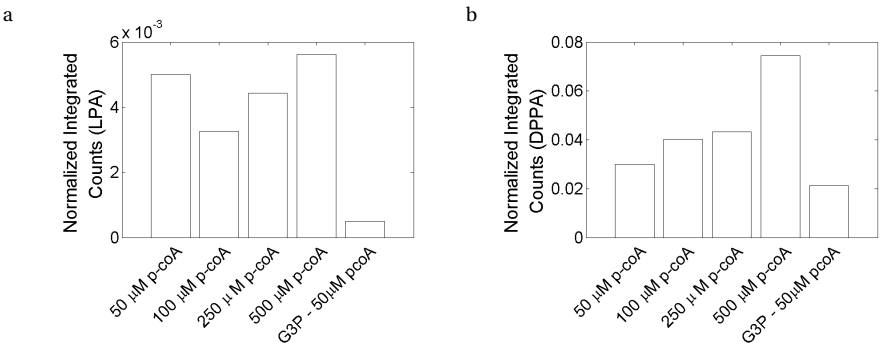

Figure 3.1: | Effect of concentration of palmitoyl CoA on LPA and DPPA production in acyltransferase reactions.
(a) LPA produced in co-expression reaction with various concentrations of palmitoyl CoA. Negative control did not contain G3P (G3P-). Increased concentration of palmitoyl CoA does not always result in increased LPA. Consumption of produced LPA by LPAAT prevents drawing strong conclusions of GPAT activity . All signals are normalized to the amount of DOPG present. (b) DPPA produced in the same set of reactions, normalized to DOPG. Amount of DPPA produced increases monotonically with palmitoyl CoA concentration but not proportionally.

In figure 3.1 we plot the amount of LPA and DPPA produced, with various concentrations of palmitoyl CoA, normalized to DOPG counts. The amount of LPA and DPPA generally increased with increasing substrate concentration, which suggests that despite the apparent precipitation above 100 μM palmitoyl CoA the reactions can still occur and even be enhanced. Note that the amount of DPPA in the 500 μM sample is certainly not 10 $\times$ the amount in the 50 μM reaction. That is an indication that there may be some inhibition of other loss of enzyme activity, that the precipitation observed has some effect on the reactions or that the kinetics are too slow to consume all the substrate. The latter can be expected to be true based on the long time scale of the reaction to consume 50 μM of substrate (approximately 15 hours) as measured in chapter 2. We thus found that a good amount of palmitoyl CoA to use in reactions was 100 μM as there was no visible precipitation and good consumption of the substrate.

3.1.2. - β -MERCAPTOETHANOL, OLD SUBSTRATES

In figure 3.2 a/b we observed if 5 mM of β-mercaptoethanol has a positive effect on the activity of GPAT and LPAAT proteins in co-synthesis and activity reactions. The motivation is that GPAT is believed to require reducing conditions to function [3], therefore β-mercaptoethanol, a reducing agent is usually included in activity buffers [3], [4]. It was found that the amount of LPA synthesis was not significantly affected, though this

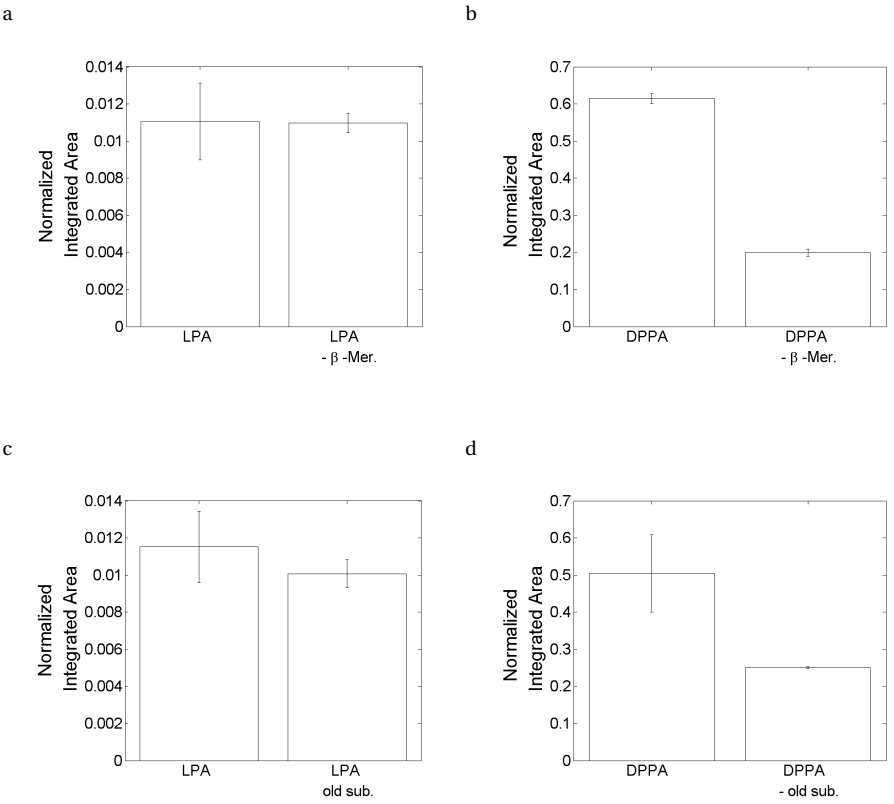

Figure 3.2: | Activity of co-expressed GPAT and LPAAT, with and without β-mercaptoethanol and with old G3P and β-mercaptoethanol.
(a/b) LPA and DPPA production in a co-expression and activity reaction with and without 5 mM β-mercaptoethanol. β-mercaptoethanol seems to enhance the production of DPPA substantially. LPA production was not substantially enhanced. Amounts are normalized to the amount of DOPG present in each reaction and error bars are from three measurements of the same sample. (c/d) LPA and DPPA production in a co-expression and activity reaction with freshly prepared and with stored β -mercaptoethanol and glycerol 3 phosphate (G3P) solutions (aqueous). Either the old β -mercaptoethanol or G3P causes a decrease in the synthesis of LPA and DPPA, either by substrate degradation (G3P), enzyme activity (β -mercaptoethanol) or possibly also protein expression (β -mercaptoethanol). Amounts are also normalized to DOPG present and error bars for the freshly prepared substrates are from 3 injections each of three preparations of the same sample and for the old substrates three measurements of the same sample

is likely due to the fact that LPA that is produced in both reactions is mostly consumed by the LPAAT. In the case of DPPA it was indeed found that there was more DPPA with β - mercaptoethanol than without. That is an indication that at least one of the enzyme reactions is more efficient in the presence of the reducing agent, or possibly also the protein expression by the PURE system and therefore the amount of active protein. A similar experiment is shown in figure 3.2 c/d where β - mercaptoethanol and G3P solutions in MQ that had been stored at -20 °C for a few days were tested against freshly prepared solutions. It was found that at least one of the old solutions experienced some degradation. This is inferred from the decrease of LPA and DPPA signal. G3P hydrolysis could affect the amount of available active substrate and therefore the amount of product produced. Degradation of β-mercaptoethanol would have the same effect as not including it, as was done in the previous experiment.

3.1.3. G3P IN PURE SYSTEM OR LIPIDS

It was found that in an early co-expression and activity experiment that there was significant lipid signal in the negative control, which was a sample where G3P was omitted. A pool of PURE*frex* was made and split into six vials containing palmitoyl CoA. To three of them G3P was added and to three MQ was added. It was found that there was nearly 70 % of the signal in the negative LPA sample as in the positive, and 55% of the DPPA signal in the negative as compared to the positive. This lead us to believe that there was G3P contamination either in the lipids as supplied by Avanti, possibly due to degradation, in the PURE*frex*, either from the solutions purified by companies, or in the DNA templates. Therefore the negative control was changed to omitted palmitoyl CoA and the counts in the negative samples decreased to the blank levels.

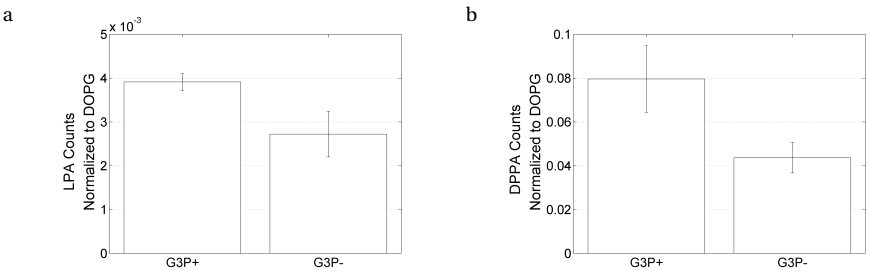

Figure 3.3: | G3P contamination in the PURE reaction or lipids as indicated by synthesis of LPA and DPPA in -G3P samples.
(a) Normalized LPA signal for a co-expression reaction with and without G3P shows negative sample as having approximately 70 % of the positive (b) similarly the normalized DPPA signal shows negative sample as having approximately is 55 % of the positive signal. The fact there there are counts in the G3P - samples that are beyond the blank values (LPA ~0.0003 DPPA ~0.003) implies that G3P was present in G3P - reactions. The observation was found on multiple days. Error bars are from three semi independent repeats made from the same pool of PURE*frex* system.

3.1.4. PURIFICATION OF PROTEOLIPOSOMES BY DYNABEADS®

In addition to the experiments of liposome purification by flotation assay for confirming the presence of proteoliposomes in solution, experiments were made to purify proteoliposomes by extraction with Dynabeads®. In these experiments liposomes containing DSPE-PEG-biotin were bound to streptavidin coated magnetic beads (Dynabeads® M-270), that were then washed to remove non liposome associated proteins.

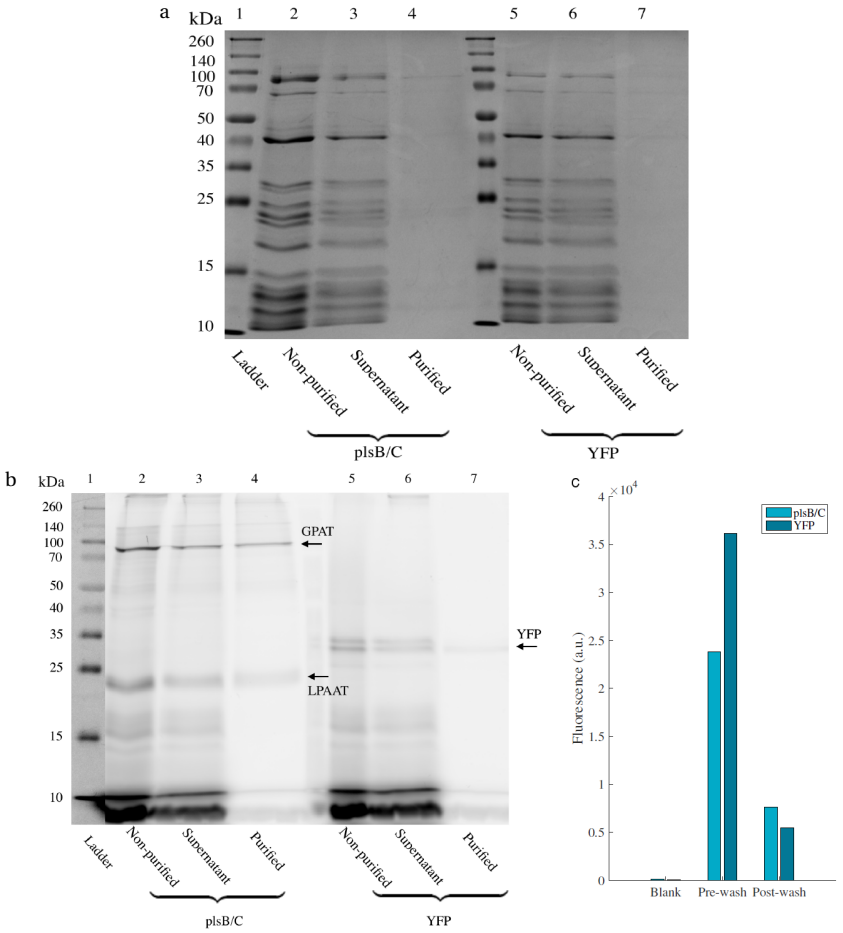

Figure 3.4: | Proteoliposome purification by Dynabeads® shows membrane association of GPAT and LPAAT. (a) SDS-page coomassie stained gel showing the lanes of non purified liposomes, supernatant from the first washing step and purified liposomes, for both GPAT/LPAAT and YFP. The non purified and supernatant lanes contain PURE*frex* background proteins whereas washed Dynabeads® purified samples do not. (b) shows the same gel as in a) imaged on a typhoon scanner to detect FluoroTect ™ GreenLys labeled lysines incorporated during translation. All lanes show presence of protein, showing that GPAT/LPAAT are liposome-associated but also some YFP is. (c) shows the fluorescence of Rhodamine-DHPE labelled liposomes bound to Dynabeads® before and after washing steps as well as blank of beads without liposomes. This result shows that 15-32 % of liposomes are retained when subjected to Dynabeads® purification.

Figure 3.4 a shows that when washing steps are made, the background PURE system proteins are removed. All lanes except for the ladder are derived from expressing indicated proteins in PURE*frex* in the presence of liposomes. The non-purified samples (lanes 2 and 5) are samples containing expressed proteins as well as liposomes, without purification by Dynabeads®, the supernatant samples (3 and 6) are the first wash of the Dynabeads® purified samples containing unbound liposomes and proteins, and the purified samples (lanes 4 and 7) are the washed Dynabeads® containing bound liposomes and proteins. The signal in the non-purified and supernatant samples shows much stronger presence of PURE*frex* proteins than the purified samples, implying that binding of liposomes and washing indeed removes PURE*frex* proteins from the purified samples. Figure 3.4 b is the same gel as in a except imaged with a typhoon scanner that visualizes the presence of FluoroTect™ GreenLys labelled lysines incorporated during translation. For GPAT and LPAAT it is clear that the bands are retained even in the washed samples, which implies that the proteins are associated with liposomes that bound the Dynabeads®. Surprisingly, the negative control sample of YFP also contains a protein band. This may be due to a truncation of the YFP product. In lane (5), the YFP non purified sample there are two bands, and in the purified sample (lane 7) only one of them remains, the lower of the two. This band may represent a truncated or misfolded product that can expose hydrophobic parts that bind to liposomes, or it may simply be that translation of YFP in the presence of liposomes allows some interaction of hydrophobic residues that prevents correct folding and causes YFP to bind to the membrane. Figure 3.4 b) shows the fluorescence of rhodamine labeled liposomes in the GPAT/LPAAT samples as well as the YFP samples as measured with excitation wavelength of 554 nm and an emission wavelength of 610 nm before and after washing steps as well as a blank. This gives the fraction of liposomes purified as 32 % and 15 % for GPAT/LPAAT and YFP samples respectively. Possible reasons for less than 100% recovery are that liposomes are sheared from the surface of the beads during washing steps, or that not all the liposomes initially bind to the beads for unknown reasons. We did not assess the recovery rate of liposomes with the flotation assay and as such we cannot compare with this Dynabeads®method. As far as the separation of the GPAT and LPAAT from PURE system proteins, both methods seem to be effective.

3.1.5. TEM IMAGES OF SYNTHESIZED PROTEINS

It was found that GPAT forms tubular structures when overexpressed in *E. Coli* [1] and we wanted to observe if the same structures form with our *in vitro* synthesized proteins. We synthesized GPAT and LPAAT separately in both the absence and presence of liposomes and imaged these samples with transmission electron microscopy (TEM). The samples with GPAT and liposomes showed tubular structures as shown in figure 3.5 a-c). The samples with GPAT in the absence of the liposomes showed no such structures (not shown). It has been reported that phospholipids are also part of the tubular structures [1]. Our experiments confirm these findings since liposomes were a requirement to obtain the structures. On the other hand, the fibres found in literature have a diameter of approximately 32 nm whereas the ones we measured have a diameter of approximately 4 nm. The difference can possibly be due to the way the structures are formed as opposed to structural differences in the proteins themselves. In literature it has been reported

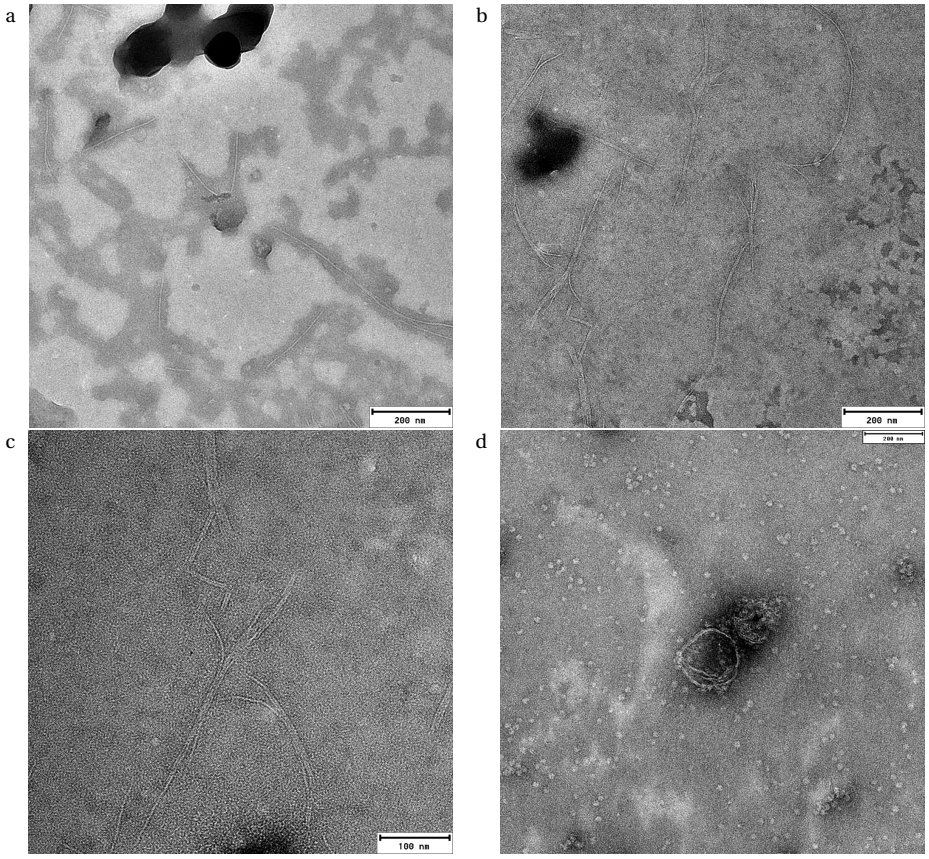

Figure 3.5: | TEM images of *in vitro* synthesized GPAT that forms tubular structures.
Transmission electron microscopy images of a 5-μl GPAT synthesis reaction including liposomes. The sample was negatively stained using 2% uranyl acetate. (a-c) Tubular structures formed by the oligomerization of GPAT. (a/b) The images are the 42,000× magnification of a 1000× diluted sample. (c) The image is the 72,000× magnification of a 1000× diluted sample. It can be seen that the tubular structures can aggregate to form even bigger tubular structures. d) An image of what seems to be a liposome. The white dots are ribosomes. This image is a 30,000× magnification of a 100× diluted sample. Altogether these images show that *in vitro* synthesized GPAT can form tubular structures reminiscent of that seen in literature [1]

that heat shock proteins are required for the tubular structures to form [5]. It was suggested that the heat shock proteins are involved in packing the the GPAT proteins into the tubes. The tubes that form in our system do so without the heat shock proteins. The LPAAT samples with and without liposomes did not show any tubular structures. This fact confirms that these tubular structures were formed by GPAT and not a PURE*frex* protein.

3.1.6. OPTIMIZATION OF EXPRESSION OF *plsB*

To optimize the expression of the *plsB* and *plsC* gene products we performed *in vitro* translation (IVT) and *in vitro* transcription translation (IVTT) reactions and analyzed

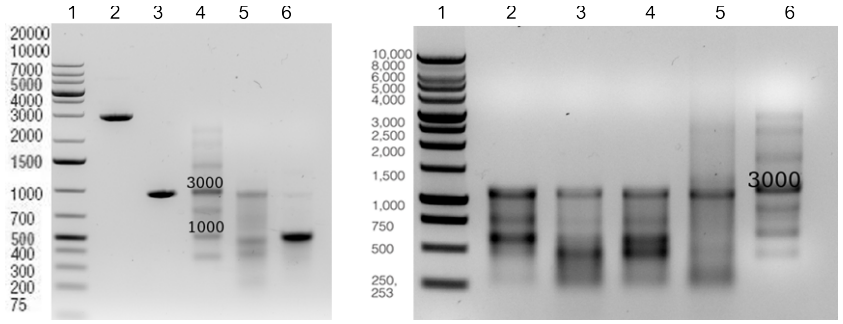

Figure 3.6: | *In vitro* transcription of *plsB* and *plsC* gene products reveals optimal template form.
(Left panel) Lane 1: GeneRuler 1kb plus, Lane 2: *plsB* PCR product, Lane 3: *plsC* PCR product, Lane 4: ssRNA ladder NO362S, Lane 5: IVT of *plsB* PCR product, Lane 6: IVT of *plsC* PCR product. Expression of *plsC* mRNA from PCR product is clean and efficient. *PlsB* mRNA expression is of low yield with many side products. (Right panel), (*plsB* mRNA) Lane 1: Benchtop DNA ladder, Lane 2: Increased Nucleotides, Lane 3: 30 degrees incubation, Lane 4: control, Lane 5: express from plasmid, lane 6: ssRNA ladder NO362S. The lane with the most *plsB* mRNA and the least side products is that derived from plasmid.

resulting RNA and protein with agarose and polyacrylamide gels respectively. Figure 3.6 shows in lane 2 and 3 the full length PCR product of the *plsB* and *plsC* genes at the correct molecular weights (*PlsB*: 4726 bp/2.9 MDa, *plsC*: 956bp/590kDa) as predicted by the sequences. In lanes 5 and 6 the mRNA product of a IVT reaction of *plsB* and *plsC* PCR products shows that the cleanliness and efficiency of making mRNA of *plsC* is high, but for *plsB* there are truncated products and low yield.

The right panel of figure 3.6 shows an additional IVT of the *plsB* genes to optimize the production of mRNA. Lanes 2, 3 and 4 are *plsB* PCR product with additional NTPs, a

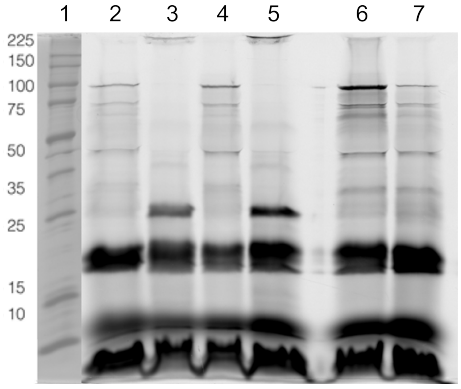

Figure 3.7: | *In vitro* transcription/translation of *plsB* and *plsC* gene products.
(a) Lane 1: V849A protein ladder (coomassie), Lane 2: *plsB* PCR increased resources, Lane 3: *plsC* PCR increased resources, Lane 4: *plsB* control, Lane 5: *plsC* control plasmid, lane 6: *plsB* plasmid 4X DNA, lane 7: *plsB* plasmid 1x DNA. Amount of GPAT only increases when increased template is used (lane 6). GPAT and LPAAT yield do not increase when increased resources (lanes 2 3) are used compared to a control without (lanes 4 5).

lower expression temperature (30 °C) and a positive control respectively. Lane 5 is with the *plsB* plasmid purified directly from *E Coli*. It is clear that lanes 2 and 3 do not show significant improvement over the positive control, lane 5 on the other hand, where the *plsB* plasmid is used, has slightly improved yield of mRNA and there are less side products. That was the motivation for employing the plasmid throughout other experiments.

We also expressed the *plsB* and *plsC* genes in the PURExpress® IVTT system (figure 3.7). PURExpress® is a variant of the PURE system made by New England Biolabs, with his-tagged proteins, and is modified from the original composition [6] to improve protein yield. The proteins were expressed from PCR products in lanes 2 (*plsB*) and 3 (*plsC*) with additional NTPs, amino acids and tNRAs (see below for complete method). Lanes 4 (*plsB*) and 5 (*plsC*) were controls also with PCR products. Lane 6 (*plsB*) and lane 7 (*plsB*) were expressed from plasmids with eight-fold and two-fold the total mass of DNA as in the PCR product. As can be seen, the increased resources do not have a significant affect on the amount of translated product, nor is the amount of GPAT greatly increased with the plasmid unless additional template is added. Despite these facts, due to improvements at the mRNA level we chose to use the *plsB* plasmid over the PCR product in our experiments.

3.1.7. EFFECT OF EDTA ON LPA AND DPPA SIGNAL

During the course of experiments it was observed that for sequential injections of the same sample in the LC-MS, a different number of total integrated counts for the DPPA and LPA signals would be measured. That is to say, a decrease in the DPPA signal and an increase in the LPA signal. There were issues with the autosampler, which is a robot

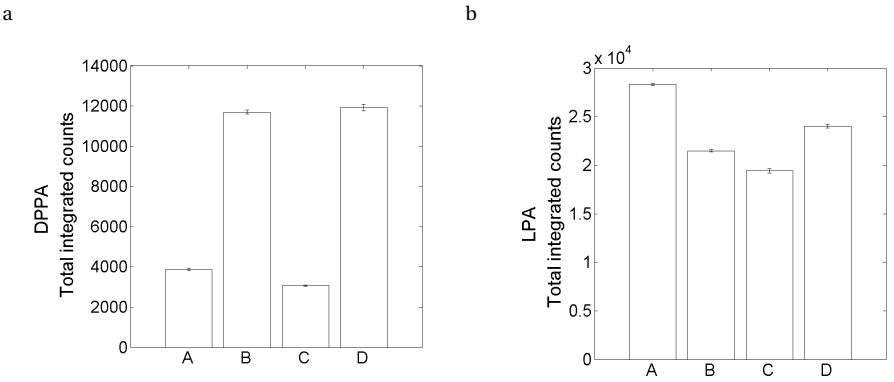

Figure 3.8: | Effect of EDTA on the signal of LPA and DPPA in LC-MS.
Column A: 90% Methanol w. 10 % buffer (2mM acetylacetone), Column B: 100% Methanol (2mM acetylacetone), Column C: column A + 25 μM $FeCl_3$, Column D: column A + 5mM EDTA
(a) the effect of various sample injection solvents on DPPA signal in the LC-MS. The presence of metal salts (columns 1 and 3) without compensating chelating action of EDTA (column 4) causes a decrease in DPPA signal (b) the effect of various sample injection solvents on LPA signal in the LC-MS. There is less of a pronounced effect on LPA and it does not correlate with the DPPA and the metal salt hypothesis.

which injects the samples, that were eventually solved. In addition we also had the hypothesis that metal ions from the liquid chromatography system could be affecting the mass spectrometry results. To test the effect of metal salts on the signal of LPA and DPPA we made four injections of the lipids (LPA and DPPA, along with DOPC, DOPE ,DOPG ,Cardiolipin liposomes) in four injection solvents conditions (for a total of 16 injections). The solvents were: (methanol with 2 mM acetylacetone mixed with PURE buffer to have 90% methanol, 10% PURE buffer (see methods)), (100% methanol with 2 mM acetylacetone), (methanol with 2 mM acetylacetone mixed with PURE buffer to have 90% methanol, 10% PURE buffer and in addition 25 μM $FeCl_3$), and (methanol with 2 mM acetylacetone mixed with PURE buffer to have 90% methanol, 10% PURE buffer and 5 mM EDTA (total)). We found that for DPPA the sample with PURE salts ($MgCl_2$, K glutamate) and methanol had less signal than the sample without PURE salts. Adding $FeCl_3$ seem to slightly worsen the effect and adding 5 mM EDTA to the sample completely removed the effect. For the LPA signal the sample with PURE salts had greater signal than the sample without, in correlation with the observation that LPA increased over sequential injections since contamination with metals would gradually increase. Confusingly the trend was not observed with the addition of $FeCl_3$. Addition of EDTA seemed to decrease the LPA signal as compared to the sample with PURE salts only. Overall we thus speculate that metal ions are modulating interactions between the analytical column and DPPA and LPA, and thus are varying the amount of lipids that elute. Interestingly the effect was not as drastic with LPA and it was not correlated with that of DPPA. The main message is that EDTA can affect the signal of LPA and DPPA, in particular it can improve that of DPPA in the liquid chromatography mass spectrometry method.

3.2. METHODS

3.2.1. BUFFERS

PURE buffer (20 mM HEPES, 14 mM magnesium acetate, 180 mM potassium glutamate pH 7.6)

3.2.2. CONCENTRATION OF PALMITOYL COA

PROTEIN SYNTHESIS

All reactions were combined protein expression and activity reactions. *PlsB* (GPAT) and *plsC* (LPAAT) templates were included at 10 ng/μl, Superase was included in the reaction at 0.4U/μl as well as 2 mg/ml of 400-nm liposomes of standard composition (DOPC, DOPE, DOPG, cardiolipin liposomes mol ratio 50.8:35.6:11.5:2.1) were also included. β-mercaptoethanol was included at 5 mM and G3P in positive reactions at 500 μM. The reactions were added to 0.2-ml eppendorf tubes containing dried palmitoyl CoA to the concentrations indicated in the figure. The reactions were incubated for 3 h at 37 °C and then incubated overnight at 22 °C.

LIQUID CHROMATOGRAPHY-MASS SPECTROMETRY

Samples were measured by standard method of liquid chromatography mass spectrometry as described in section 3.3.1 without EDTA in the sample preperation.

3.2.3. - β-MERCAPTOETHANOL, OLD SUBSTRATES

PROTEIN SYNTHESIS

For both experiments, a standard PURE*frex* reaction was assembled with 10 ng/μl of *plsB* (GPAT) and *plsC* (LPAAT) templates, 0.4 U/μl Superase, 0.4 mg/ml 400-nm DOPC, DOPE, DOPG, cardiolipin liposomes (mol % 50.8:35.6:11.5:2.1). In the -β-mercaptoethanol experiment, G3P was also included in both samples at a concentration of 500 μM and 5 mM of β-mercaptoethanol was included in the positive only. For the old substrates experiment the 5 mM β-mercaptoethanol and the 500 μM G3P included in the positive control (from 35.7 mM and 3.5 mM solutions in MQ respectively) were prepared fresh and in the old substrates sample, the solutions were stored at -20 °C for a few days before use. All experiments were performed in a 0.2-ml Eppendorf PCR tube in which dried palmitoyl CoA to a final concentration of 100 μM was present. For - β-mercaptoethanol experiment expression and activity was at 37 °C for 2.5 hours and then the sample was moved to room temperature overnight. For old substrates experiment expression and activity was at 37 °C overnight.

LIQUID CHROMATOGRAPHY-MASS SPECTROMETRY

After the overnight reaction samples were prepared with the standard sample preparation technique as described in section (3.3.1) (without EDTA). For the experiment where β-mercaptoethanol experiment was omitted from the negative, three injections of the same sample were made. The LPA and DPPA signals of the injection replicates were divided by the corresponding DOPG signals. Then the average and standard error of the DOPG normalized values were taken. For the "old substrates experiment" the following procedure was used: for the fresh substrate sample, three preparations of the same sample were made. Each of the three preparations were injected 3 ×. The values of the LPA and DPPA signal were divided by corresponding DOPG signals. The averages were taken across the three injections of each preparation and then the mean and standard error were taken across the three preparations. For the old substrate sample a single sample was prepared and injected 3 ×. The LPA and DPPA signals were divided by the DOPG signal and then the average and standard error of the triplet were taken.

3.2.4. G3P IN PURE SYSTEM OR LIPIDS

PROTEIN SYNTHESIS

All reactions were combined protein expression and activity reactions. *PlsB* (GPAT) and *plsC* (LPAAT) template were included at 10 ng/μl, Superase was included in the reaction at 0.4 U/μl and 2 mg/ml of 400-nm liposomes of standard composition (DOPC, DOPE, DOPG, cardiolipin liposomes mol % 50.8:35.6:11.5:2.1) were also included. β-mercaptoethanol was included at a concentration of 5 mM and G3P in positive reactions at a concentration of 500 μM. The reactions were added to 0.2-ml eppendorf tubes containing dried palmitoyl CoA at 100 μM final concentration. The reactions were incubated for 2.5 h at 37 °C and then incubated overnight at 22 °C.

LIQUID CHROMATOGRAPHY-MASS SPECTROMETRY

After reaction each of three identical vials were subjected to the standard sample preparation from section (3.3.1) (without EDTA) and injected 3 ×. The LPA and DPPA signal of

the injection replicates were divided by that of DOPG, and the averages taken across the three normalized injection replicates. Then the resulting three averages were themselves averaged and the standard error calculated.

3.2.5. PURIFICATION OF PROTEOLIPOSOMES BY DYNABEADS®

PROTEIN SYNTHESIS

Protein synthesis was carried out in the standard manner in the PURE*frex* IVTT system. Either *plsB* (GPAT) and *plsC* (LPAAT) template were included at 10 ng/μl or emYFP template at a concentration of 10 ng/μl . Superase was included at 0.5 U/μl and FluoroTect™ Green Lysine was included at 20 × dilution. Liposomes included were 400 nm and of standard composition (DOPC, DOPE, DOPG, cardiolipin liposomes mol % ratio 50.8:35.6:11.5:2.1) with the addition of 0.5% of the total lipid mass consisting of Rhodamine-DHPE and 0.1% of the total lipid mass consisting of DSPE-PEG-Biotin. The liposomes were included at a final concentration of 1.667 mg/ml. Proteins were expressed for 3 h at 37 °C. After protein expression 40 × diluted RNase ONE ™ and 20 × diluted DNAse I were added to the reactions that were incubated for an additional hour.

DYNABEADS® PURIFICATION

For the binding and washing to Dynabeads®, the beads were suspended in their container by vortexing and 30 μl was transferred to an 1.5-ml eppendorf tube. Two hundred microliter of PURE buffer was added, the mixture was vortexed and then put on a magnetic stand. The magnet draws the Dynabeads® to the side of the Eppendorf and the buffer can be removed without disturbing the beads. This process was repeated twice to remove the storage solution. After washing but before final removing of buffer, 10 μl (5%) of the beads were removed for the blank fluorescence measurement. After removing buffer, 11.5 μl of GPAT/LPAAT-expressed PURE system and 11.5 μl of YFP-expressed PURE system was added to separate vials containing washed beads and then 20 μl of PURE buffer was added to each. The mixtures were incubated while gently rotating, for 1h at room temperature and mixed by slowly pipetting up and down every 20 min. After incubation, 1.66 μl of bead solution was added to 8.34 μl of PURE buffer representing another 5% of the original number of beads to be used as a the pre-wash fluorescence measurement. The original Eppendorf tube was then put on the magnet stand for 2 min and then the first supernatant was removed and kept for measurement on the gel. The beads were subsequently washed four times by adding 200 μl PURE buffer, mixed by pipetting up and down, then putting it on the magnetic stand for 2 min and then removing the supernatant. The beads were then resuspended in 20 μl of PURE buffer and 1.11 μl (5% of the original number of beads) was taken and mixed with 8.89 μl of PURE buffer for the post-wash fluorescence measurement. Then the remaining suspended beads and liposomes were directly added to 5 × SDS loading buffer. For the unpurified controls 10.29 μl of appropriate expressed PURE system was mixed with 5 × SDS loading buffer and added to the gel. For the supernatant sample 1.49 μl of the supernatant was first removed for fluorescent measurement (not shown) and the rest was mixed with 5 × SDS loading buffer and added to gel. All samples were incubated at 65 °C for 5 minutes before loading on a 12% polyacrylamide gel.

	x-res.(2) B	x-res.(3) C	c. B(4)	c. C(5)	4x B plas.(6)	B plas.(7)
A solution	5	5	5	5	5	5
B solution	3.75	3.75	3.75	3.75	3.75	3.75
Superase	0.25	0.25	0.25	0.25	0.25	0.25
Green Lys	0.25	0.25	0.25	0.25	0.25	0.25
template	250ng P	250ng P	250ng P	250ng P	2166ng p	533.5ng p
Extra B	2.5	2.5	x	x	x	x
MQ	x	x	2.5	2.5	x	2.782
Total	13.31	14.44	13.31	14.44	13.31	13.03

Table 3.1: Reaction compositions for optimizing of GPAT and LPAAT expression. P=PCR, p=plasmid, numbers in title correspond to lane numbers of figure 3.7. x-res=extra resources, i.e. solution B, c.=control, 4xB=4x amount of *plsB* plasmid, B plas=1x amount of *plsB* plasmid.

3.2.6. TEM IMAGES OF SYNTHESIZED PROTEINS

PROTEIN SYNTHESIS

Protein synthesis was carried out in the standard manner in the PURE*frex* IVTT system. Either *plsB* (GPAT) or *plsC* (LPAAT) template was included at 10 ng/μl. Superase was also included in the reaction. In images shown in figure 3.5, 400-nm liposomes were included of standard composition (DOPC, DOPE, DOPG, cardiolipin mol % 50.8:35.6:11.5:2.1). Proteins were expressed for 3 h at 37 °C. Samples were stained with 2% uranyl acetate and imaged on a transmission electron microscope.

3.2.7. *PlsB* AND *plsC* CONSTRUCTS AND OPTIMIZATION

PlsB and *plsC* plasmids were obtained from Dr. Yutetsu Kuruma [3]. The plasmids carried an ampicillin selection marker and were thus cultured in medium containing ampicillin. Plasmids were purified with a PureYield™ plasmid miniprep kit. When linear PCR constructs were required the following primers were used: plsB fwd 5' CATTCGCCATTCAGACTACG 3', plsB rev 5'GACTATGATTACGCCGGTAC 3' and plsC Fwd 5'TCGACTCTAGAGGATCTCG 3' plsC Rev 5'CCTCAAGACCCGTTTAGAG 3'. To verify the length of *plsB* and *plsC* PCR products (lanes 2 and 3 figure 3.6 left panel) they were run on a 1% agarose gel. mRNA was obtained by expressing constructs using the RiboMAX™ large scale RNA production system and products run on an agarose gel. For the initial expression experiment (left panel lanes 5 and 6 of figure 3.6) the standard protocol was used with 500 ng of template consisting of PCR products of *plsB* and *plsC*. The expression was at 37 °C for 3 h. For optimization of *plsB* mRNA expression the standard protocol with the following modifications was used: Lane 2 - normal, 500 ng PCR, lane 3 - expression at 30 °C, 500 ng PCR, Lane 4 - 3 × amount of NTPs, 500 ng PCR, lane 5 - plasmid, 500 ng plasmid. For protein expression *in vitro* transcription and translation the yields of produced full-length protein were compared by including FluoroTect™ Green Lysine in the PURE Express system. The complete reaction assembly is shown in table 3.1.

3.2.8. EDTA

An experiment was performed using the standard liquid chromatography-mass spectrometry (LC-MS) technique with four different solvents used for sample preparation,

with 5 μM of LPA and DPPA along with 0.2 mg/ml of 50.8:35.6:11.5:2.1 mol. % DOPC, DOPE, DOPG, cardiolipin liposomes. The solvents were the following:

- Methanol containing 2 mM of acetylacetone was mixed with PURE Buffer to have a composition of 90% methanol, 10% PURE Buffer.
- 100% methanol containing 2mM of acetylacetone.
- Methanol containing 2 mM of acetylacetone was mixed with of PURE Buffer to have a composition of 90% methanol, 10% PURE Buffer and in addition 25 μM $FeCl_3$ was added.
- Methanol containing 2 mM of acetylacetone was mixed with of PURE Buffer to have a composition of 90% methanol, 10% PURE Buffer and in addition 5 mM EDTA was added.

3.3. LABORATORY TECHNIQUES

This section of the thesis includes some details of important techniques used in the laboratory that were newly developed. It is not an exhaustive description of techniques developed but rather a guide to inform future students through difficult procedures not part of the common knowledge of the Christophe Danelon lab at Bionanoscience in Delft.

3.3.1. LIQUID CHROMATOGRAPHY-MASS SPECTROMTRY

This section contains details on liquid chromatography mass spectrometry methods developed for the results of this chapter and chapters 2 and 4.

SAMPLE PREPARATION

The reaction mixture contains liposomes with proteins and other components of the PURE system along with the DNA templates coding for the lipid synthesizing enzymes, mRNA, the enzymes themselves, other additives, substrates and products. We used the simplest sample preparation approach, which was to dilute the sample with 100 % methanol containing 2 mM acetylacetone (see section 3.3.1). Methanol is less polar than water, it therefore disrupts the electrostatic screening of electrostatic forces between molecules, which causes proteins and nucleic acids to precipitate. The precipitates were then removed by centrifugation. The lipids being less polar and charged than DNA and protein remain in solution, and they can be injected into the mass spectrometer.

LIQUID CHROMATOGRAPHY METHOD

In all experiments 5 μl samples were injected into a liquid chromatography system (Agilent 1260) equipped with a XSELECT HSS T3 2.5μm analytical column. This column consists of C18 carbon chains bound to a high strength silica beads. As such the beads are very hydrophobic, and in an hydrophilic solvent, lipids will tend to bind the to column whereas in a hydrophobic solvent they will elute. The sample was thus initially injected in methanol (intermediate hydrophilicity) and pushed into the column in a relatively hydrophilic solvent (mobile phase A) which allows the lipids to bind the column. Then

Time (m)	Solvent A (60% Acetonitrile)	Solvent B (90% Isopropanol)
0	100%	0%
1	90%	10%
1.5	35%	65%
10	30%	70%
11	5%	95%
11.5	3%	97%
12	100%	0%
15.5	stop	stop

Table 3.2: The gradient used to separate lipids by liquid chromatography. Solvent B is more hydrophobic than solvent A, and thus the gradient moves from hydrophilic to hydrophobic during course of the method. Most of the lipids elute between 35% solvent A and 30% solvent A, that is why the slowest rate of change of the solvents occurs between 1.5 and 10 min.

a gradient was applied to a more hydrophobic solvent (mobile phase B), which elutes the various compounds sequentially. The exact scheduling of the solvent composition is based on a method developed in another lab [7][8], and is given in table 3.2. The specific composition of mobile phase A consisted of 60% acetonitrile, 40% deionized water, 7 mM ammonium formate 0.0114% formic acid and 2 mM acetylacetone. The mobile phase B was 90% isopropanol, 10% acetonitrile 0.0378% formic acid and 2 mM acetylacetone. The reason for the acetylacetone is that it binds metal ions. It is hypothesized that metals ions caused peak broadening for lysophosphatidic acid (LPA) and phosphatidic acid (PA) which was due to interactions between the metal ions and the phosphate group of the lipids and the analytical column [9]. The acetylacetone was also included in the sample and in later experiments, so was EDTA. EDTA served a similar purpose as to the acetylacetone (see section 3.1.7). An important consideration is that EDTA, being hydrophilic, will not bind the column and should not be allowed to enter the ion source as it may corrode it. Therefore the first minute of the column eluent was put to waste instead of the MS.

MASS SPECTROMETRY METHOD

The basic operation principles of the mass spectrometry operating in multiple reaction monitoring (MRM) mode are as follows. A diagram of a triple quadrapole setup with important components is shown in figure 3.9. The eluent from the liquid chromatography is sprayed from a nebulizer which forms small droplets with the aid of a nebulizing gas flow. The nebulizer is at ground, and a capillary is at a positive potential (in negative mode) which ionizes the droplets. The droplets break and the solvent evaporates aided by the flow of heated nitrogen drying gas until which single ions are formed. The droplets and eventually ions are simultaneously drawn towards the capillary by the electric field. They then pass through the capillary. After exiting the capillary, there is a voltage which helps to draw the ions into the skimmer. This is called the *Fragmentor Voltage*. The skimmer is an octapole ion guide which keeps the ion beam focused until it enters the first quadrapole. The first quadrapole acts as an ion filter. Two of the rods are at negative po-

tential and two of the rods are positive potential. There is also an AC (radio frequency) voltage applied to the rods with the positive rods being 180 degrees out of phase with the negative rods. The combined effect is that the ions travel in a spiral path, whose exact trajectory depends on both the mass to charge (m/z) ratio of the ions, and the voltages applied. As such the first quadrupole analyser can be set to pass only ions of a given m/z. In MRM mode, the first quadrapole looks at specific (m/z) ratios for a specified dwell time. For instance it can look at the mass to charge ratio of corresponding to DOPE (742.5) and DOPG (773.5) for 100 ms each. After these ions are filtered they are passed into a collision cell. In addition to focusing the ions with a hexapole (though it is referred to as second quadrapole), there are two potentials across the cell. The *Cell Accelerator Voltage* which is constantly applied and clears the cell of all ions, and the *Collision Energy* (in eV), which is an additional voltage which also accelerates the ions but is only present temporarily. There is also nitrogen in the collision cell, as the speed of the molecules increases due the the collision energy, the ions collide energetically with the gas and fragment into smaller ions. These fragments then pass into a third quadrapole which operates with the same principles as the first. It also timeshares for fragment ions of various m/z, for instance the intact DPPA ion (647.5) fragments in multiple possible ways including an ion of 152.9 (m/z), an ion of 255.1 (m/z) and an ion of 391.1 (m/z). The ions are then collided with a dynode which produces electrons that are then collided with an electron multiplier and then detected. The term multiple reaction monitoring (MRM) mode refers to the fact that the first and second quadrapole are continuously switching between monitoring specific combinations of intact and fragment ions, which allows for

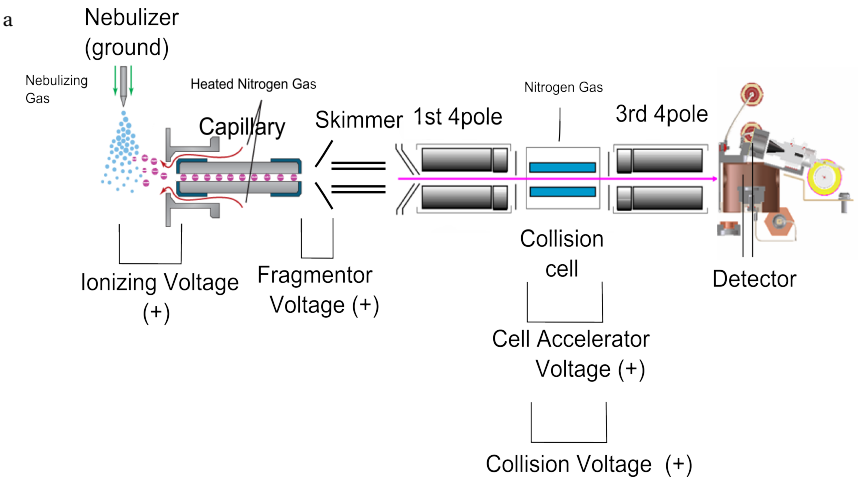

Figure 3.9: | Diagram of Mass Spectrometer.
A diagram of a triple quadrapole mass spectrometer showing important features. Of primary importance are the first quadrapole, the collision cell and the third quadrapole. The first quadrapole filters intact ions based on m/z ratio, the collision cell fragments them and the third quadrapole filters the the fragments again based on the m/z ratio. Also indicated are the locations of the fragmentor voltage, cell accelerator voltage, and collision voltage (also called collision energy and measured in eV) which are optimized by the Agilent optimizer for the various lipids studied. Adapted from the Agilent QQQ Concepts Guide.

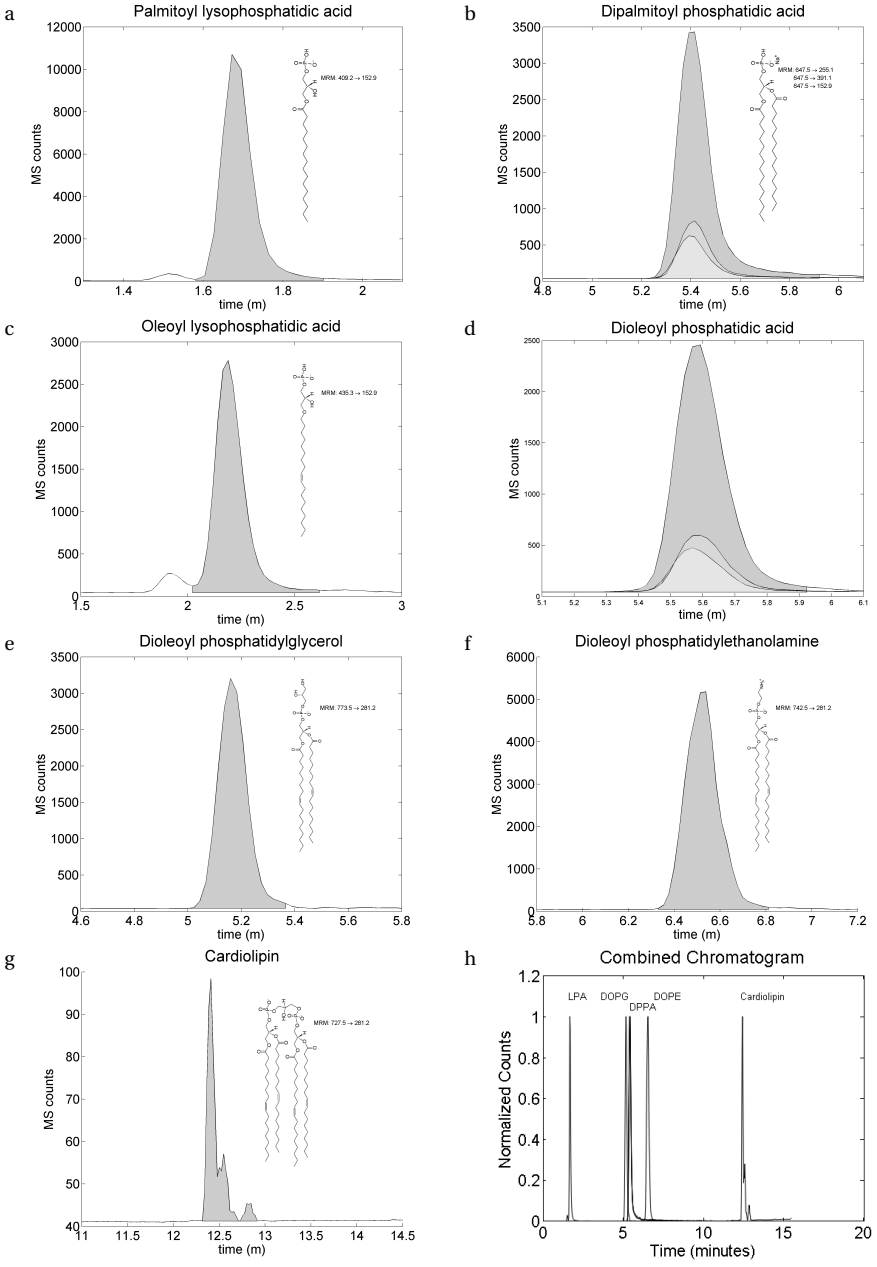

Figure 3.10: | Lipid chromatograms of liquid chromatography mass spectrometry method.
(a-g) Chromatograms of various lipid species detected in chapter 2 via mass spectrometry in MRM mode. Highlighted areas are used to calculate the total integrated counts. (h) A complete normalized chromatogram from a typical experiment with the species LPA, DOPG, DPPA, DOPE, and cardiolipin elute sequentially.

the sensitive detection of multiple species.

Compound Name	LPA(16:0)	PA(16:0/16:0)	PA(16:0/16:0)	PA(16:0/16:0)
Formula	C19H39O7P	C35H69O8P	C35H69O8P	C35H69O8P
Mass (Da)	410.24	648.47	648.47	648.47
Precursor (m/z)	409.2	647.5	647.5	647.5
Product (m/z)	152.9	152.9	255.1	391.1
Fragmentor (V)	100	210	210	210
Cell Acc. (V)	7	7	7	7
Collision (eV)	13	33	29	17
Abundance	4236	2219	13222	3156
Polarity	Negative	Negative	Negative	Negative

Table 3.3: Mass spectrometer settings for MRM transitions of 16:0 LPA and 16:0/16:0 PA.

Compound Name	PE(18:1/18:1)	PG(18:1/18:1)	CL(1'[18:1/18:1],3'[18:1/18:1])
Formula	C41H78NO8P	C42H79O10P	C81H150O17P2
Mass (Da)	743.55	774.54	1457
Precursor (m/z)	742.5	773.5	727.5
Product (m/z)	281.2	281.2	281.2
Fragmentor (V)	140	190	140
Cell Acc. (V)	7	7	7
Collision (eV)	25	37	29
Abundance	N/A	9597	7282K
Polarity	Negative	Negative	Negative

Table 3.4: Mass spectrometer settings for MRM transitions of DOPE, DOPG, and Cardiolipin.

Compound Name	LPA(18:1)	PA(18:1/18:1)	PA(18:1/18:1)	PA(18:1/18:1)
Formula	C21H41O7P	C39H73O8P	C39H73O8P	C39H73O8P
Mass (Da)	436.26	700.5	700.5	700.5
Precursor (m/z)	435.3	699.5	699.5	699.5
Product (m/z)	152.9	281.2	153	417.2
Fragmentor (V)	160	190	190	190
Cell Acc. (V)	7	7	7	7
Collision (eV)	17	37	37	17
Abundance	38003	40466	6838	9599
Polarity	Negative	Negative	Negative	Negative

Table 3.5: Mass spectrometer settings for MRM transitions of 18:1 LPA and 18:1/18:1 PA.

To be able to measure the lipids eluting from the liquid chromatography step, the instrument must have its settings tuned to optimize the signal of the various intact ions

and fragment ions. Specifically it adjusts the Fragmentor Voltage, Cell Accelerator Voltage and Collision Energy (eV). This process is performed automatically by Agilent software when it is told which specific intact ion to search for. The results for all ions detected in chapter 2 are listed in tables 3.3, 3.4, and 3.5 . A completed MRM method, then timeshares between various ions of interest adjusting all settings to look at intact and fragment ions corresponding to a given compound. Chromatograms of those ions are given in figure 3.10 a-g. Figure 3.10 h is an example of a chromatogram obtained during a typical experiment with a completed MRM method. Lipids LPA, DOPG, DPPA, DOPE and cardiolipin elute from the column sequentially and are detected by the mass spectrometer.

3.3.2. LIPID HANDLING

Here we provide a guide to handling of the lipids used in this thesis to facilitate future experiments.

DOPC, DOPG, DOPE, cardiolipin and other glycerophosphoplipids

Lipids used for forming liposomes are purchased from Avanti Polar Lipids in chloroform. They include but are not limited to dioleoylphosphatidylcholine, dioleoylphosphatidylglycerol, dioleoylphosphatidylethanolamine and cardiolipin. These lipids come in a glass ampule of which the neck must be broken. The lipids are thus first aliquoted into glass vials with a PTFE lined lid (Sigma 27134 Vials, 2mL - PTFE lined cap) using Hamilton syringes rinsed 5 × in chloroform and the outside of the needle washed with ethanol (and dried). This ensures that the lipids are not contaminated. Lipids are either dried under argon flow and stored under argon and marked with mass to be redissolved in chloroform at a later date, or otherwise stored in chloroform *without* storing under argon to prevent evaporation and concentration changes. Vials are stored at -20 °C with Parafilm around the lid. For experiments, lipid volumes are measured with Gilson Microman pipettes using capillary pistons, which ensures accurate pipetting of volatile solvents and therefore lipid quantities. It may be that the plastic tips leach compounds into the chloroform, though if so, we have not found that to interfere with experiments.

Palmitoyl-CoA and oleoyl-CoA

These fatty acid CoAs are purchased from Avanti Polar Lipids in powder form. To measure specific amounts of lipid the following procedure is used. The known mass of fatty acyl CoA is first dissolved in a known amount of solvent giving a known concentration. Avanti reports that the total amount of fatty acyl CoA may be greater than the amount indicated by as much as 10%, so there is immediate uncertainty in the actual quantity of lipids. The lipids readily dissolve in a mixture of Chloroform:Methanol:Water in an 80:20:2 ratio. The *miscibility of these solvents depends quite sensitively on the ratio* so normally an amount of 20 ml is made for accuracy in measuring of solvents. Hamilton syringes, rinsed first in chloroform and then 80:20:2 C:M:W, then rinsed on the outside with ethanol (and dried), are used to measure quantities of 80:20:2 C:M:W to dissolve the lipids. Amounts are then measured by volume into the same glass vials as above. The solvent is then evaporated in bell jar glass desiccator overnight with an open valve to allow solvent to evaporate. The desiccator is *not put under vacuum.* If so, some of the

dried lipids in powder form will become airborne and the *accuracy of quantities will be lost*. The same can be said for using argon flows. Vials are stored at -20 °C with parafilm to ensure sealing of the vials. Before use the fatty acyl CoAs are redissolved in 80:20:2 C:M:W with Gilson Microman pipettes as above.

Palmitoyl LPA and dipalmitoyl PA

These lipids are purchased from Avanti Polar Lipids in powder form. To measure the amount of CoA, they are first dissolved in a known amount of solvent giving a known concentration. Avanti reports that the total amount of lipid may be greater than the amount indicated by as much as 10%. The lipids dissolve rather poorly in a mixture Chloroform:Methanol:Water in a ratio of 65:35:8. Ammonium hydroxide can be added to improve solubility but it also degrades the lipids and may effect the pH of solutions downstream. To allow the LPA and particularly the DPPA to dissolve, although Avanti suggests that concentrations of 10 mg/ml can be obtained, we found that it was better not to use concentrations above 1 mg/ml. The remaining procedures are the same as above as for palmitoyl CoA and oleoyl CoA except with 65:35:8 C:M:W as a solvent.

Oleoyl LPA and dioleoyl PA

Due to the unsaturation of fatty acid tails these simple phospholipids readily dissolve in chloroform. They are thus purchased from Avanti Polar Lipids dissolved in chloroform, and handled as DOPC, DOPE etc.

REFERENCES

[1] W. O. Wilkison, J. P. Walsh, J. M. Corless, and R. M. Bell, "Crystalline arrays of the escherichia coli sn-glycerol-3-phosphate acyltransferase, an integral membrane protein," *The Journal of Biological Chemistry*, vol. 251, no. 21, pp. 9951–9968, 1986.

[2] P. P. Constantinides and J. M. Steim, "Solubility of palmitoyl-coenzyme a in acyltransferase assay buffers containing magnesium ions," *Archives of biochemistry and biophysics*, vol. 250, no. 1, pp. 267–270, 1986.

[3] Y. Kuruma, P. Stano, T. Ueda, and P. L. Luisi, "A synthetic biology approach to the construction of membrane proteins in a semi-synthetic minimal cells," *Biochimica et Biophysica Acta*, vol. 1788, pp. 567–574, 2009.

[4] P. R. Green, A. H. Merril, and R. M. Bell, "Membrane phospholipid synthesis in escherichia coli purification, reconstitution, and characterization of sn-glycerol-3-phosphate acyltransferase," *The Journal of Biological Chemistry*, vol. 256, no. 21, pp. 11 151–11 159, 1981.

[5] W. Wilkison and R. Bell, "sn-glycerol-3-phosphate acyltransferase tubule formation is dependent upon heat shock proteins (htpr)." *Journal of Biological Chemistry*, vol. 263, no. 28, pp. 14 505–14 510, 1988.

[6] Y. Shimizu, T. Kanamori, and T. Ueda, "Protein synthesis by pure translation systems," *Methods*, vol. 36, no. 3, pp. 299–304, 2005.

[7] G. Astarita, J. H. McKenzie, B. Wang, K. Strassburg, A. Doneanu, J. Johnson, A. Baker, T. Hankemeier, J. Murphy, R. J. Vreeken *et al.*, "A protective lipidomic biosignature associated with a balanced omega-6/omega-3 ratio in fat-1 transgenic mice," *PloS one*, vol. 9, no. 4, p. e96221, 2014.

[8] V. Gonzalez-Covarrubias, M. Beekman, H.-W. Uh, A. Dane, J. Troost, I. Paliukhovich, F. M. Kloet, J. Houwing-Duistermaat, R. J. Vreeken, T. Hankemeier *et al.*, "Lipidomics of familial longevity," *Aging Cell*, vol. 12, no. 3, pp. 426–434, 2013.

[9] D. Siegel, H. Permentier, and R. Bischoff, "Controlling detrimental effects of metal cations in the quantification of energy metabolites via ultrahigh pressure-liquid chromatography–electrospray-tandem mass spectrometry by employing acetylacetone as a volatile eluent modifier," *Journal of Chromatography A*, vol. 1294, pp. 87–97, 2013.

4

HEADGROUP MODIFYING ENZYMES

Here we extend the in vitro lipid biosynthesis from the acyltransferases presented in chapter 2 to six new phospholipid headgroup modifying enzymes. These enzymes are those responsible in E. coli for the synthesis of 5 new lipids from phosphatidic acid, and other precursors. The end products of the two pathways reconstituted are phosphatidyl glycerol and phosphatidyl ethanolamine. In this chapter we briefly describe what is known about the six enzymes from literature. We then proceed to demonstrate that we were able to synthesize these enzymes in the PURE system, and measure their activity by LC-MS.

4.1. INTRODUCTION

To achieve growth of liposomes and eventually minimal cells, it is necessary that the lipids produced are able to sustain the functions of the cell boundary. Besides complex functions such as facilitating division and transport of molecules the most basic function required of the cellular lipid membrane is the ability to form stable bilayers. There is not much in the literature on the subject of forming vesicles with lysophosphatidic acid or phosphatidic acid, which suggests that they are not good at forming bilayers. If one considers the ratio of the diameter of the headgroup to the diameter of the tail (or tails) of the lipids then lysolipids have values greater than one (relatively large headgroups) and phosphatidic acids have values less than one (relatively large tails). It can be considered that the farther this ratio is from 1, the harder it will be to form stable bilayers due to the inability to pack in a flat sheet (for phosphatidylcholine, which is most frequently used to form bilayers, the value is close to 1). As such modifying the PA produced in our vesicle system so that it has a larger headgroup, will help it form stable bilayers. It is widely reported that the composition of *E. coli* membranes is approximately 80% diacylphosphatidylethanolamine (XXPE) and 20% diacylphosphatidylglycerol (XXPG) with a small fraction of cardiolipin [1] [2] [3]. Therefore it is natural to pursue making XXPE and XXPG in the *E. coli* based PURE system and as such they were our initial targets for synthesis. The enzymes required for the synthesis of XXPE and XXPG from phosphatidic acid are shown in figure 4.1

4.1.1. DETAILS OF SYNTHESIS PATHWAY

CDSA

The first reaction of the pathway for the synthesis of XXPE and XXPG is where a phosphatidic acid, cytosine tri-phosphate (CTP) and a proton react to form cytosine di-phosphate-diacyl glycerol with the release of diphosphate. This reaction is performed by the gene product of cdsA (phosphatidate cytidylyltransferase). The molecular weight of the protein as predicted by the nucleotide sequence is 31 kDa and the previously observed molecular weight is 27kDa. Sequence analysis predicts eight transmembrane helices [4] and databases list it as localized to the inner membrane of *E. coli* [4]

PSSA

The first committed step of synthesizing XXPE from phosphatdic acid is the formation of phosphatidylserine. The gene product of pssA (diacylphosphatidylserine synthase) ligates L-serine to CDP diacylglycerol via a ping pong reaction mechanism releasing CMP and a proton [5] [6]. The enzyme does so without a requirement for divalent metal ions [6]. It was originally thought that the enzyme was ribosome associated (both 30S and 50S) [5]). It was later discovered however that the association may have been an artifact of cell purification as physiological levels of polyamines prevented ribosome association [7]. PssA is now considered to be a peripheral membrane protein that associates with membranes via its lipid substrate and may spend time membrane-bound as well as free in the cytoplasm [6]. The predicted molecular weight from the nucleotide sequence is 52 kDa [8].

a

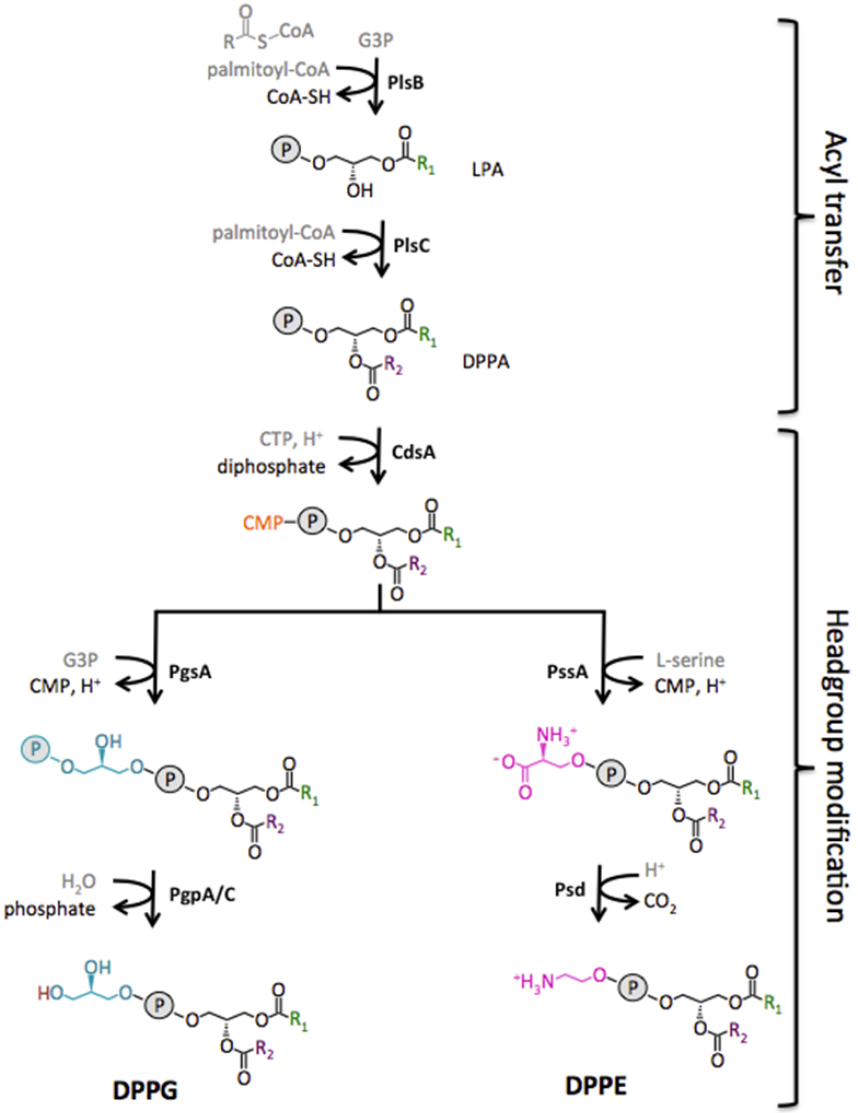

Figure 4.1: | Glycerophospholipid headgroup modification enzyme pathways.
The pathways for synthesizing XXPE and XXPG from phosphatidic acid consist of five reactions each. The reactions are catalyzed by enzymes which are the products of the genes listed in the figure. For the final step of synthesis of XXPG there are three alternative enzymes: pgpA, pgpB, and pgpC, two of which (A/C) were studied here.

PSD

The final step in the formation of XXPE is the decarboxylation of phosphatidylserine by the gene product of psd (phosphatidylserine decarboxylase). In this reaction dia-

cylphosphatidylserine (XXPS) and a proton react and diacylphosphatidylethanolamine and carbon dioxide are released. The enzyme itself is a heterodimer, produced from a single polypetide which cleaves itself postranslationally [9] [10]. Phosphatidylserine decarboxylase is located at the inner membrane[11] [12]. The predicted molecular weight from the nucleotide sequence is 35 kD [13].

PGSA

The first committed step of synthesizing XXPG from phosphatidic acid is the formation of phosphatidylglycerolphosphate. The gene product of pgsA (phosphatidylglycerophosphate synthase) accepts CDP diacylglycerol and ligates *sn*-glycerol-3-phosphate to it releasing diacylphosphatidyl glycerol phosphate, CMP and a proton. It is an integral membrane protein [6] located at the inner membrane [10]. The enzyme has an absolute requirement for magnesium to function [14]. The predicted molecular weight from the nucleotide sequence is 20 kDa. [15]

PGPA, PGPC (PGPB)

The final step in the formation of XXPG is the dephosphorylation of diacylphosphatidylglycerol phosphate (PGP) to diacylphosphatidylglycerol (XXPG). There are three enzymes (phosphatidylglycerolphosphatases) which can perform the hydrolysis reaction and they are the products of *pgpA*, *pgpB* and *pgpC* genes. PgpA and pgpB act on several phospholipids including PA, lyso-PA and PGP [16]. PgpA contains a single transmembrane segment and an active site that faces the cytoplasm [17]. PgpB was originally thought to be an outer membrane phosphatase, but more recent results indicate an inner membrane location [18]. PgpC is predicted to have a single transmembrane domain with its active site facing the cytoplasm [17]. Overexpression of pgpA caused primarily PGP phosphatase activity [19], while overexpression of pgpB caused phosphatase activity toward all three substrates with a relativity small PGP phosphatase activity [20] [21] and pgpC had activity specific to PGP [17] [16]. The molecular weight of pgpA from sequence analysis is 19kD [22], that of pgpB is 29 kD [23], while from experiment it is 28 kD [24], and that of pgpC from sequence prediction is 24.439 kD [25].

To our knowledge we are the first to attempt to express and study the complete synthesis pathway for XXPE and XXPG in an *in vitro* synthesis reaction. There are previous works with some similarity, such as an early work where phosphatidylcholine (PC) was produced from rat microsomes solubilized with lysophosphatidyl choline and oleoyl-CoA and containing l-acyl-sn-glycero-3-phos-phorylcholine acyltransferase, which produced membrane from the solubilizing lysosphosphatitdyl choline and oleoyl CoA [26]. Later phosphatidylcholine producing PC vesicles were made from purified proteins (glycerol 3 phoshate acyltransferase, lysophosphatidic acid acyltransferase, phosphatidate phosphatase and cytidinediphosphocholine phosphocholinetransferase) from pig liver reconstituted in phosphatidylcholine vesicles [27]. These works focused on phosphatidylcholine with purified proteins. Here, we show that we can produce the membrane-forming lipids XXPG and XXPE as well as there intermediates from *in vitro* synthesized proteins.

4.2. RESULTS

Initially we expressed the proteins in an *in vitro* transcription translation reaction in the presence of FluoroTect™ Green Lysine (BODIPY labeled lysine tRNA) and observed the produced protein products on an SDS page gel. Figure 4.2 a shows the expression of six proteins (pgpA, pgpC, pgsA, cdsA, pssA, psd) and controls (pssA, plsB) from the genes indicated in the figure. The gel on the left is a 15% polyacrylamide gel for identifying the smaller proteins, and the other gel is a 12% polyacrylamide. The red arrows indicate the expected molecular weight of the proteins either from sequence information or from experiment (see section 4.1). These results show that the constructs (see methods, section 4.4) are capable of expressing a polypeptide of, or close to, the expected molecular weight.

We then immediately attempted to measure the activity of the six proteins by liquid chromatography mass spectrometry (LC-MS). In order to do so it was necessary to develop multiple reaction monitoring transitions, whereby the molecules of interest are selected for in a quadrapole mass filter, fragmented into smaller molecules, and then these molecules filtered in another mass filter and finally detected. For enzyme activity we used palmitoyl CoA, glycerol-3-phosphate (G3P), cytidine tri-phosphate (CTP) and L-serine as substrates and expressed all enzymes in the pathway up to the one producing the molecule of interest. This was done in the presence of liposomes. We were able to detect dipalmitoyl phosphatidylglycerol (DPPG, *plsB-plsC-cdsA-pgsA-pgpA/C*), dipalmitoyl phosphtidylethanolamine (DPPE, *plsB-plsC-cdsA-pssA-psd*) and dipalmitoyl phosphatidylserine (*plsB-plsC-cdsA-pssA-psd*). As we did not have standards available to use to develop transitions, they were developed by first injecting the complex sample mixture into a column and eluting the lipids with the same liquid chromatography method as discussed in chapter 3. The details of the transitions are indicated table 4.1.

Compound Name	16:0/16:0 PG (pgpA)	16:0/16:0 PG (pgpC)	16:0/16:0 PE (psd)	16:0/16:0 PS (pssA)
Formula	C38H75O10P	C38H75O10P	C37H74NO8P	C38H74NO10P
Mass (Da)	722.51	722.51	691.52	735.51
Precursor (m/z)	721.5	721.5	690.5	734.5
Product (m/z)	255.2	255.3	255.1	255.1
Fragmentator (V)	220	70	230	180
Collision (eV)	45	45	37	41
Cell Acc.(V) .	4	4	4	4
Abundance	3233	1667	1231	645
Polarity	Negative	Negative	Negative	Negative

Table 4.1: | MRM transitions of DPPG and DPPE.
Details of DPPG and DPPE MRM transitions developed with Agilent optimizer. Two instances of DPPG were due to the use of pgpA and pgpC, to make the lipid, though the transition settings found for pgpA were also more effective for pgpC.

Already from using the developing the multiple reaction monitoring transitions to detect dipalmitoyl phoshatidylglycerol (DPPG), dipalmitoyl phosphatidylethanoamine (DPPE) and dipalmitoyl phosphatidylserine (DPPS), we knew we could make these mole-

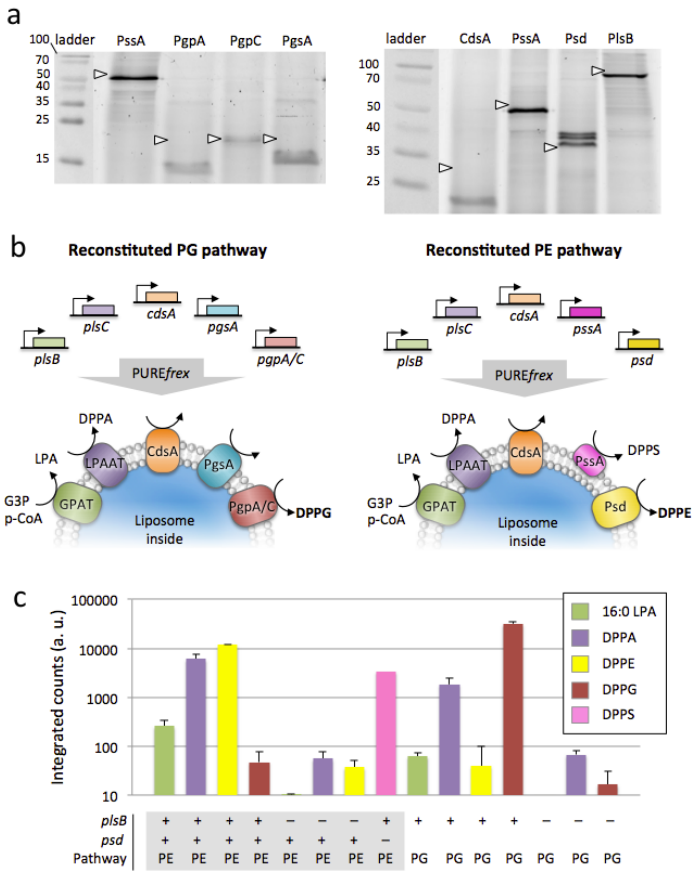

Figure 4.2: | Functional reconstitution of complete biosynthesis pathways for PE and PG lipids.
(a) Fluorescence scans of SDS-PAGE gels for the headgroup modifying enzymes produced in the PURE system. Fluorescently labeled lysine residues were incorporated during translation. The left gel is 15% polyacrylamide. In addition to the *pssA* gene product that was used as a control, the gene products of *pgpA*, *pgpC* and *pgsA* were synthesized. The right gel is 12% polyacrylamide and, besides the *plsB* gene product used as a control, the genes *cdsA*, *pssA* and *psd* were expressed. Size markers are in kDa. The arrowheads point to the protein molecular mass as expected from the nucleotide sequence of the genes. (b) Schematic of the inside-out proteoliposome reconstitution experiments and enzymatic cascade reactions, where all genes of a given pathway were expressed in PURE*frex* and all specific substrates were supplied. (c) LC-MS data reporting lipid production in the PE and PG pathways under various experimental conditions. Combined gene expression and lipid biogenesis was carried out as illustrated in (b) using 25 ng of each linear DNA templates, 500 μM G3P, 100 μM palmitoyl-CoA, 1 mM CTP and 500 μM L-serine. Details of MS signatures for the different lipids are reported in table 4.2. Lipids DPPE and DPPG were unambiguously detected in a pathway-specific manner. No PG is produced in the reconstituted PE pathway. Likewise, no PE was detected in the PG pathway. When the *plsB* gene is omitted the complete pathways are shut down. In the absence of the psd enzyme, PE was not detected and its substrate lipid DPPS accumulated. Note that the MRM data for PS come from the MS optimizer results, not from separate experiments as used for the other compounds. Data are mean and s.e.m. of three independent experiments, except for the negative controls without *plsB* gene where two independent experiments were conducted. For each replicate the same sample was injected between one and four times in the MS, their averaged value was calculated and data are reported as the mean and standard error across the different trials.

cules via *in vitro* synthesized proteins in the PURE system. The presence of these lipids implied the functioning of all enzymes, including both variants of pgpA/C (see separate column for pgpA and pgpC in table 4.1). To confirm the activity of the enzymes we measured again with the complete LC-MS method described below and performed two additional repeats that validated the synthesis of DPPE and DPPG. For these experiments with increased number of lipids we used a dynamic MRM method, details of which can be found in methods, section 4.4. Figure 4.2 c shows the result of mass spectrometry measurements for: the complete pathway of DPPE (column 1-4), the DPPE pathway with GPAT removed (column 5-7), the DPPE pathway with psd removed (column 8) the complete DPPG pathway (column 9-12) and the DPPG pathway with GPAT removed (column 13-15). DPPG and DPPE synthesis is confirmed by three repeats and the negative controls by two repeats which indicates unambiguously the functionality of the complete pathways. In addition, figure 4.2 c, column 8, shows that it was possible to detect phosphatidylserine (as shown in table 4.1).

An attempt to achieve a larger percentage increase in liposome size was made by reducing the vesicle concentration. In this additional experiment, 0.04 mg/ml (47 μM of lipids) DOPG/DOPE/cardiolipin liposomes with composition of 54.5:35.6:10 mol % were included in a one-pot reaction with all the enzymes for the synthesis of DOPG and DOPE expressed (plsB, plsC, cdsA, pgsA, pgpA, pssA, psd). This was done in the presence of 500 μM L-Serine, 500 μM G3P, 1 mM CTP (additional to that in PURE system) and 100 μM oleoyl CoA. There was not significant synthesis of DOPG or DOPE over the control samples which could be either due to: few proteins successfully incorporated in proteoliposomes at low liposome concentration, or liposomes disrupted by oleoyl CoA acting as surfactant. It was however found that 100 μM of p-CoA with 100 μM of lipids in the form of 400-nm liposomes did not affect the liposome size distribution as measured by light scattering. Further experiments will be required to achieve true autopoesis and growth of liposomes.

4.3. DISCUSSION

Here we show that in addition to lysophosphatidic acid and phosphatidic acid we can make phospholipid headgroup-modifying enzymes. We focus here on making phosphatidylglycerol and phosphatidylethanolamine which together make the largest fraction of the *E. coli* lipidome. Due to the astonishing ability of the PURE system to synthesize functional membrane proteins, we predict that in the future it will be possible to synthesize other lipids. Examples include phosphatidylcholine, which can be made from phosphatidylethanolamine with a single enzyme from *Rhodobacter sphaeroides* [28] and cardiolipin which can be made from phosphatidylglycerol with cardiolipin synthase A or B and from phosphatidylethanolamine and phosphatidylglycerol combined with cardiolipin synthase C [29]. Since it is now possible to synthesize lipids forming stable liposomes the obvious immediate goal is to obtain growth of liposomes that are truly self reproducing (with respect to the lipids, if not yet the entire content of the minimal cell). We already attempted this by measuring an increase of DOPG and DOPE and though we encountered difficulties in preliminary experiments, we maintain it will be possible with our system. It may be an obstacle that the fatty acyl CoA lipid precursors may act as a surfactant when overloaded in the membrane, or it may simply be that the protein in-

corporation efficiency at low vesicle concentration is the obstacle. Alternatively to measuring a total increase in the amount of lipids, there are other methods to detect growth. These include using C13 labeled oleoyl CoA which would separate orthogonally newly synthesized lipids from existing lipids, or the commonly used FRET assay for fatty acid vesicle growth [30]. Eventually it may be necessary to synthesize fatty acids from more hydrophilic components by expressing the complete *E. coli* fatty acid synthesis pathway a project which is being pursued in the lab of Yutetsu Kuruma (Tokyo). It may also be that acyl carrier proteins (ACPs) are more water soluble than acyl CoAs and act less as a surfactant. Eventually the ability to synthesize a variety of lipids may prove useful in achieving the complex functions for a minimal cell, for example division [31]. This is discussed further in chapter 6.

4.4. METHODS

4.4.1. EXPRESSION OF PROTEINS AND SDS GELS

PURE*frex* reactions were assembled with 10 ng/μl of coding template (as indicated in figure 4.2 a), 0.5 U/μl Superase RNAse inhibitor with 20 × dilution of FluoroTect™ Green Lysine tRNA in 10 μl of total volume. Reactions were incubated at 37 °C for three hours. For the left panel of figure 4.2 a samples had 1 μl of RQ1 DNAse and RNAse One added and were then incubated for an additional hour to digest background of Green Lysine tRNA. Samples were then incubated at 60 °C for 10 min with SDS loading dye, run on a 15 % or 12 % SDS polyacrylamide gel with 37.5:1 ratio of acrylamide:bis acrylamide and imaged on a Typhoon fluorescent gel scanner (Amersham Biosciences) with BODIPY-FL settings.

4.4.2. MRM METHOD DEVELOPMENT

To develop the MRM transitions it was necessary to directly attempt the activity assays since presynthesized standards were not available for all compounds of interest. PURE*frex* reactions were assembled as above except that for each reaction the pathway was truncated at the molecule of interest. E.g. the phosphatidylserine reaction had genes: plsB, plsC, cdsA, pssA. The LC method of chapter 3 was run in the Agilent optimizer software which automatically searched for the settings for the compounds of interest. To do that it requires the molecular weight of the intact neutral molecules. The optimal settings of the parameters are given in table 4.1, the meaning of which are discussed in chapter 3. It was possible to detect DPPG, DPPE, and DPPS, which all flew in the MS as singly charged species. It was not possible to detect the intermediates CDP-dipalmitoylglyerol diphosphate or dipalmitoyl phosphatidylglycerol phosphate as singly charged species with the masses we predicted, though it may be possible if the correct charge state can be obtained from a complete scan of the m/z (mass to charge) ratios below 1000 m/z.

4.4.3. SYNTHESIS OF DPPG,DPPE

SYNTHESIS AND ACTIVITY OF PROTEINS

PURE*frex* reactions were assembled with standard components and in addition 0.4U/μl Superase RNAse inhibitor, 500 μM L-Serine, 500 μM G3P and 1mM CTP (extra) and 0.4

mg/ml of 400-nm liposomes (composition: DOPC, DOPG, DOPE, cardiolipin 50.8, 35.6, 11.5, 2.1 mol.%). Genes for the pathways of DPPG synthesis (*plsB*, *plsC*, *cdsA*, *pgsA*, *pgpA*) or DPPE synthesis (*plsB*, *plsC*, *cdsA*, *pssA*, *psd*) were included at concentration of 5 ng/μl each. Negative controls were the same pathways without *plsB*. After assembly, but before transfer to 37 °C for incubation, the reactions were added to dried palmitoyl CoA in an Eppendorf 0.2 ml PCR tube for a final concentration of 100 μM. The reactions were incubated overnight at 37 °C. Two repeats of the above experiment were performed with a third repeat of the positive only (the same experiment was used for developing MRM transitions). For liquid chromatography mass spectrometry the method described in chapter 3 was followed, though in addition to the 2 mM acetylacetone 5 mM EDTA was included in methanol to chelate metal ions (also discussed in chapter 3).

For mass spectrometry a dynamic MRM method was used. This differs from the standard MRM method in that the mass spectrometer is set to observe compounds in a scheduled manner. An example of the scheduling is given in table 4.2 and an example of a chromatogram obtained is given in figure 4.3. The peak position was in fact slightly unstable during initial measurements. As such the windows chosen for the compounds were quite wide and the times in the example chromatogram do not correspond directly to those in the method given as an example. The reason for the shift was likely due to problems with the HPLC pump, which caused a change in the pressure profile between injections. This indicates that the solvent composition was varying between injections. The pump has since been repaired and the retention times should be taken as a guideline for future methods.

FORMATION OF GENE PRODUCTS

The constructs of *cdsA*, *pgsA*, *pgpA*, *pgpC*, *pssA*, *psd* were all constructed from *E. coli* MG1655 (K12) genomic DNA which was extracted with GenElute Bacterial Genomic DNA

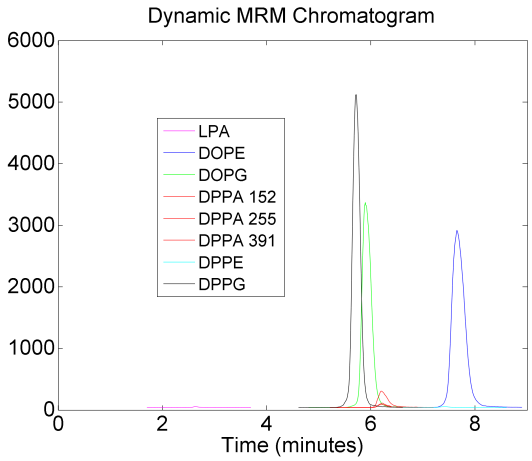

Figure 4.3: | Scheduled dMRM measurement.
A dynamic multiple reaction monitoring measurement (dMRM) that monitors any given compound for a fraction of the total liquid chromatography method.

Compound Name	Precursor Ion	Product Ion	Ret Time (min)	Δ Ret Time
LPA_16-0	409.2	152.9	2.2	3
PA_16-0_16-0	647.5	391.1	5.8	3
PA_16-0_16-0	647.5	255.1	5.8	3
PA_16-0_16-0	647.5	152.9	5.8	3
PE_16-0_16-0	690.5	255.1	6.5	5
PE_18-1_18-1	742.4	281.2	7	5
PG_16-0_16-0A	721.5	255.2	5.4	3
PG_16-0_16-0C	721.5	255.3	5.4	3
PG_18-1_18-1	773.5	281.2	5.6	3
Cardiolipin	727.5	281.2	12.4	2

Table 4.2: Retention times and windows for various lipids detected with dynamic MRM (dMRM) method used in this chapter

Kit (Sigma Aldrich). The genes were cloned into a pET11a backbone by Gibson assembly [32] [33]. For each amplification of a target gene four primers were used. A forward primer with the following regions in the 5'-3' direction: a region overlapping the pET11a sequence and a region overlapping the gene of interest. A reverse primer with the same structure (pET11a homology, gene of interest homology). A set of short primers homologous to part of the pET11a sequences were used to amplify the pET11a vector into a linear fragment to be used in the Gibson assembly. The primers used are listed in table 4.3.

The thus assembled plasmids were then cultured in *E. coli*, and purified with PureYield™ plasma miniprep system. The PCR products used as DNA templates for PURE system reactions were made by amplifying the genes from the pET11a vectors with the following primers:
HG Fwd: 5'-GGATCTCGACGCTCTCCCTTATG-3'
HG Rev: 5'-GATATCCGGATATAGTTCCTCC-3'.

fwd: random-pET11a -EG11371 pgpC
TGGACAGCAAATGGGTCGCGGATCCGGCTGCttgGCAACTCACGAGCGTCG
fwd - pET11a
GCAGCCGGATCCGCG
rev: random-pET11a -EG11371 pgpC
AGCAGCCAACTCAGCTTCCTTTCGGGCTTTGctaTTCCAGTTGCTGGAGTTCACC
rev-pET11a
CAAAGCCCGAAAGGAAGCTGA
fwd: random-pET11a -EG10704 pgpA
TGGACAGCAAATGGGTCGCGGATCCGGCTGCatgACCATTTTGCCACGCCA
fwd - pET11a
(idem) GCAGCCGGATCCGCG
rev: random-pET11a -EG10704 pgpA
AGCAGCCAACTCAGCTTCCTTTCGGGCTTTGctaCGACAGAATACCCAGCGG
rev-pET11a
(idem) CAAAGCCCGAAAGGAAGCTGA
fwd: random-pET11a -EG10706 pgsA
TGGACAGCAAATGGGTCGCGGATCCGGCTGCatgCAATTTAATATCCCTACGTTGCTTACAC
fwd - pET11a
(idem) GCAGCCGGATCCGCG
rev: random-pET11a -EG10706 pgsA
AGCAGCCAACTCAGCTTCCTTTCGGGCTTTGtcaCTGATCAAGCAAATCTGCACGC
rev-pET11a
(idem) CAAAGCCCGAAAGGAAGCTGA
fwd: random-pET11a -EG10775 psd
TGGACAGCAAATGGGTCGCGGATCCGGCTGCttgTTAAATTCATTTAAACTTTCGCTACAGTACATTCTGC
fwd - pET11a
(idem) GCAGCCGGATCCGCG
rev: random-pET11a -EG10775psd
AGCAGCCAACTCAGCTTCCTTTCGGGCTTTGttaGACCTGGTCTTTTTTGTCGTCAACCA
rev-pET11a
(idem) CAAAGCCCGAAAGGAAGCTGA
fwd: random-pET11a -EG110781 pssA
TGGACAGCAAATGGGTCGCGGATCCGGCTGCatgTTGTCAAAATTTAAGCGTAATAAACATCAACAAC
fwd - pET11a
(idem) GCAGCCGGATCCGCG
rev: random-pET11a –EG110781 pssA
rv–EG110781 pssA
AGCAGCCAACTCAGCTTCCTTTCGGGCTTTGttaCAGGATGCGGCTAATTAATCGGT
rev-pET11a
(idem) CAAAGCCCGAAAGGAAGCTGA
fwd: random-pET11a -EG10139 cdsA
TGGACAGCAAATGGGTCGCGGATCCGGCTGCttgCTGAAGTATCGCCTGATATCTGC
fwd - pET11a
(idem) GCAGCCGGATCCGCG
rev: random-pET11a –EG10139 cdsA
AGCAGCCAACTCAGCTTCCTTTCGGGCTTTGttaAAGCGTCCTGAATACCAGTAACAACAAG
rev-pET11a
(idem) CAAAGCCCGAAAGGAAGCTGA

Table 4.3: Primers used for the Gibson assembly of headgroup modifying enzymes.

REFERENCES

[1] W. Dowhan, "Molecular basis for membrane phospholipid diversity: why are there so many lipids?" *Annual Review of Biochemistry*, vol. 66, pp. 199–323, 1997.

[2] D. Oursel, C. Loutelier-Bourhis, N. Orange, S. Chevalier, V. Norris, and C. M. Lange, "Lipid composition of membranes of escherichia coli by liquid chromatography/tandem mass spectrometry using negative electrospray ionization," *Rapid Communications in Mass Spectrometry*, vol. 21, no. 11, pp. 1721–1728, 2007.

[3] S. Furse, H. Wienk, R. Boelens, A. I. de Kroon, and J. A. Killian, "E. coli mg1655 modulates its phospholipid composition through the cell cycle," *FEBS letters*, vol. 589, no. 19, pp. 2726–2730, 2015.

[4] UniProt. (2015) Uniprotkb - p0abg1 (cdsa_ecoli). [Online]. Available: http://www.uniprot.org/uniprot/P0ABG1

[5] C. R. Raetz and E. P. Kennedy, "The association of phosphatidylserine synthetase with ribosomes in extracts of escherichia coli," *Journal of Biological Chemistry*, vol. 247, no. 7, pp. 2008–2014, 1972.

[6] W. Dowhan, "A retrospective: use of escherichia coli as a vehicle to study phospholipid synthesis and function," *Biochimica et Biophysica Acta (BBA)-Molecular and Cell Biology of Lipids*, vol. 1831, no. 3, pp. 471–494, 2013.

[7] K. Louie and W. Dowhan, "Investigations on the association of phosphatidylserine synthase with the ribosomal component from escherichia coli." *Journal of Biological Chemistry*, vol. 255, no. 3, pp. 1124–1127, 1980.

[8] EcoCyc. (2015) Pssa - eg10781. [Online]. Available: http://www.ecocyc.org/ECOLI/NEW-IMAGE?type=GENE&object=EG10781

[9] Q.-X. Li and W. Dowhan, "Structural characterization of escherichia coli phosphatidylserine decarboxylase." *Journal of Biological Chemistry*, vol. 263, no. 23, pp. 11 516–11 522, 1988.

[10] W. Dowhan, "Phosphatidylglycerophosphate synthase from escherichia coli," *Methods in enzymology*, vol. 209, pp. 313–321, 1992.

[11] R. M. Bell, R. D. Mavis, M. Osborn, and P. R. Vagelos, "Enzymes of phospholipid metabolism: localization in the cytoplasmic and outer membrane of the cell envelope of escherichia coli and salmonella typhimurium," *Biochimica et Biophysica Acta (BBA)-Biomembranes*, vol. 249, no. 2, pp. 628–635, 1971.

[12] D. A. White, F. R. Albright, W. Lennarz, and C. A. Schnaitman, "Distribution of phospholipid-synthesizing enzymes in the wall and membrane subfractions of the envelope of escherichia coli," *Biochimica et Biophysica Acta (BBA)-Biomembranes*, vol. 249, no. 2, pp. 636–642, 1971.

[13] EcoCyc. (2015) Psda -eg10775. [Online]. Available: http://www.ecocyc.org/ECOLI/NEW-IMAGE?type=GENE&object=EG10775

[14] T. Hirabayashi, T. J. Larson, and W. Dowhan, "Membrane-associated phosphatidylglycerophosphate synthetase from escherichia coli: purification by substrate affinity chromatography on cytidine 5'- diphospho-1, 2-diacyl-sn-glycerol sepharose," *Biochemistry*, vol. 15, no. 24, pp. 5205–5211, 1976.

[15] EcoCyc. (2015) Psda -eg10706. [Online]. Available: http://www.ecocyc.org/ECOLI/NEW-IMAGE?type=GENE&object=EG10706

[16] T. Icho and C. Raetz, "Multiple genes for membrane-bound phosphatases in escherichia coli and their action on phospholipid precursors." *Journal of Bacteriology*, vol. 153, no. 2, pp. 722–730, 1983.

[17] Y.-H. Lu, Z. Guan, J. Zhao, and C. R. Raetz, "Three phosphatidylglycerol-phosphate phosphatases in the inner membrane of escherichia coli," *Journal of Biological Chemistry*, vol. 286, no. 7, pp. 5506–5518, 2011.

[18] T. Touzé, D. Blanot, and D. Mengin-Lecreulx, "Substrate specificity and membrane topology of escherichia coli pgpb, an undecaprenyl pyrophosphate phosphatase," *Journal of Biological Chemistry*, vol. 283, no. 24, pp. 16 573–16 583, 2008.

[19] T. Icho, "Membrane-bound phosphatases in escherichia coli: sequence of the pgpa gene." *Journal of Bacteriology*, vol. 170, no. 11, pp. 5110–5116, 1988.

[20] M. El Ghachi, A. Derbise, A. Bouhss, and D. Mengin-Lecreulx, "Identification of multiple genes encoding membrane proteins with undecaprenyl pyrophosphate phosphatase (uppp) activity in escherichia coli," *Journal of Biological Chemistry*, vol. 280, no. 19, pp. 18 689–18 695, 2005.

[21] D. A. Dillon, W.-I. Wu, B. Riedel, J. B. Wissing, W. Dowhan, and G. M. Carman, "The escherichia coli pgpb gene encodes for a diacylglycerol pyrophosphate phosphatase activity," *Journal of Biological Chemistry*, vol. 271, no. 48, pp. 30 548–30 553, 1996.

[22] EcoCyc. (2015) Psda - eg10704. [Online]. Available: http://www.ecocyc.org/ECOLI/NEW-IMAGE?type=GENE&object=EG10704

[23] ——. (2015) Ppgb - eg10705. [Online]. Available: http://www.ecocyc.org/ECOLI/NEW-IMAGE?type=GENE&object=EG10705

[24] T. Icho, "Membrane-bound phosphatases in escherichia coli: sequence of the pgpb gene and dual subcellular localization of the pgpb product." *Journal of Bacteriology*, vol. 170, no. 11, pp. 5117–5124, 1988.

[25] EcoCyc. (2015) Ppgc - eg11371. [Online]. Available: http://www.ecocyc.org/ECOLI/NEW-IMAGE?type=GENE&object=EG11371

[26] D. W. Deamer and V. Gavino, "Lysophosphatidylcholine acyltransferase: purification and applications in membrane studies," *Annals of the New York Academy of Sciences*, vol. 414, no. 1, pp. 90–96, 1983.

[27] P. K. Schmidli, P. Schurtenberger, and P. L. Luisi, "Liposome-mediated enzymatic synthesis of phosphatidylcholine as an approach to self-replicating liposomes," *Journal of the American Chemical Society*, vol. 113, no. 21, pp. 8127–8130, 1991.

[28] V. Arondel, C. Benning, and C. R. Somerville, "Isolation and functional expression in escherichia coli of a gene encoding phosphatidylethanolamine methyltransferase (ec 2.1. 1.17) from rhodobacter sphaeroides." *Journal of Biological Chemistry*, vol. 268, no. 21, pp. 16 002–16 008, 1993.

[29] B. K. Tan, M. Bogdanov, J. Zhao, W. Dowhan, C. R. Raetz, and Z. Guan, "Discovery of a cardiolipin synthase utilizing phosphatidylethanolamine and phosphatidylglycerol as substrates," *Proceedings of the National Academy of Sciences*, vol. 109, no. 41, pp. 16 504–16 509, 2012.

[30] I. Chen and J. W. Szostak, "A kinetic study of the growth of fatty acid vesicles," *Biophysical Journal*, vol. 87, 2004.

[31] Y. Sakuma and M. Imai, "Model system of self-reproducing vesicles," *Physical review letters*, vol. 107, no. 19, p. 198101, 2011.

[32] D. G. Gibson, L. Young, R.-Y. Chuang, J. C. Venter, C. A. Hutchison, and H. O. Smith, "Enzymatic assembly of dna molecules up to several hundred kilobases," *Nature Methods*, vol. 6, no. 5, pp. 343–345, 2009.

[33] D. G. Gibson, H. O. Smith, C. A. Hutchison III, J. C. Venter, and C. Merryman, "Chemical synthesis of the mouse mitochondrial genome," *Nature Methods*, vol. 7, no. 11, pp. 901–903, 2010.

5

STUDYING GPAT AND LPAAT WITH FLUORESCENCE

As part of our investigation into the ability to grow liposomes via in vitro synthesized GPAT (glycerol 3 phosphate acyltransferase) and LPAAT (lysophosphatidic acid acyltransferase), we developed methods for studying the activity of these enzymes via light. These methods were: (i) a fluorogenic assay that detects the presence of CoA in solution, which is released upon the reaction of acyl-CoA with glycerol 3 phosphate (G3P) or lysophosphatidic acid (LPA) and (ii) a fluorogenic/color change assay based upon the change of the optical properties of a NBD (nitrobenzoxadiazole)-labeled fatty acid. These changes principally occurred when the fatty acid was incorporated into liposomal membranes, either as a free fatty acid, attached to CoA, as in palmitoyl CoA or attached to the glycerol backbone of a lipid, as in lysophosphatidic acid or phosphatidic acid. Both methods were developed initially in the absence of a better tool (eventually LC-MS) to study the activity of the enzymes, though they offer some interesting possibilities for microscopy studies as well as high throughput and kinetics studies. We found that the CoA method could be used to study LPAAT only, due to the fact that the assay is only functional in non-reducing conditions and that the reducing environment required by GPAT saturates the assay. The NBD method was found to be effective to study the activity of LPAAT and the combination of GPAT and LPAAT though there remains some open questions as to whether fluorescence and color changes observed correspond directly to the activity of GPAT and LPAAT or if there are some other reactions/processes involved.

5.1. INTRODUCTION

Optical methods for studying the activity of GPAT and LPAAT can complement mass spectrometry offering many advantages. For instance if the activity of GPAT and LPAAT can be measured by a fluorescence change, it can easily used be to study the enzymes in small volumes and in a high-throughput manner. That is true for both the assays developed in this chapter. An advantage of the NBD assay is it also possible to make real-time measurements, which is not possible with the CoA assay or mass spectrometry. It may also be possible to directly image growth of liposomes in a microscope with the NBD method. This can complement existing methods for measuring volume expansion with FRET signal [1]. To the best of our knowledge it is a new development to study GPAT and LPAAT activity optically.

5.2. RESULTS

5.2.1. COA ASSAY

Enzo Life Sciences produces a proprietary assay for the measurement of activity of acyltransferases, using acyl CoAs as substrates, by a non-fluorogenic substrate which becomes fluorescent upon reacting with CoA, which is released by the acyltransferase reactions studied here. GPAT, DHFR, LPAAT and LacI were expressed separately in the presence of liposomes. DHFR and LacI were chosen because the templates were plasmid and PCR product respectively in analogy to the constructs used for GPAT (gene:*plsB*) and LPAAT (gene:*plsC*). The resulting solutions of liposome with incorporated proteins (proteoliposomes, as is shown in chapter 3) were dialyzed to remove small molecules, in particular DTT, which is known to give false positive results in the assay [2]. That was done using a floating dialysis membrane as indicated in figure 5.1 a. A membrane floats on buffer and the sample is pipetted on top of the membrane that allows small molecules to pass through. The dialyzed proteoliposomes solutions are then adjusted so that the buffer composition was similar to that previously reported [3] i.e. for GPAT enzyme the final buffer was that of GPAT buffer II, and for LPAAT the buffer was that of LPAAT buffer I. There is an important difference in the buffers from those used in literature [3] in that β-mercaptoethanol was omitted from the GPAT buffer, which could have the same effect as DTT on the assay and meant that the buffers would have been mildly oxidizing due to the presence of oxygen in solution. Another important difference was the doubling of NaCl in the GPAT buffer to 400 mM and addition of 200 mM of NaCl to the LPAAT buffer. This was done to prevent the precipitation of palmitoyl CoA by magnesium ions [4]. The resulting solutions were reacted with palmitoyl CoA, and in the case of LPAAT, also 16:0 lysophosphatidic acid (LPA). The samples were then measured for the presence of CoA via a fluorogenic assay that forms a fluorescent product from CoA and proprietary molecule as indicated in figure 5.1 b. Figure 5.1 c shows that GPAT sample did not have significantly more CoA over the LacI control (P value=0.9237), this may be expected since it is known that GPAT requires reducing conditions to function [3]. The LPAAT sample on the other hand has less than 1/4 chance of obtaining the indicated result if the LPAAT and lacI samples are equivalent (i.e. the null hypothesis is true, P value=0.2306), which suggests that LPAAT is active in the conditions studied. All samples had more CoA signal than the blank, which was the buffer provided with Enzo assay. This could be due to

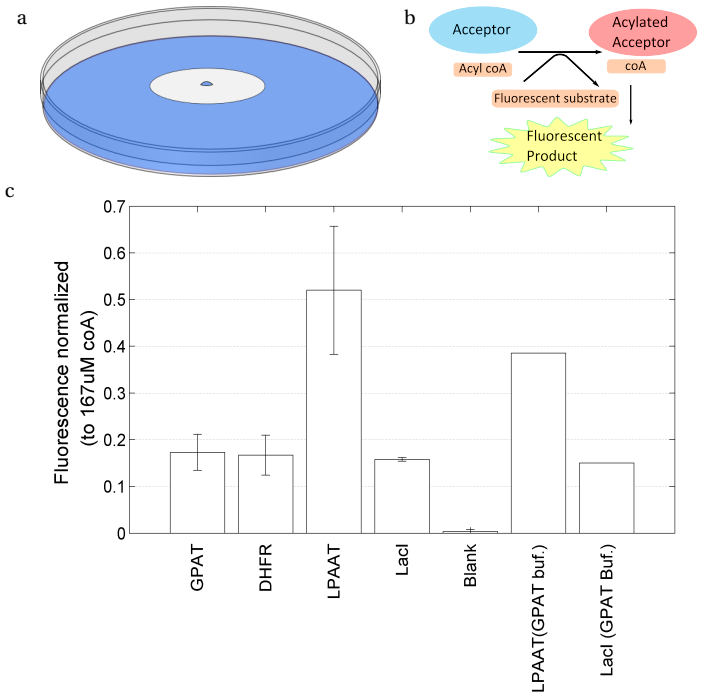

Figure 5.1: | Acyltransferase activity with fluorescent CoA assay.
(a) After protein synthesis in the PURE*frex* system, DTT was removed from samples using floating membranes with pores that allowed small molecules, but not the 100-nm SUVs to pass through them. (b) One of the products of the acyltransferase reaction, CoA was detected fluorescently upon its reaction with a substrate that became fluorescent after that reaction. (c) The activity of the enzymes (GPAT, LPAAT) in various buffers were compared to controls consisting of other enzymes (DHFR, LacI) not expected to have activity. Error bars are from two independent repeats.

hydrolysis of the thioester at the pH considered (GPAT pH 8.4, LPAAT pH 9.0 [5], which would release CoA from the palmitoyl group. It was also found that LPAAT was active in the GPAT buffer II (non-reducing) as compared to lacI in the same buffer.

We also found that it was possible to remove the DTT and other small molecules from solution with ZebaSpin Desalting Columns with 7K MWCO and then measure with the CoA assay, though data is not included here.

The CoA assay was used to further explore the activity of LPAAT, and it was attempted to measure the activity of GPAT as well, the results of which are shown in figure 5.2. This was done by adding a small amount of DTT that possibly would not saturate the CoA assay, but perhaps allow the reducing conditions believed to be required for GPAT to be functional (buffer: GPAT Buffer 10 μM DTT). It was again found that GPAT did not have any significant signal beyond what was found with a control protein of DHFR, neither for the instance where a small amount of DTT was added (columns 1+2) after dialysis, nor in a control where the dialysis was used to remove the DTT entirely (GPAT/DHFR columns 3+4). It was however found that when LPAAT was synthesized and dialyzed

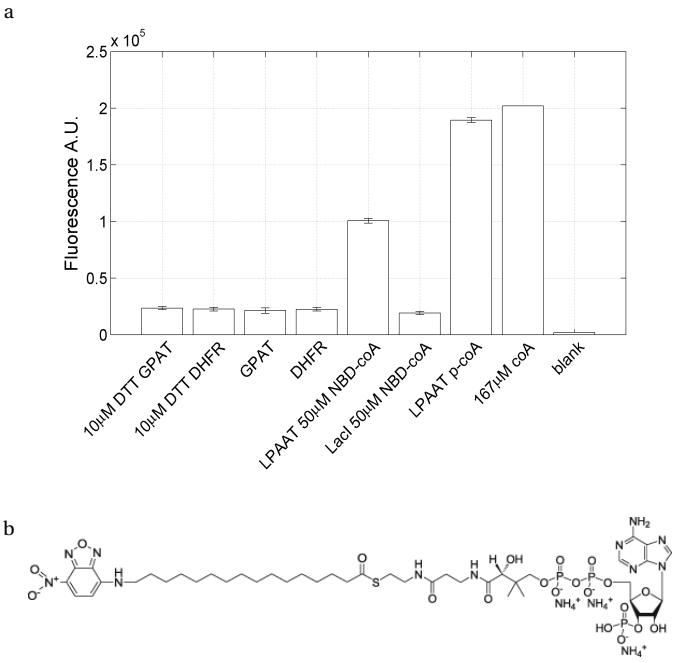

Figure 5.2: | Additional acyltransferase activity measurements with fluorescent CoA assay including with NBD palmitoyl CoA substrate.
(a) The CoA assay was used to study the activity of the GPAT enzyme with a non assay saturating amount of DTT (columns 1+2). Also the previous experiment, where DTT was completely removed by dialysis was repeated as a control (columns 3,4). In neither case was activity detected over the control. It was also used to compare the activity of LPAAT enzyme with an NBD labeled palmitoyl CoA to a control with lacI (columns 5,6). A second control was made with LPAAT and unlabeled palmitoyl CoA (column 7). It was found that both the labeled and non labeled molecules released more CoA in the presence of the LPAAT enzyme than the labeled molecule in the presence of lacI, and that the unlabeled molecule was more active than the labeled molecule. Error bars are from multiple measurements of the same sample. (b) the structure of the NBD palmitoyl CoA molecule used here and throughout the chapter.

to remove DTT (buffer: LPAAT Buffer I) and then mixed with LPA and NBD palmitoyl CoA, that there was more production of CoA in the LPAAT sample over the LacI sample (columns 5 +6) which suggested that NBD palmitoyl CoA can be used as an LPAAT substrate. We employed the NBD palmitoyl CoA in this reaction to confirm its activity as a complement to using it alone to detect GPAT and LPAAT activity (section 5.2.3). A positive control performed under the same conditions except with palmitoyl CoA in place of NBD palmtioyl CoA, suggests the activity of the LPAAT in the studied condition (column 7). We also attempted to oxidize the DTT in a GPAT reaction by adding oxidized glutathione after mixing GPAT proteoliposomes and GPAT buffer, but before applying the CoA assay. We found however that glutathione did not prevent DTT from saturating the CoA assay (not shown). Error bars in this section are from repeat measurements of the fluorescence only and not independent experiments.

5.2.2. MASS SPECTROMETRY OF NBD LIPIDS

To confirm the reactivity of NBD palmitoyl CoA, as measured by the CoA assay and by fluorescence of the NBD itself (see following sections), we assayed by mass spectrometry GPAT and LPAAT together in GPAT Buffer IV + 66 μM G3P with both the substrates palmitoyl CoA and NBD palmitoyl CoA simultaneously present. The result, as seen in figure 5.3 b/c was the detection of a molecule with m/z corresponding to a phosphatidic acid with two fatty acid tails, one with NBD and one without, though the NBD label could be at the distal end of either of the fatty acid tails. Figure 5.3 b is an extracted ion current (m/z 830.034) chromatogram (EIC) with a peak at ~5.4 min and figure 5.3 c is part of the m/z spectra for the corresponding peak in the total ion current chromatogram (TIC). This indicates that GPAT or LPAAT or both are active with the NBD-palmitoyl CoA as a substrate (the MS in this experiment cannot distinguish between molecules with the fatty acid of the sn-1 position labeled or with the sn-2 position and the mass spectra was only to m/z 1000, below the mass of the doubly labeled molecule). NBD 16:0 LPA was not detected, though neither was 16:0 LPA. The latter indicates that under the present conditions, we would not expect to detect the labeled NBD 16:0 LPA. In other words we expect if the labeled LPA molecule was produced it was subsequently consumed. The above results only indicate that at least one of the enzymes accepts the NBD palmitoyl CoA as a substrate, though that gives insight in the following sections that the measured changes in optical properties are indeed due to activity of enzymes. It remains to be determined if both enzymes can use the NBD palmitoyl fatty acyl CoAs as substrates.

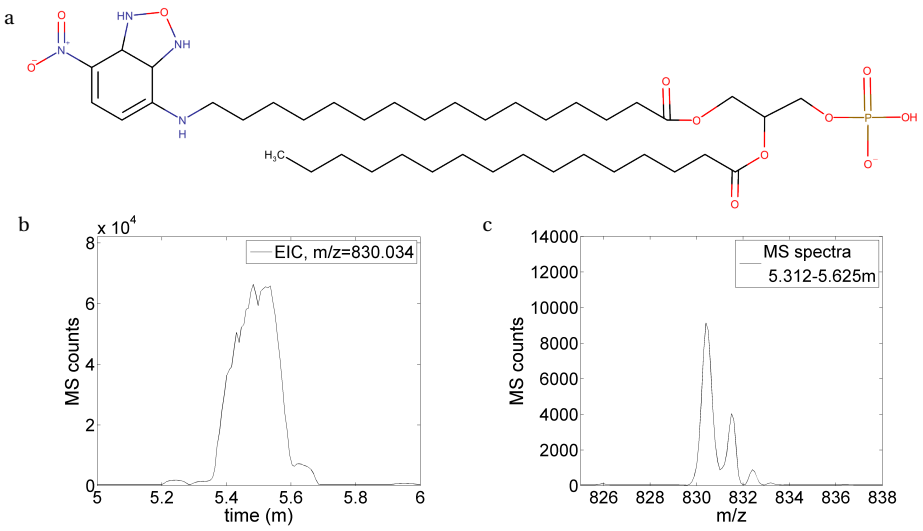

Figure 5.3: | LC-MS of assay of acyltransferase activity with NBD palmitoyl CoA as substrate.
(a) The NBD labeled phosphatidic acid detected in panel b, mass 830.034 g/mol (the position of the NBD is not yet determined) (b) Detection of m/z peak at 830.034 Da/e in an extracted ion chromatogram corresponds to a type of phosphatidic acid with two acyl groups, one that is 16:0 palmitic acid, and a second that is NBD palmitic acid. (c) A mass spectra from 5.312-5.625 min showing the specified peak of the NBD labeled DPPA, along with three additional isotopic peaks. The position of the labeled and unlabeled fatty acid groups is as of yet unspecified and thus whether GPAT, LPAAT or both are active with this substrate remains to be investigated.

5.2.3. NBD PALMITOYL COA IN MEMBRANES

First we studied only NBD palmitoyl CoA with and without membranes. Unlabeled palmitoyl CoA in solution with liposomes is known to partition mostly in liposome membranes [6] but due to its partial solubility in the buffers used [4], some of it will remain in solution. We therefore expect that in the presence of liposomes, NBD labeled palmitoyl CoA is likely to also partition mostly in liposomes due to a similar structure. We wanted to see the effect of the labeled fatty acyl coA entering the membrane on the fluorophore. We thus mixed it with buffer, and then added it to other buffer solutions with and without liposomes. Fluorescence emission spectra were measured and indeed it was found that the sample with liposomes was more fluorescent than the sample without (figure 5.4). Thus it may support our hypothesis that it may be possible to detect transfer of the fatty acid group to either the sn-1 position of G3P, or the sn-2 position of LPA, if those reactions would cause an increase of NBD concentration in the membrane.

To investigate the partitioning of NBD palmitoyl CoA in the membrane in further detail, we made an experiment where a solution of NBD palmitoyl CoA had successive additions of liposomes in LPAAT Dialysis Buffer. If there was additional increase of fluorescence upon multiple additions of liposomes, it would indicate that their had remained some NBD palmitoyl CoA in solution that was then incorporated into liposomes since it was observed that liposomes alone are non-fluorescent (figure 5.5 c). It is also known that NBD self quenches at high concentrations in membranes [7], which complicates the matter because there is also a possible decrease of fluorescence when sufficient concentration of NBD labeled molecules are in the liposome membranes. Although palmitoyl CoA partitions almost completely in the membrane [6] NBD is partially hydrophilic [8], which could cause NBD palmitoyl CoA to be more soluble in aqueous buffers than palmitoyl CoA. A complicated kinetics was observed upon the titration (figure 5.5 b). Multiple processes must be involved that may include but not be limited to the following (figure 5.5 a). The process that we hope to observe is the intact NBD palmitoyl CoA en-

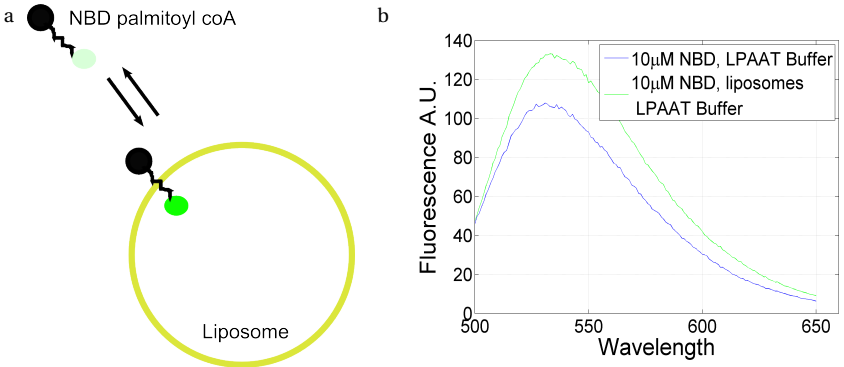

Figure 5.4: | Increase of NBD fluorescence upon insertion of NBD fluorophore into liposomal membranes. (a) Palmitoyl CoA is labeled with the fluorophore NBD at the end of the acyl chain and displays an increase in fluorescence in the presence of liposomes due to the fact that NBD is more fluorescent in a hydrophobic environment and NBD palmitoyl CoA is at least partially incorporated into membranes (see figure 5.10) (b) NBD palmitoyl CoA fluorescence is greater in the presence of liposomes then in the absence.

tering the membrane from aqueous solution. That could result in fluorescence increase due to environment sensitivity of the NBD, or decreases due to quenching. There is also possible hydrolysis of the thioester between the CoA and fatty acid at pH 9.0 in buffer used, which is known to occur [5] and may in turn lead to the formation of fatty acids aggregates, micelles or bilayers or some combination thereof resulting in subsequent quenching of fluorophore. The labeled fatty acid without CoA is also likely to prefer the membrane environment, which for the same reasons as for the intact NBD palmitoyl CoA could cause increase or decrease in fluorescence. Two negative controls, one with NBD palmitoyl CoA without added liposomes, which has fluorescence of only 15 units, and one with liposomes without NBD palmitoyl CoA, that has fluorescence of less than 5 units, show that the effect is due to the interaction of the NBD palmitoyl CoA with the liposomes (figure 5.5 c). This rules out the NBD palmitoyl CoA lysing to NBD palmitic acid and forming micelles or aggregates hypothesis but not the others. Altogether it was difficult to determine exactly the processes that were occurring without further study, though it was clear that fluorescence changes were occurring and it was decided to investigate whether enzymes would have an effect on the complex fluorescence signal.

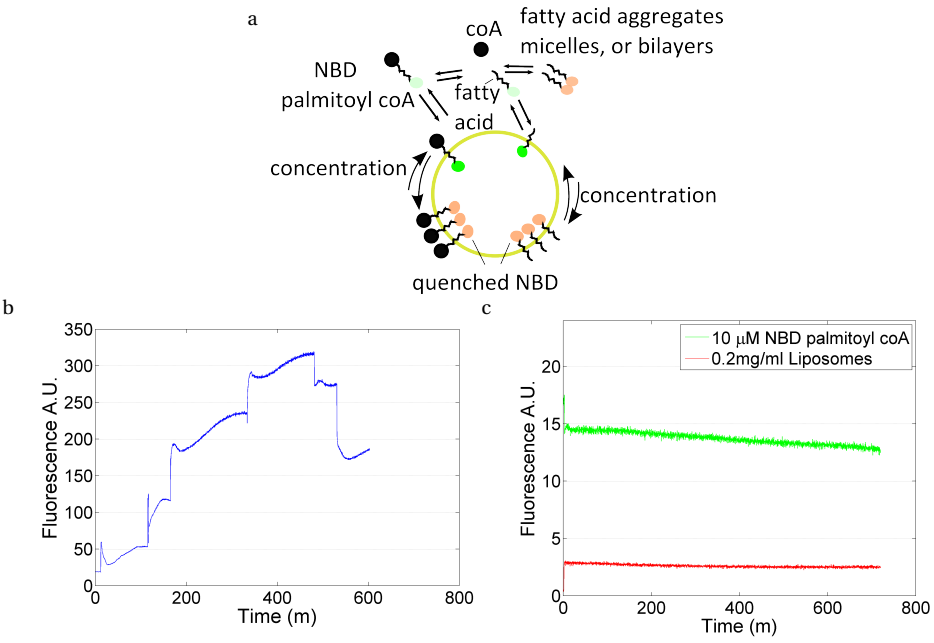

Figure 5.5: | Long titration of NBD palmitoyl CoA with liposomes.
(a) Some of the hypothesized chemical equilibria which can explain the complex kinetics of titration of NBD-CoA with liposomes. NBD palmitoyl CoA can enter the membrane, it can increase in concentration or alternatively it can be hydrolyzed to become free fatty acid that can form micelles and then enter the membrane, also with the possibility of increase in concentration. (b) the kinetics observed when liposomes are added in 6 steps (at discontinuities in the fluorescence levels) to a 10 μM NBD CoA solution. (c) The fluorescence of 10 μM palmitoyl-coA in LPAAT buffer is stable and less than the values in the presence of liposomes. Similarly the fluorescence of liposomes in LPAAT buffer is minimal and stable.

In addition to all the mechanisms described in figure 5.5 for the change in fluorescence in the absence of enzymes, there are possible new dynamics occurring upon the addition of the acyltransferase enzymes. In figure 5.6 a the hypothesized processes are illustrated. If the GPAT enzyme can use NBD palmitoyl CoA as a substrate, then NBD 16:0 LPA will form. NBD lysophosphatidic acid will be at least partially in the membrane of the liposomes [9], and may have different solubility than NBD palmitoyl CoA in the membrane and buffer which may cause and increase or decrease in concentration of NBD in the membrane. When the LPAAT enzyme is active with either palmitoyl CoA or NBD palmitoyl CoA and NBD 16:0 LPA, or 16:0 LPA substrate (LPAs as produced by GPAT or supplied directly), it can produce 16:0/16:0 DPPA with doubly labeled or singly labeled NBD. The DPPA products are expected to be mainly membrane soluble and thus accumulate in the membrane (see DPPA localization by Dynabeads® in chapter 2). Figure 5.6 a) (left panel) shows LPA and palmitoyl CoA as being in equilibrium with the membrane and environment and DPPA as accumulating and quenching. Figure 5.6 a) (right panel) shows the situation when the amount of NBD-palmitoyl CoA is decreased by a factor of 50. Again NBD palmitoyl coA and NBD 16:0 LPA are in equilibrium with between the membrane and the buffer and DPPA is thought to accumulate in the membrane. Here though and instead of quenching of NBD upon accumulation of NBD in the membrane, there is only enough NBD labeled lipids (particular NBD DPPA) to cause an increase in fluorescence due to environment sensitivity of NBD.

In the first two columns of panel b of figure 5.6 the activity of LPAAT compared to LacI, assayed in LPAAT Buffer I (with dialysis to remove DTT) with 50 μM of NBD-palmitoyl CoA and 33 μM of LPA is presented. The result that the LPAAT sample was less fluorescent can be attributed at partly to the accumulation of NBD-DPPA in the membrane causing quenching of the flurophore. This further suggests the LPAAT can accept and use NBD-palmitoyl CoA as a substrate. Note that there is no non-labeled palmitoyl CoA in this experiment, which suggest the enzyme is active with the *labeled* palmitoyl CoA. Columns 3 and 4 show GPAT and DHFR assayed in GPAT buffer III with in addition 33.3 μM NBD palmitoyl CoA and 66.6 μM G3P. The lack of difference in the samples does not necessarily mean that the GPAT was inactive, simply there is not a significant change in the amount of NBD in the membrane. Columns 5 and 6 are again the activity of LPAAT against LacI except 400 nm liposomes were used instead of the normal 100 nm. That may increase the effects observed when NBD-DPPA is potentially made due to increased probability of enzymes and substrates and thus products to be in the same liposome. The buffer was in this instance LPAAT buffer I with in addition 33.3 μM NBD palmitoyl CoA and 33.3 μM LPA included in the reaction. The quenching effect appears to be more pronounced in this instance. In columns 7 and 8 LPAAT and LacI are compared again in LPAAT buffer I, though with less substrate i.e 1.65 μM NBD palmitoyl CoA and 6.66 μM LPA. In this instance, as suggested in the right cartoon of figure 5.6 panel a, the increase of fluorescence of NBD in the hydrophobic membrane environment causes an increase in signal in the LPAAT over the LacI sample. In columns 9,10 the activity of LPAAT compared to lacI with oxidized glutathione (oxidizing buffer i.e. LPAAT Glutathione) with 33.3 μM of NBD palmitoyl CoA and 33.3 μM of LPA was studied. It was found that quenching occurred in this case suggesting LPAAT is active in a strong oxidizing environment. Likewise in columns 11 and 12, the activity of LPAAT compared to lacI

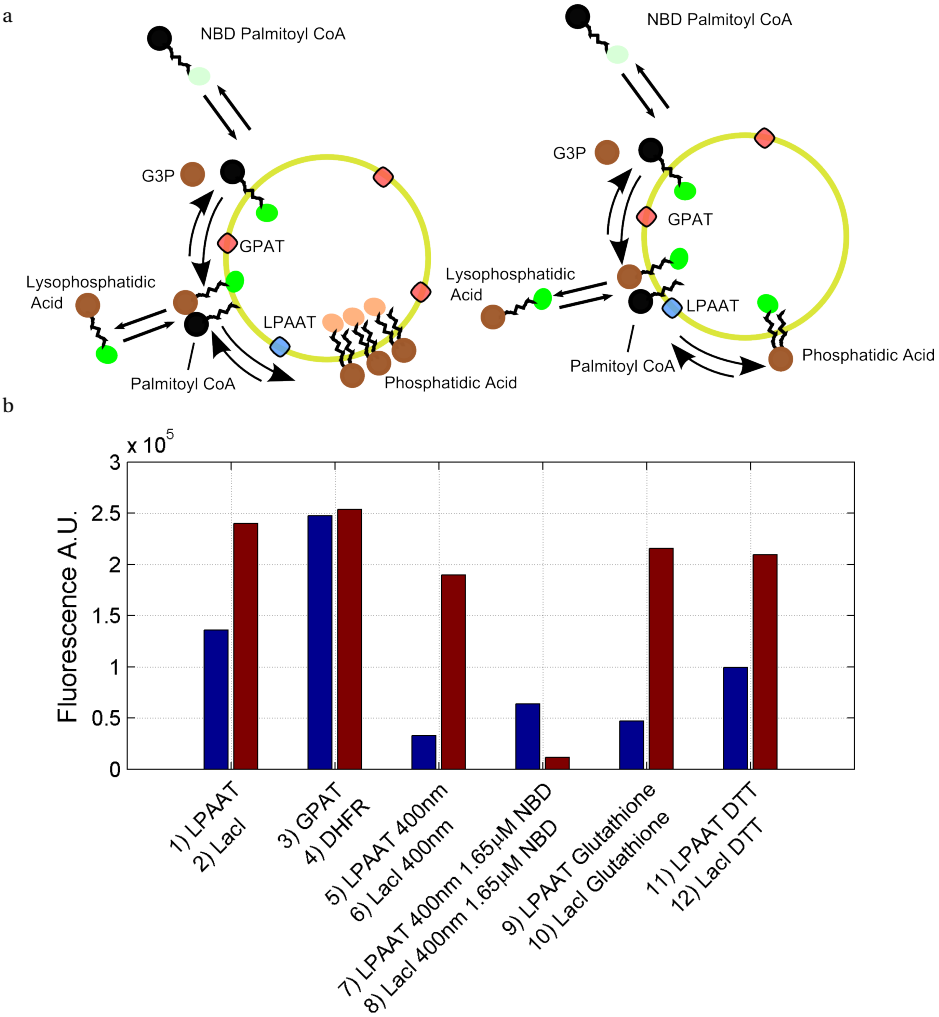

Figure 5.6: | Study of acyltransferase activity with NBD palmitoyl CoA.
(a) The hypothesized mechanisms for enzyme-induced fluorescence decrease at high NBD palmitoyl concentrations due to quenching of NBD (left), and fluorescence increase due to environmental sensitivity at low NBD palmitoyl CoA concentrations (right). (b) LPAAT and GPAT activities studied with fluorescence decrease due to quenching (columns 1-6 and 9-12) and fluorescence increase (columns 7 and 8). LPAAT has a decrease in signal due to the quenching of fluorophores over lacI controls in columns 1/2 5/6 9/10 11/12. GPAT does not cause a decrease in fluorescence over the negative control of DHFR in columns 3/4. When less NBD palmitoyl CoA (1.65 μM instead of 50μM>x>33.3μM) is included in the solution, the fluorescence is increased in the LPAAT signal likely due to the concentration and environmental sensitivity of NBD fluorophore when it moves from the aqueous hydrophilic environment to the membranous hydrophobic environment

with DTT (reducing buffer i.e. LPAAT buffer II, the DTT is in the PURE) with 33.3 μM of

NBD palmitoyl CoA and 33.3 μM of LPA was studied. It was also found that quenching occured in this case suggesting that LPAAT can be active in reducing conditions too.

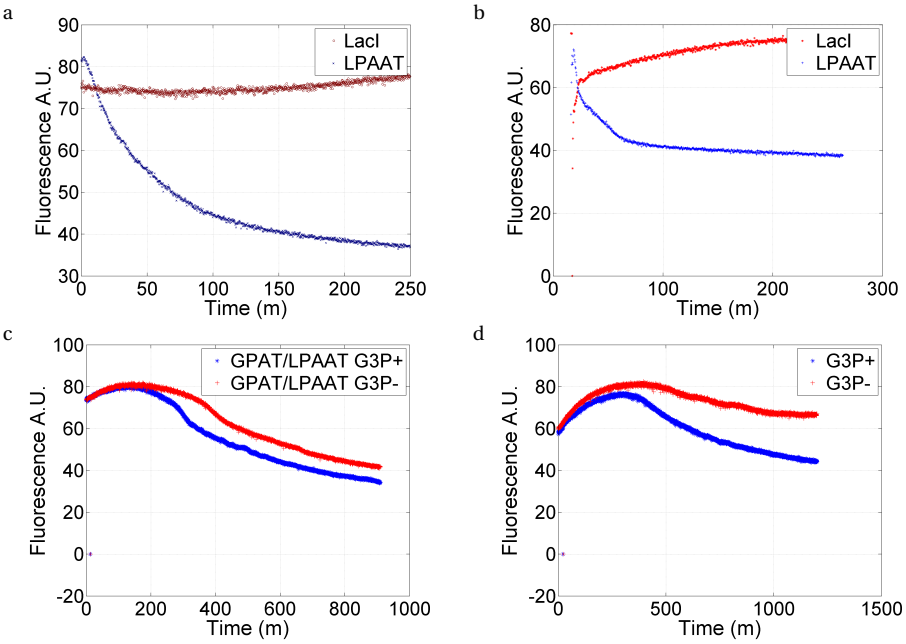

Figure 5.7: | Kinetics of GPAT and LPAAT reactions as studied by NBD palmitoyl CoA quenching.
(a) kinetics of conversion of 16:0 LPA into 16:0 - NBD 16:0 DPPA in real time by LPAAT as measured by quenching of fluorescence in LPAAT buffer I. Control is with LacI in place of LPAAT (b) same as a) only in a GPAT buffer IV that is reducing. (c) Kinetics of combined GPAT and LPAAT in a GPAT buffer V with NBD palmitoyl CoA, palmitoyl CoA included in the reaction and G3P in the positive but not in the negative (G3P+/-) (d) Similar to c in that the buffer conditions are the same except for increased substrate concentration and larger diameter of liposomes (see text).

Having established that a sample containing LPAAT proteoliposomes, NBD palmitoyl CoA and LPA in a LPAAT buffer could cause a decrease in fluorescence compared to a sample containing synthesized LacI, NBD palmitoyl CoA, LPA and liposomes in LPAAT buffer (figure 5.6), we were interested if we could measure a kinetics of this process. Figure 5.7 a shows the progression of such a reaction measured in real time in a spectrofluorometer. Qualitatively, the initial rate is the fastest and constant, and then begins to saturate at 30 minutes. The reaction continues until beyond the window of measurement, though 95% of the total observed change occurs after 150 min. This is in contrast to the kinetics measured with mass spectrometry (chapter 2), where this level is not reached until approximately 10 hours. This does not mean there is a discrepancy, because: a) the quenching assay may not be linear and this was not tested, b) the substrate concentrations were 33.3 μM NBD palmitoyl CoA and 33.3 μM NBD LPA in this quenching kinetics, and 50 μM NBD palmitoyl CoA and 50 μM LPA in the mass spectrometry and furthermore the liposome concentration was 0.4 mg/ml in the MS kinetics and 2 mg/ml here. We were also interested to see if the kinetics could be measured in a

reducing environment since unlike the CoA assay the NBD quencing assay worked without removing DTT (figure 5.6 b columns 11 12). Figure 5.7 b shows quenching kinetics in reducing buffer with pH 8.4 (GPAT Buffer IV). The kinetics are not identical between the case with reducing (GPAT Buffer IV) and non reducing (LPAAT buffer I) buffer though in both there is clearly a difference in the sample with LPAAT and that with LacI. These two experiments show that we can monitor the course of an LPAAT reaction with NBD palmitoyl CoA, and together with the mass spectrometry data, proves that NBD palmitoyl phosphatidic acid labeled at at least one position can form. This therefore suggests that the NBD quenching assay is a real way to monitor LPAAT kinetics in both oxidizing and reducing conditions. Although we were not able to detect the activity of GPAT alone with the NBD palmitoyl CoA quenching method (figure 5.6 b columns 3 4), either due to the inability of GPAT to react with NBD palmitoyl CoA, or due to the fact that 16:0 NBD LPA likely partitions between the membrane and the aqueous phase similarly to 16:0 NBD palmitoyl CoA, we reasoned that GPAT and LPAAT in combination may be able to produce a change in fluorescence due quenching caused by the accumulation of 16:0 NBD labeled phosphatidic acid. Figure 5.7 c shows in reducing conditions at pH 8.4 (GPAT Buffer V), the quenching kinetics due to the lipid synthesis activity of proteoliposomes with both GPAT and LPAAT in the membrane. The positive sample contains G3P while the negative does not, and both samples have 33 μM NBD palmitoyl CoA and 33 μM palmitoyl CoA. There is a difference in the fluorescence between the samples. In figure 5.7 d we tried to enhance the differences by increasing the substrate compositions to 100 μM, as well as the size of the liposomes in order to increase the loading of 16:0 NBD DPPA in individual liposomes. There was indeed an increase in the difference between the positive and negative control. The fact that the kinetics are not monotonically decreasing, and that there is activity in the negative samples where G3P is ommited can again either be due to the other processes mentioned, or also due to the fact that there

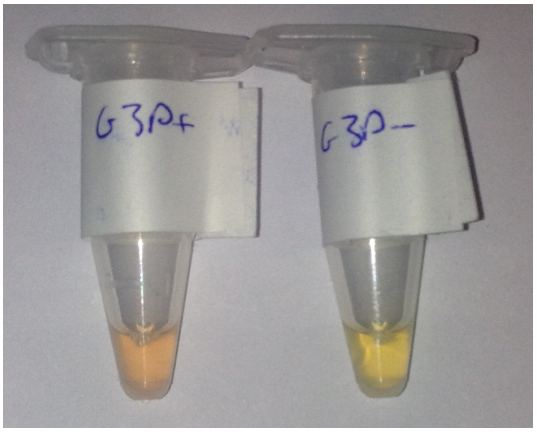

Figure 5.8: | Concentration of NBD in the membrane causes an optical (color) change.
A color change in the NBD dye after reacting NBD palmitoyl CoA, palmitoyl CoA and G3P in the presence of GPAT and LPAAT was observed by visual inspection, which effectively is a measurement of all emitted, transmitted and reflected light.

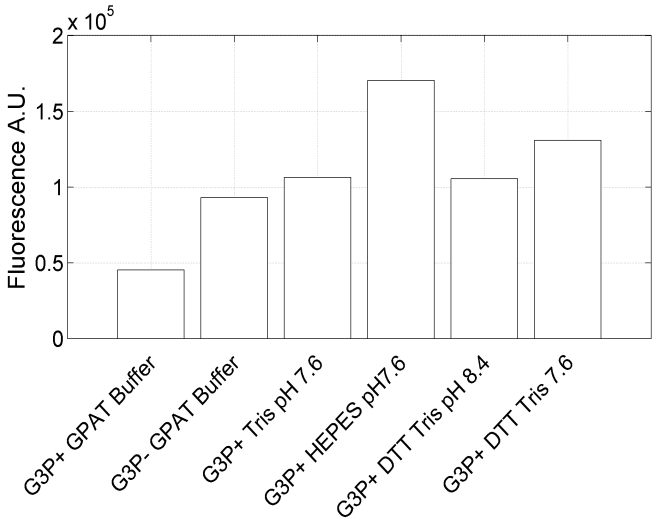

Figure 5.9: | GPAT and LPAAT combined quenching assays.
The fluorescence quenching assay for the activity of GPAT and LPAAT was tried in various buffers, and was found to be most effective in the "GPAT" Buffer. Buffer composition is indicated.

may be G3P contamination in the lipids or PURE system as we found in mass spectrometry experiments of chapter 3. This would allow DPPA to be formed in negative samples Here the kinetics correspond well with the mass spectrometry experiments, as there is a clear increase in the rate of activity after 4 hours, and the entire process takes at least tens of hours to occur.

In addition to the difference in fluorescent signal between the positive sample with G3P and the negative sample without (figure 5.7 d) we were able to distinguish the samples by eye and by photography (figure 5.8). This is effectively a measurement of all emitted, reflected and transmitted light. We attempted to measure these changes by absorbance spectroscopy, but due to lack of appropriate instrumentation we were not able to resolve samples consistently with that technique.

Having found that it was possible to measure a process catalyzed by GPAT and LPAAT in reducing GPAT buffer of pH 8.4 via quenching of fluorescence, we investigated this phenomenon in various buffers. The results are shown in figure 5.9. Though we later found in chapter 2 that we could form DPPA from palmitoyl CoA and G3P in various buffers, the data here was inconclusive with an enzyme catalyzed process as the signal varied between the positive samples with G3P in various buffers. Although we later confirmed by LC-MS that the formation of 16:0-16:0 (NBD) DPPA was occurring in the GPAT buffer the conclusion cannot be extended to the various buffers here without further experimentation.

5.2.4. MICROSCOPY STUDIES

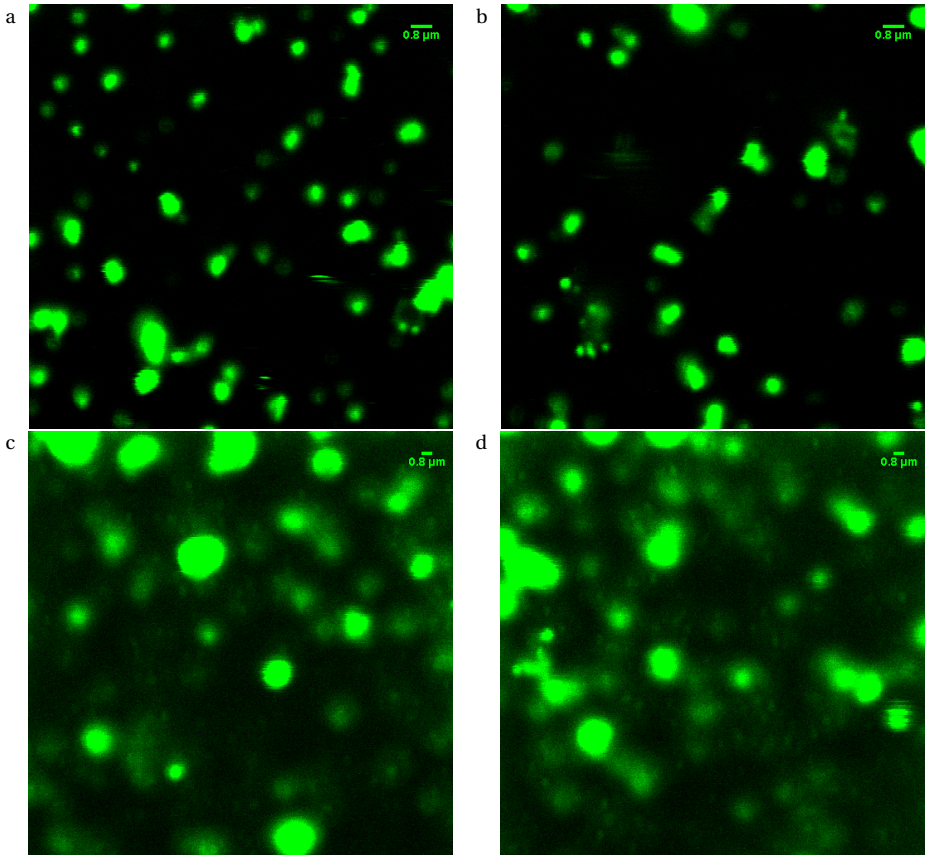

Figure 5.10: | Fluorescence microscopy study of GPAT and LPAAT activity with NBD palmitoyl CoA. (a/b) 800-nm liposomes with *plsB* and *plsC* genes expressed and in PURE*frex* and supplied with glycerol 3 phosphate NBD-palmitoyl CoA and palmitoyl CoA. (c/d) Negative control consisting of 800-nm liposomes with DHFR/LacI expressed and supplied with G3P palmitoyl CoA and NBD palmitoyl CoA, L-serine, and cytidine triphoshate. We have the hypothesis that reaction of NBD palmitoyl CoA and palmitoyl CoA with G3P catalyzed with GPAT and LPAAT (a/b) removes the semi soluble fatty acyl CoAs from solution by creating the more membrane soluble DPPA (single or doubly labeled with NBD). Comparing the GPAT and LPAAT sample to the DHFR and lacI, there is more background signal in the DHFR/LacI as the fatty acyl CoAs remain partly in the buffer solution.

In figure 5.10 we see further evidence that NBD labeled molecules (palmitoyl CoA, LPA, DPPA) are situated in the membrane before and after reaction with GPAT *plsB* and LPAAT *plsC*. Panels a/b are with GPAT and LPAAT expressed catalyzing the formation of NBD-DPPA as found in the mass spectrometry section, whereas panels c/d are with the genes for DHFR/LacI which do not catalyze reactions with palmitoyl CoA . The reaction conditions are the co-expression and activity conditions (see methods) found in chapter 2 to be effective for the activity of GPAT and LPAAT together. The laser power and camera settings were the same for both sets of images, nevertheless it is not appropriate to

directly compare intensities due to saturation of pixels. That being said there is clearly NBD labeling the membrane in both cases suggesting that NBD as NBD palmitoyl CoA is in the membrane at significant concentration before reaction with GPAT and LPAAT, and afterwards NBD is also in the membrane, either in the form of remaining NBD palmitoyl CoA or synthesized NBD LPA or NBD DPPA. It is interesting to note the background in the non reacted sample is higher compared to the reacted sample, this could be attributed to amphiphilic NBD palmitoyl CoA in solution or in micelles in the non reacted sample, that upon reaction is incorporated into the membrane. Conversely it could be simply due to positioning near the surface of the microscope slide in the sample, and as such further experiments are required to confirm that 16:0 NBD DPPA is incorporated into the membrane increasing the concentration there and reducing it in the bulk.

5.3. DISCUSSION

In this chapter, we studied the activity of GPAT and LPAAT with light. We found that a fluorogenic assay of CoA could be used to suggest that LPAAT was active in the presence of proteoliposomes. Due to the fact that GPAT requires reducing conditions to function it was not possible to study its activity. The assay was also limited insofar as it requires a dialysis step and is not a continuous measurement. Nevertheless, it proved useful as it was the initial experiment that suggested there was acyltransferase activity of an enzyme (LPAAT) being synthesized in the PURE system. The NBD palmitoyl CoA quenching and fluorescence increase assays were found to be more effective. Though they had limitations in that many chemical and physical processes could be occurring in our system, it did seem to imply activity of both GPAT and LPAAT protein in various experiments. That is because all samples containing GPAT and LPAAT are compared to a negative control with the same buffer conditions, we thus consider that the differences observed are caused by the GPAT and LPAAT. It may also be true that those enzymes do not synthesize product but rather increases hydrolysis of the substrates leading to dynamics alternate to those suggested in figure 5.6. This in turn means that a change in the fluorescence signal suggests rather than confirms proper enzyme activity. Quenching assay experiments, in particular the kinetics experiments of figure 5.7 should be repeated. The fact that LPAAT appeared to be active with NBD palmitoyl CoA only, the fact that this situation also gave signal in the CoA assay and the fact that it was also possible to find a hybrid DPPA molecule with an NBD labeled and non labeled tail in the mass spectrometry is altogether evidence that NBD palmitoyl CoA can be used by LPAAT. It was ambiguous as to whether GPAT can accept NBD palmitoyl CoA as a substrate. In both cases an experiment with the MS and separate enzymes would confirm which of the two or both are active. Furthermore experiments, with NBD palmitoyl CoA indicated it could also be used for microscopy studies. Due to inexperience with microscopy, experiments should be repeated, though there is hope that the technique could be used to prove that the synthesized DPPA is being accumulated in the membrane and NBD palmitoyl CoA removed from solution. In conclusion, it is possible to study GPAT and LPAAT activity in the PURE system optically, which adds to the set of available tools for studying GPAT and LPAAT.

5.4. METHODS

5.4.1. CoA ASSAY METHOD

PROTEIN SYNTHESIS

In figures 5.1 and 5.2 proteins were synthesized in the PURE*frex* cell-free translation system. The concentration of *plsB* (GPAT) and DHFR templates was 3.4 nM and those of *plsC* (LPAAT) and LacI were 16.9 nM. In all PURE reactions 2 mg/ml of 100-nm DOPC, DOPE, DOPG, cardiolipin liposomes (mol ratio 50.8:35.6:11.5:2.1) were included along with 0.2U/ul of Superase RNAse inhibitor. Protein synthesis was carried out for 3 hours at 37 °C.

DIALYSIS TO REMOVE DTT

In order to remove DTT which would give false positives in the assay used, synthesized protein was dialyzed against an appropriate buffer. In all experiments of figures 5.1 and 5.2, the synthesized protein samples were dialyzed by floating dialysis (whereby a dialysis membrane floats on the surface of a buffer and the sample is pipetted onto the floating membrane) using V-Series membranes from Millipore with 25 nm pore size. *PlsB* (GPAT) and DHFR samples were dialyzed against GPAT Dialysis Buffer, while *PlsC* (LPAAT) and LacI samples were dialyzed against LPAAT Dialysis Buffer. After dialysis, the total volume of each sample was adjusted to 100 μl by adding various components. For figure 5.1 the resulting final buffer composition for GPAT (*PlsB*) and DHFR was GPAT buffer II and for LPAAT (*PlsC*) and LacI it was LPAAT Buffer I. For figure 5.2 the final buffer composition of the GPAT and DHFR with 10 μM DTT samples was GPAT Buffer 10 μM DTT. For the GPAT and DHFR samples it was GPAT Buffer II and for the LPAAT/LacI with NBD palmitoyl CoA or simply palmitoyl CoA it was LPAAT Buffer I

PROTEIN ACTIVITY

In figure 5.1 GPAT and DHFR protein and liposome solutions were added to vials containing dried palmitoyl CoA for final concentration of 66 μM. LPAAT and LacI protein and liposome solutions were added to vials containing dried palmitoyl CoA and 16:0 LPA for a final concentration of 33.3 μM each. Samples were incubated for 2 hours at 22 °C. In figure 5.2 for GPAT/DHFR with 10 μM DTT and GPAT/DHFR the concentration of palmitoyl CoA was 66.6 μM and for the NBD CoA LPAAT/LacI the concentration of NBD palmitoyl CoA was 50 μM and that of LPA was 33.3 μM.

ACTIVITY ASSAY

Enzo Life sciences produces a proprietary assay for the measurement of concentrations of CoA which indirectly reports the activity of the acyltransferases. The assay works by reacting co-enzyme A with a substrate which becomes fluorescent after the reaction. According to protocol, for each measurement 25 μl of sample was mixed with of transferase assay buffer, 50 μl of cold isopropanol and 50 μl of detection solution containing pre-fluorogenic substrate. Samples were incubated for 10 min and then measured in a plate reader with excitation wavelength of 380 nm and emission wavelength of 520 nm.

5.4.2. MASS SPECTROMETRY OF NBD LIPIDS

PROTEIN SYNTHESIS AND ACTIVITY

A PURE*frex* reaction was assembled with 3.4 nM of *plsB* and 16.9 nM of *plsC* template along with 0.4 U/μl Superase and 2 mg/ml of 400-nm liposomes (DOPC, DOPE, DOPG, cardiolipin liposomes mol % ratio 50.8:35.6:11.5:2.1). The proteins were expressed at 37 °C for 3 h. The synthesized proteoliposomes were then diluted to have buffer composition of GPAT Buffer III and mixed with dried NBD palmitoyl CoA and palmitoyl CoA to a concentration of 66 μM each. The pool was then split and 66 μM G3P was added to the positive sample and they were both incubated at 22 °C overnight.

MASS SPECTROMETRY

The sample was treated in the same manner as described in chapter 2. I.e. it was diluted 10 × in methanol with 2 mM acetylacetone, centrifuged and the precipitate injected into the LC-MS system. The mobile phases and gradient were the same as in all other experiments, whereas the mass spectrometry method differed. In place of multiple reaction monitoring mode the mass spectrometer was operated in negative MS2 mode. In this mode ions are negative and the first and second quadrapoles pass all ions and the third quadrapole performs a 500-ms scan over a broad range of m/z 100-1000. The fragmentor is set to 135 V, the cell accelerator is set to 7 V and the electron multiplier voltage to -500 V

5.4.3. FLUORESCENCE INCREASE IN THE PRESENCE OF LIPOSOMES

10 μl of 100 μM NBD palmitoyl CoA in LPAAT Buffer I was mixed with 1 μl of 20 mg/ml 100 nm liposomes (DOPC, DOPE, DOPG, Cardiolipin mol ratio 50.8:35.6:11.5:2.1, containing Pure Buffer I) and an 89 μl of LPAAT Buffer I. A control was made with 10 μl of 100 μM NBD palmitoyl CoA in LPAAT buffer I and an additional 90 μl LPAAT buffer I. The samples were added to a Cary Eclipse Spectrophotometer from Agilent in glass cuvettes at room temperature and excited at 478 nm and the emission scanned from 500 nm to 650 nm.

5.4.4. NBD LIPOSOME TITRATION

First, 100-nm liposomes (DOPC, DOPE, DOPG, cardiolipin liposomes mol ratio 50.8, 35.6, 11.5, 2.1) containing PURE buffer I were diluted to 4 mg/ml and to have similar final composition as that of LPAAT Dialysis Buffer. Then, a solution of 10.5 μM NBD palmitoyl CoA in the same LPAAT Dialysis Buffer was made. Following that,114 μl of 10.5 μM NBD CoA solution was added to a cuvette. At each major discountinous change of intensity, 6 μl of liposome solution was added to the NBD CoA solution. For the negative control without liposomes a solution of 10.5 μM NBD CoA in LPAAT Dialysis Buffer was added to the cuvette and supplemented once with LPAAT Dialysis Buffer alone instead of liposomes. For negative control without NBD palmitoyl CoA 6 μl of 4 mg/ml liposomes were diluted in 114 μl of LPAAT buffer. All reactions were monitored at 25 °C with excitation at 478 nm and emmission at 530 nm.

Name	NBD P-coA conc.	G3P or LPA	Buffer
LPAAT, LacI	50 μM	33.3 μM LPA	LPAAT Buf. I
GPAT, DHFR	33.3 μM	66.6 μM G3P	GPAT Buf. III
LPAAT 400 nm LacI 400nm	33.3 μM	33.3 μM LPA	LPAAT Buf. I
LPAAT 1.65 μM NBD LacI 1.65 μM NBD	1.65 μM	6.66 μM LPA	LPAAT Buf. I
LPAAT Glutathione, LacI Glutathione	33.3 μM	33.3 μM LPA	LPAAT Gluta.
LPAAT DTT, LacI DTT	33.3 μM	33.3 μM LPA	LPAAT Buf. II

Table 5.1: Buffer type and substrate composition for NBD activity assay experiments.

5.4.5. NBD QUENCHING AND FLUORESCENCE INCREASE ASSAYS

PROTEIN SYNTHESIS

Protein synthesis in figure 5.6 were carried out in a similar manner to that of figure 5.1 (coA assay method) except where indicated 400-nm liposomes were used. The concentration of DNA templates was 3.4 nM for all *plsB*/DHFR experiments and 16.9 nM for all plsC/lacI experiments.

NBD-BASED ACTIVITY ASSAYS

After protein synthesis samples were diluted with buffers and added to substrates including NBD palmitoyl CoA. The one exception is figure 5.6 column 1 and 2 which also underwent dialysis against LPAAT dialysis buffer before dilution. The samples were allowed to react 2 h at 22 °C and then fluorescence was measured at 486 nm excitation with 540 nm emission. In figure 5.6 the concentrations of substrate and buffers are as listed in the table 5.1.

5.4.6. NBD QUENCHING ASSAY KINETICS

PROTEIN SYNTHESIS

Protein synthesis was carried out in a similar manner to figure 5.1 (coA assay method) except for figure 5.7d where 400-nm liposomes were used. DNA template concentrations were for *plsB* and DHFR 3.4nM and for *plsC* and lacI they were 16.9 nM

QUENCHING ACTIVITY ASSAY

In figure 5.7 a, 5-μl proteoliposomes were dialyzed against LPAAT dialysis buffer. The resulting proteoliposomes were mixed with 11.66 μl of LPAAT Adjustment Buffer, added to dried NBD palmitoyl CoA and allowed to equilibrate for 30 min. 33.33 μl of LPAAT Dialysis Buffer was added to dried LPA. The two were then mixed to start the reaction, with the final buffer conditions and substrates concentrations being indicated in table 5.2 below. The reaction was performed at 22 °C and monitored in a spectrophotometer with excitation wavelength of 486 nm and emission of 540 nm. In figure 5.7 b undialyzed liposomes were used. 5-μl of proteoliposome solution was mixed with 11.66 μl of GPAT

Panel letter	NBD P-CoA conc.	Palmitoyl CoA or LPA	Buffer
a	33.3 μM	33.3 μM LPA	LPAAT Buf. I
b	33.3 μM	33.3 μM LPA	GPAT Buf. IV
c	33.3 μM	33.3 μM P-CoA	GPAT Buf V (+/-)
d	100 μM	100 μM P-CoA	GPAT Buf VI(+/-)

Table 5.2: Buffer conditions and substrate concentrations used in NBD palmitoyl CoA quenching kinetics.

Adjustment Buffer, added to dried NBD palmitoyl CoA and allowed to equilibrate for 30 min. 33.3 μl of GPAT Adjustment Buffer was added to the LPA. The two were then mixed and reacted as in figure 5.7 a. The method for figure 5.7 c,d were identical to each other except for the concentration of substrates and that in panel d, 400 nm liposomes were used. 5-μl undialyzed proteoliposomes were mixed with 45 μl of GPAT adjustment buffer to have the buffer composition indicated in table 5.2, added to dried NBD and allowed to equilibrate for 30 min. To start the reaction, G3P was added to the positive cuvette and MQ to the control for a final concentration 100 μM (Figure 5.7 c) or 300 μM (figure 5.7) (also indicated by the buffer type in tables 5.2 and 5.3). The reactions were monitored as in other panels.

5.4.7. NBD QUENCHING, BUFFER STUDY

PROTEIN SYNTHESIS

Protein synthesis was carried out in a similar manner to figure 5.1 (CoA assay method) except for figure 5.7 where 400-nm liposomes were used. For all reactions 3.4 nM of *plsB* and 16.9 nM of *plsC* template were employed.

QUENCHING ASSAYS

After protein synthesis, 2.5-μl undialyzed proteoliposomes were mixed to a final volume of 25μl to have the buffer types of those indicated in the figure and whos composition are given in table 5.3. These solutions were added to 100 μM NBD palmitoyl CoA and 100 μM palmitoyl CoA. Reactions were incubated overnight at 22 °C and then measured in a fluorescence plate reader at excitation 486 nm and emission 540 nm.

5.4.8. MICROSCOPY STUDY

The microscopy experiments were made by initially performing one-pot reactions combining protein synthesis and activity as developed in chapter 2. Amounts corresponding to 2.5 μM of NBD palmitoyl CoA and 2.5 μM of palmitoyl CoA in 5 μl volume were dried in 0.2-ml Eppendorf PCR tubes. The 5-μl PURE system reactions were assembled with 0.4 U/μl Superase RNAse inhibitor, 0.2 mg/ml 800 nm DOPC, DOPE, DOPG, cardiolipin liposomes (mol ratio 50.8:35.6:11.5:2.1) with 0.1 % DSPE PEG biotin, as well as 500 μM G3P, 1 mM addtional cytidine triphosphate (CTP), 5 mM β-mercaptoethanol, and 500 μM L-Serine. Included in the reactions were either templates for *plsB* (3.4 nM) and *plsC* (16.9 nM) or DHFR (2.9 nM) and lacI (24.4 nM). The CTP and L-serine were included because there was another sample, which did not make it to the microscope,

that included the lipid headgroup modifying genes of chapter 4. The reactions were incubated overnight at 37 °C. After reactions microscopy chambers were prepared by using adhesive coated (double sided) silicone sheet with a small hole punctured in it fixed on a microscope cover slide and later sandwiched between the cover glass and a microscope slide. Liposomes were immobilized by first filling the chambers with BSA biotin (2 mg/ml) and then incubating for 10 min followed by washing with PURE*frex* buffer 3 ×. The chambers were than filled with neutravidin (2 mg/ml) and incubated for 10 min before washing with PURE*frex* buffer 6 ×. Finally the sample was applied in the chamber and the microscope slide added. Samples were imaged on a Nikon Eclipse Ti E with a 514 nm laser at 20.4 % power with a dichroic mirror reflecting wavelengths 400-457/514 nm. The emission filter was 540nm/30nm. The pinhole was 54.9 μm, and the scan speed was 0.25 frames per second. The photomultiplier tube high voltage was 41 V with an offset of -14 V.

Buffer Name	Buffer Composition
GPAT Dialysis Buffer	150 mM TrisHCl pH 8.4, 400 mM NaCl, 3 mM $MgCl_2$
LPAAT Dialysis Buffer	100 mM TrisHCl pH 9.0, 200 mM NaCl, 0.5 mM $MgCl_2$
GPAT Buffer I	150 mM TrisHCl pH 8.4, 400 mM NaCl, 3 mM $MgCl_2$, 1 mg/ml BSA, 100μM G3P
LPAAT Buffer I	100 mM TrisHCl pH 9.0, 200 mM NaCl, 0.5 mM $MgCl_2$, 1 mg/ml BSA
GPAT Buffer II	150 mM TrisHCl pH 8.4, 400 mM NaCl, 3 mM $MgCl_2$, 1 mg/ml BSA, 66.6 μM G3P
GPAT Buffer 10μ DTT	150 mM TrisHCl pH 8.4, 400 mM NaCl, 3 mM $MgCl_2$, 1 mg/ml BSA, 66.6 μM G3P, 10 μM DTT
PURE Buffer I	50 mM HEPES pH 7.6, 100 mM Potassium Glutamate, 13 mM $MgCl_2$
PURE Frex	20 mM HEPES pH 7.6, 180 mM Potassium Glutamate, 14 mM $MgCl_2$
GPAT Buffer III	135 mM TrisHCl pH 8.4, 360 mM NaCl, 2.7 mM $MgCl_2$, 1 mg/ml BSA, 10x dil PURE
LPAAT Gluthatione	90 mM TrisHCl pH 9.0, 180 mM NaCl, 0.45 mM $MgCl_2$, 1 mg/ml BSA, 10x dil PURE 3.33 mM Glutathione oxidized
LPAAT Adjustment Buffer	100 mM TrisHCl pH 9.0, 200 mM NaCl, 0.5 mM $MgCl_2$ 1.42 mg/ml BSA
GPAT Adjustment Buffer	150 mM TrisHCl pH 8.4, 400 mM NaCl, 3 mM $MgCl_2$ 1 mg/ml BSA
LPAAT Buffer II	90 mM TrisHCl pH 9.0, 180 mM NaCL, 0.45 mM $MgCl_2$, 1 mg/ml BSA, 10x dil PURE
GPAT Buffer IV	135 mM TrisHCl pH 8.4, 360 mM NaCL, 2.7 mM $MgCl_2$, 0.9 mg/ml BSA, 4.5 mM β-Mercaptoethanol 10x dil PURE
GPAT Buffer V	135 mM TrisHCl pH 8.4, 360 mM NaCL, 2.7 mM $MgCl_2$, 0.9 mg/ml BSA, 4.5 mM β-Mercaptoethanol 100 μM G3P (+/-) 10x dil PURE
GPAT Buffer VI	135 mM TrisHCl pH 8.4, 360 mM NaCL, 2.7 mM $MgCl_2$, 0.9 mg/ml BSA, 4.5 mM β-Mercaptoethanol 300 μM G3P (+/-) 10x dil PURE Frex
GPAT Buffer IV + 270 μM G3P	135 mM TrisHCl pH 8.4, 360 mM NaCl, 2.7m M $MgCl_2$, 0.9 mg/ml BSA, 4.5 mM β-Mercaptoethanol 270 μM G3P 10x dil PURE
GPAT Buffer IV + 66 μM G3P	135 mM TrisHCl pH 8.4, 360 mM NaCl, 2.7 mM $MgCl_2$, 0.9 mg/ml BSA, 4.5 mM β-Mercaptoethanol 66 μM G3P 10x dil PURE
Tris HCl pH 7.6 + G3P	135 mM Tris HCl pH 7.5, 360 mM NaCl, 2.7 mM $MgCl_2$, 0.9 mg/ml BSA, 4.5 mM β-Mercaptoethanol, 270 μM G3P 10x dil PURE
HEPES pH 7.6 G3P+	45 mM Tris HCl pH 7.6, 360 mM NaCl, 2.7 mM $MgCl_2$, 0.9 mg/ml BSA, 4.5 mM β-Mercaptoethanol, 270 μM G3P 10x dil PURE
0.9 mM DTT Tris pH 8.4 G3P+	135 mM Tris HCL pH 8.4, 360 mM NaCl, 2.7 mM $MgCl_2$, 0.9 mg/ml BSA, 4.5 mM β-Mercaptoethanol, 0.9 mM DTT 270 μM G3P 10x dil PURE
0.9mM DTT Tris pH 7.6 G3P+	135 mM Tris HCL pH 7.6, 360 mM NaCl, 2.7 mM $MgCl_2$, 0.9 mg/ml BSA, 4.5 mM β-Mercaptoethanol, 270 μM G3P 10X dil PURE

Table 5.3: Various buffer compositions used in this chapter.

REFERENCES

[1] I. Chen and J. W. Szostak, "A kinetic study of the growth of fatty acid vesicles," *Biophysical Journal*, vol. 87, 2004.

[2] E. L. Sciences. (2015) Acyltransferase activity kit. [Online]. Available: http://static.enzolifesciences.com/fileadmin/files/manual/ADI-907-026_insert.pdf

[3] Y. Kuruma, P. Stano, T. Ueda, and P. L. Luisi, "A synthetic biology approach to the construction of membrane proteins in a semi-synthetic minimal cells," *Biochimica et Biophysica Acta*, vol. 1788, pp. 567–574, 2009.

[4] P. P. Constantinides and J. M. Steim, "Solubility of palmitoyl-coenzme a in acyltransferase assay buffers containing magnesium ions," *Archives of Biochemistry and Biophysics*, vol. 250, no. 1, pp. 267–270, 1986.

[5] P. J. Bracher, P. W. Snyder, B. R. Bohall, and G. M. Whitesides, "The relative rates of thiol–thioester exchange and hydrolysis for alkyl and aryl thioalkanoates in water," *Origin of Life and Evolution of Biospheres*, vol. 41, pp. 399–412, 2011.

[6] M. A. Requero, F. M. Goni, and A. Alonso, "The membrane-perturbing properties of palmitoyl-coenzyme a and palmitoylcarnitine. a comparative study," vol. 34, pp. 10 400–10 405, 1995.

[7] R. S. Brown, J. D. Brennan, and U. J. Krull, "Self-quenching of nitrobenzoxadiazole labeled phospholipids in lipid membranes," *Journal of Chemical Physics*, vol. 100, p. 6019, 1994.

[8] D. Ramierz, W. Ogilvie, and L. Johnston, "Nbd-cholesterol probes to track cholesterol distribution in model membranes," *Biochim Biophys Acta*, vol. 1798, 2010.

[9] H. Jespersen, J. H. Andersen, H. J. Ditzel, and O. G. Mouritsen, "Lipids, curvature stress, and the action of lipid prodrugs: Free fatty acids and lysolipid enhancement of drug transport across liposomal membranes," *Biochimie*, vol. 94, pp. 2–10, 2012.

6

EVOLUTION, DIVISION AND MICROCHAMBERS

In the preceding chapters, we studied experiments performed in the lab during the course of four years. Though these were fruitful, there were many avenues that we explored that were either partially completed, or that we simply did not have time to pursue in depth. In this chapter we present some speculative ideas and initial experiments in the direction of in vitro evolution, and compartmentalization of reactions. To begin we explore the meaning of evolution, since from our perspective it is a word that is somewhat loosely defined. Then having settled upon a definition of evolution, we examine how it can be applied to the minimal cell and present the two keys to evolution. To be specific about how evolution can be applied in the laboratory we briefly present some experiments from the field of in vitro evolution. With that inspiration we propose three experiments based upon in vitro replication of DNA in compartments. Connecting back to the work of chapter 2 we explore the idea of dividing liposomes through lipid synthesis [1]. Finally in a brief experimental section, we present a few results obtained from a project on compartmentalization of reactions in fabricated microchambers, both for studying the effects of small volumes on biochemical reactions, such as protein synthesis in the PURE system, and as a tool for in vitro evolution.

6.1. THOUGHTS ON FUTURE DIRECTIONS

6.1.1. DEFINITION OF EVOLUTION

The semi-synthetic minimal cell is an ambitious project. To achieve the goals outlined in the introduction, it will require significant complexity. Though part of the goal of the minimal cell is to have a designed and controlled system, it is very likely that parts of such a complex system will be beyond rational design. Just as the electrical or mechanical engineer must sometimes use the tools of numerical modeling and simulation for difficult problems, so will the synthetic biologist need to resort to evolution. In this section the question of what is evolution, and what is required for it is examined, and then in the following sections we give examples of how it can be applied to the minimal cell.

What is evolution? some definitions of evolution are:

¨The gradual development of something¨ - Google

¨the process by which different kinds of living organism are believed to have developed from earlier forms during the history of the earth.¨ - Oxford English Dictionary

¨Biological evolution, simply put, is descent with modification¨ - Charles Darwin

The first definition, it seems is far too broad. Coastlines can erode, weather patterns develop and though well these may be considered to be evolving, it seems this definition is not precise enough or not applicable to biology. Living things are conscious, complex physico-chemical systems, they have strategies and awareness, whereas coastlines and weather patterns do not. In the introduction part of our definition of a living system was a complex system of molecules, which through the use of energy builds the physical and chemical catalysts that comprise the system. Are any alterations to this system evolution? We could broadly say that evolution occurs when random modifications to parts of a complex living system, affect a part of that systems' ability to sustain itself, for better or worse. This definition does not specify where such a system starts and ends, as living systems often do not have clear boundaries. A bacteria living in a human gut, requires the human host, which in turn requires the appropriate environment to thrive. However, it is always possible to make boundaries in a system to define individuals and this is how we get to the Darwinian definition. *Staphollococcus aureus* is not *Escherichia coli*, is not *Mus musculus*, is not *Homo sapiens*, moreover Celine Dion is not Vladimir Putin. Once we have an individual biological unit, the organism, we could say that a modification of which occurs internal to that unit and affects its survival is evolution of that individual. Here we have not specified that evolution is necessarily genetic, nor that reproduction is a requirement. New languages, tools, and behaviors certainly can be seen as forms of evolution, and can occur within a generation. A possible definition could be

I) Evolution: Changes in a part of living system (organism), which allows its continued existence in its environment.

While it is clear that under this definition an organism can evolve without reproducing, it is interesting to consider if an organism can truly survive without reproducing. It is

true that the molecules of life do not exist in their most thermodynamically stable states – that much is obvious due to their low entropy. Something must be done to maintain these states in the long term. The two strategies are to be repaired or recycled. In principle if an organism could repair or recycle all of its components, it could be immortal. Practically however this appears not to be a strategy, even in single celled organisms [2] – this is likely due to energetic cost to repair and recycle compared to starting over. That brings us to our working definition of evolution.

II) Evolution: Changes in a part of living system (organism), which allows its continued existence in its environment, which over long time scales, implies descent with modification.

6.1.2. APPLYING EVOLUTION TO THE MINIMAL CELL

Having elaborated and explored the meaning of evolution, we will return to practical questions about how we can use evolution to aid in our design of living systems.

The end goal as stated in the introduction is to have a cell which can be programmed and continuously survive in a laboratory environment, where a relatively complex mixture of nutrients are provided. We have discussed the minimal cell in the introduction as having the ability to metabolize, have a container which specifies a boundary that can grow and divide, representing the unit of replication, and have genes which encode the above processes and that can themselves be replicated with the possibility for mutation, which is necessary for evolution. That is to say, we will have a replicating evolving semi autonomous organism, able to survive in a specific laboratory environment.

We also discussed in the introduction, how in the end, the functions of the semi synthetic minimal cell will be carried out by proteins, DNA and RNA. The bottom up approach we are using is to encode protein functions in DNA, and express in the PURE system these encoded functions. There are many intermediate obstacles along the way. The accurate folding of proteins from various organisms in the new setting of a minimal cell. The activity and specificity of proteins involved in metabolism. The tuning of control networks, i.e the coordination of expression levels of proteins for the efficient coordination of cellular activities, such as when to initiate division, or DNA replication. Similarly the amount of proteins or metabolites to control the biophysical properties of the cell, e.g. the amount of membrane division proteins to properly divide a cell, the control of lipid composition to affect permeability, or to cause membrane deformations leading to cell division. How can we use evolution, i.e descent with modification, to succeed at these tasks.

The answer is that to have evolution, there are two keys, replication of the genome with some modification, (that is descent with modification), and spatial separation of individual genomes based upon there ability to perform the task at hand, that is generally referred to as the genotype to phenotype linkage. *In vitro* evolution is the field which plays with various ways to select for genomes encoding to their specific functions, at the DNA, RNA or protein level which we will now explore.

6.1.3. IN VITRO EVOLUTION: STRATEGIES FOR THE GENOTYPE TO PHENOTYPE LINKAGE

To start we will review some of the classical ways of playing with evolution in the laboratory. As is well known double stranded DNA has an aperiodic structure composed of four chemical bases A,T,C,G - which are transcribed into RNA that is then translated into proteins [3]. At both the RNA and protein level, catalysts form. Modifications can be made to the DNA sequence, which usually occurs when a copy of it is made, i.e. mutations. When this occurs, new forms of RNA and proteins can also form, which may have new physical or chemical properties that can significantly affect the properties of the system, such as protein folding, enzyme activity or more global properties such as a network property, for instance, the period of an oscillating circuit, or global physical properties such as the composition of a membrane. The sequence of DNA is referred to as the genotype and the resulting system properties are referred to as phenotypes. In classical molecular biology mutations are generated in organisms by techniques such as UV irradiation, and phenotypes are strains that for instance, are temperature-sensitive for enzyme activity. An example of that is the strain found with a temperature-sensitive version of *plsB* [4] . In the next sections we will explore via a review of the literature the types of genotype to phenotype linkages that may be used for laboratory evolution of biological systems that cannot achieve evolution autonomously, e.g. the components needed to build the minimal cell.

AN EXAMPLE OF AN IN VITRO SELECTION EXPERIMENT: BINDING

In the simplest *in vitro* evolution experiment, the phenotype of better binding of a protein to a ligand is selected for by attaching the ligand to a surface, expressing the protein from a pool of sequences that have had some variability generated in them, linking the protein to the genotype and then co-purifying the protein and the genotypic sequence that codes for the better binders thus establishing the genotype to phenotype linkage. The oldest way of doing this is based upon phage display [5], a technique whereby a sequence encoding a protein is inserted into a phage genome as a fusion to one of the phage coat proteins. A typical application of phage display is in selecting antibodies against a given target, that is immobilized to a surface and allows for the selective purification of active antibodies on the phage surface. Antibody libraries can be created by harvesting the RNA from an immune cell, creating a cDNA, performing a PCR on the VH, and VL regions of immunoglobulin genes and then constructing randomized vectors that code for a fusion protein with the coat protein, which are then electroporated into cells along with a support vector which contains the rest of the phage proteins [6]. The resulting phages displaying the proteins are harvested and used in binding experiments.

In this example we see a technique for generating sequence diversity which results in various phenotypes, and then selecting for the phenotype. Descent with modification occurs because the parent RNA sequences from the immune cell are screened, and after selection only a few of the sequences are used for therapeutic purposes. Further evolution can occur by introducing errors in the sequences and then performing additional rounds of selection [7]. A possible application of binders in a minimal cell would be to increase the affinity of DNA-binding proteins to DNA, e.g in the design of a basic form of chromatin.

SUMMARY OF IN VITRO EVOLUTION TECHNIQUES

To summarize some of the existing work in *in vitro* evolution tables 6.1 and 6.2 show techniques developed to perform directed evolution, the targets that the techniques are applicable for, their genotype to phenotype linkage, and some of their principle advantages. In general we can divide these experiments into two classes, the binding class and compartmentalization class. In the binding experiments shown in table 6.1 the genotype to phenotype linkage is based upon a variation of the phage display techniques where genotype and protein are physically linked and the phenotype is the ability of the pair to bind to a surface or a ligand, which then establishes the phenotype to genotype linkage. In the compartmentalization experiments of table 6.2 the genotype to phenotype linkage is established by co-localization of DNA and protein in an emulsion droplet or liposomes. The compartmentalization experiments can be further divided into two classes, those based upon sorting of genomes, either by cytometry or affinity and those based upon amplification of genomes.

6.1.4. PROPOSED EXPERIMENTS

Although all the types of experiments listed have potential applications for the minimal cell, it is the experiments based on amplification of the active genomes that we find particularly powerful, i.e the *RNA replication in a cell-free system* experiments of Ichihashi et al. and the *Compartmentalized Self Replication* experiments of Ghadessy et al. In the former, an RNA encoding a Qβ replicase is expressed *in vitro* in a compartment and the expressed replicase can then replicate its on genome. Compartmentalized self replication is more involved, with encapsulated cells expressing plasmids that encode proteins that allow for the amplification of the coding part of the plasmid, which is then ligated into new plasmids and put into new cells, then the cycle repeats. The strength of these experiments is that they do not require complicated sorting, or finicky binding procedures but rather rely on routine reactions that can be performed in a test tube. In fact it is the self referential amplifying quality of the experiments that make them able to undergo continuous evolution in a similar manner to living cells. The key step is to close a loop between encoding DNA, the function of some RNA or protein, and the replication of that DNA. Although we thought of many directed evolution experiments, we focus here on details of three experiments.

EVOLUTION OF A DNA POLYMERASE

As a proof of principle experiment, we propose a simple DNA replication similar to those of Ghadessy et al. in *Compartmentalized Self Replication*. We propose to express a Taq polymerase from *Thermus aquaticus* in PURE system encapsulated in an emulsion with on average less than one DNA molecule per emulsion droplet along with primers and dNTPS. Then the DNA would be replicated in a PCR reaction. The emulsion is broken and the cycle repeated. Why would we choose to use Taq polymerase? To make an evolution experiment, it is necessary that there are errors in the replication, otherwise the "modification" part of descent with modification is lost. The Taq polymerse error rate is 1/9000 and the size of the gene is 832 base pairs so approximately one in ten replications will have a mutation. Depending on the exact conditions, it may be this rate does not produce many effects on the time scale of an experiment, so it may be necessary to

Name of technique	Evolution Target(s)	Genotype to phenotype linkage	Advantages
Phage display [8]	antibodies, vaccine devlopment, protein protein interactions, peptide mimics of non peptide ligands	Protein of interest fused to coat protein of phage which contains the DNA encoding that protein	large libraries > 10^9 amplifiable in *E. coli*
Ribosome Display [9]	principally binders,e.g scFV antibodies, or DARPins, (designed ankyrin repeats)	stalled ribosome due to absence of stop codon causes mRNA to remain linked to protein	completely in vitro, allows for larger libraries, including sequence randomization through PCR,
Puromycin Derivative/mRNA peptide fusion [10]	similar to Ribosome display	Puromycin ligated to mRNA in low concentrations will specifically incorporate in a polypeptide at the C–terminus linking mRNA to protein	completely in vitro, allows for larger libraries, including sequence randomization through PCR
STABLE [11]	similar to Ribosome display	Protein of interest and streptavidin fusion. DNA with biotin tag is expressed in emulsion, streptavidin fusion binds biotin DNA then emulsion is broken and protein remains linked to DNA	stable linkage of DNA to protein, DNA more stable than RNA

Table 6.1: Various types of *in vitro* evolution based upon proteins with their genotype attached binding to ligands.

Name of technique	Evolution Target(s)	Genotype to phenotype linkage	Advantages
Microbead Display [12]	enzymes that create a molecule with free radical and fluorescent functionalities	beads that have genotype and protein phenotype linked to them react with a fluorescent molecule causing it to also bind to the beads which are sorted by flow cytometry	allows sorting of sequences that cause reaction and binding by flow cytometry
Compartmentalized Self-Replication (CSR)[13] / Cooperative CSR	polymerases, (thermostability, inhibitor resistance), enzymes linked to better production of a DNA molecule	CSR: Polyermase gene encoded in *E. coli* plasmid captured in emulsion, cells express genes and rupture and PCR polymerase replicates its own gene. Co-CSR gene that encodes a protein that makes dNTPs that allows co-encapsulated polymerase to replicate the gene	allows evolution of polymearses, transcription factors, RNA polymerases
Cell like compartmentalization [14] [15] [16]	enzymes which can modify DNA, similar to CSR	methyltransferase expressed in emulsion, methylates its own biotynalated template which prevents its cleavage by a restriction enzyme allowing purification by the biotin	extends evolution in compartments to methyltransferases
In vitro compartmentalization [17]	any substrate/product pair that can have an antibody raised for it, and also have a caged biotin moiety	beads have genotype and protein phenotype linked to them in emulsions. Protein reacts caged biotin substrate to make caged biotin product, caging is released and product binds to bead and then is labeled or purified by antibody	allows evolution of enzymes (with some requirements)
Fluorescence activation of double emulsions [18]	enzymes with fluorescent product	genes and enzymes in a double emulsion convert a non fluorescent substrate into fluorescent product and emulsion is sorted by cytometry	allows evolution of enzymes with fluorescent product
Screening of Liposomes [19]	enzymes with fluorescent product of fluorescent proteins (GFP)	liposomes encapsulate genes for variants of a fluorescent protein that are expressed and liposomes sorted by cytometry	Liposomes are more stable than double emulsions, better contain reagents
Replication in a cell-free system [20]	Qβ Replicase	Qβ Replicase mRNA is expressed in emulsion and replicates itself	positive feedback loop is self reinforcing.

Table 6.2: Various types of *in vitro* evolution based upon co encapsulation of enzymes and genomes in compartments.

further increase the rate of mutation by using an enzyme such as Mutazyme II which makes errors at a rate of about 4.5-9 mutations per kb. We can speculate on how various selection pressures should play out in the evolution. For instance if very long templates are used (with non coding regions flanking the gene to increase length and primers hybridizing at the far end of templates), and a very short extension time, then replication rate (existing Taq rate 35-100 nt/sec), and processivity (exisiting processivity 50 bp) will be selected for. Also the number of temperature cycles is important, a single cycle will give the expressed enzymes only one "chance" to replicate its genome. This should also decrease the error rate of the polymerase over rounds of expression and replication as errors that do not produce viable offspring would be more lethal. In that instance it would be better to start with the Mutazyme enzyme, and see if the error rate could be reduced. In the work of Ghadessy et al. [13], they did not generate diversity from the self replication process by the errors of the compartmentalized reactions themselves but rather by error prone PCR in an initial step before the first round of screening. It would therefore be novel and interesting to see if it would be possible to generate new variants of polymerase by making constraints on the self replication process itself. In the work of Ichihashi et al. [20] they did indeed see initially an increase in the mutation rate correlated with the number of copies made per round and it leveled out once the number of replications per round plateaued. Thus we predict that the mutation rate can be controlled by the number of PCR cycles per generation. For instance in should be possible to create polymerases with an increased mutation rate by making many copies per generation. Another possibility is to select for resistance to inhibitors such as heparin, as done by [13]. In this instance one would expect to select for better ability to amplify in the presence of heparin. It may also be possible to increase the mutation rate, because if no mutations are occurring then resistance cannot evolve, however considerations about the number of copies per cycle should be remembered. It may also be that the harshness of the conditions (concentration of heparin for instance) affects the mutation rate because new variants must be discovered faster under harsh conditions to survive. Another interesting experiment, would be to invoke competition between polymerases, which could be done by replacing the emulsion with pore-equipped liposomes, and then decreasing the total number of dNTPs, that would force the polymerases in individual liposomes to likely increase their speed of replication to compete for dNTPs. It is also possible that the rate of evolution would also increase due to the need for innovation in those harsh conditions.

Already from a simple DNA replication experiment we see that many types of experiments can be performed that may provide interesting varieties of *in vitro* evolution. We will now consider how evolution could be applied to two key areas of the minimal cell.

AMPLIFICATION OF GENES THAT ENHANCE TRANSLATION

A major obstacle to creating a minimal cell from the PURE system is that after three hours of translation, the PURE system stops. In our laboratory, we are investigating systematically possible reasons for that. There is a hypothesis that there is a small molecule toxin of some sort produced during transcription or translation that can shut down protein production. This hypothesis stems from the fact that in cell extracts an extension of the expression time of as much as 20x can occur when the reaction occurs in a dialysis chamber supplied with solution of amino acids and nucleotides from the outside [21].

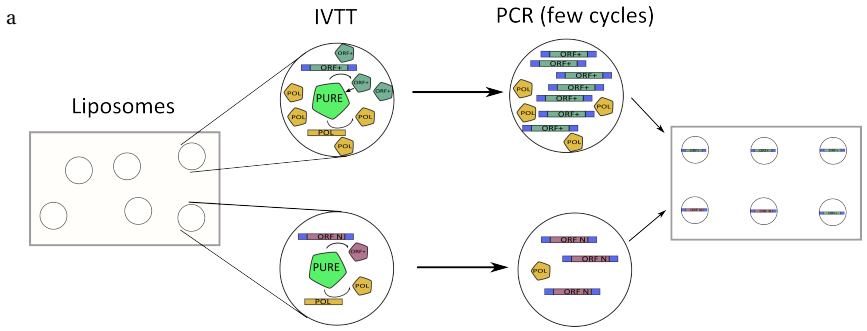

Figure 6.1: | Schematic of a *in vitro* evolution experiment to amplify genes that aid protein expression Liposomes are formed. In each liposome there is encapsulated PURE system, and ORF gene (single copy) with flanking regions identical for all ORF genes, and polymerase gene, as well as primers, NTPS (both not shown). The PURE system expresses the ORF gene and the polymerase genes. If the expression of the ORF gene improves the yield of the PURE system (ORF+), more polymerase will be expressed than if the ORF gene is neutral (ORF N). A PCR step then amplifies the ORF genes in all liposomes, the final number of ORF genes in any given liposomes will be proportional to the number of polymerases expressed in the IVTT step. The cycles repeats and eventually beneficial ORF genes (ORF+) comprise the majority of the population.

There was a similar effect when *E. coli* extracts were encapsulated inside lipid vesicles [22] and placed in a feeding solution consisting of nucleotides, amino acids, salts and sulfahydryl compounds (DTT, β mercaptoethanol). To our knowledge these results have not been reproduced in PURE system, neither in our lab or elsewhere. This points to the possibility that it is not simply a small molecule that can diffuse out of the dialysis chamber but there might be a crucial component present in the cell extract that is not present in the PURE system that allows metabolism of toxins. Similar to a concept recently introduced in the literature [23], we present a method to search for the responsible genes. We propose to encapsulate in liposomes, equipped with α-hemolysin to create an open system (to feed reactions, to enhance competition between liposomes as well as provide dilution of toxins), the PURE system, a gene encoding for a polymerase, and all 4,123 open reading frames of *E. coli* or some subset thereof as well as a primers pair (all genes would have the same flanking region) for the ORF genes and dNTPs. If the concentration of the templates is such that nearly all the liposomes contain a least one copy of the polymerase gene, along with a single gene of the open reading frame library, then when the templates are expressed, it is expected that a combination of polymerase and a random ORF gene would be expressed. Should the ORF gene enhance the lifetime of the PURE system, then an increased amount of protein, including polymerase, would be produced. If the primers encapsulated that only hybridize with the ORF constructs, and that sufficient rounds of PCR are made, so that the number of genes that pass to the next generation is proportional to the amount of polymerase, then the amplification process will favor the genes in vesicles that enhanced translation. The presence of a non helpful gene also has the effect to decrease the total number of polymerases present per vesicle, thus decreasing the viability of that compartment. This procedure is illustrated in figure 6.1. It would also be possible to perform the experiment with increased numbers of ORF genes per cell, so that allosteric effects could be selected for. It should be that

after multiple rounds of selection, the population of genes would decrease to only a few helpful genes. In either case, i.e. with single copy or multiple copy genes, after several rounds of encapsulation and replication, the genes can be sequence by next generation sequencing technologies, that spatially separate individual molecules before amplifying them and then obtaining sequence information from the amplified group of molecules [24]. Comparing sequence information to a full genome sequence of *E. coli* will allow the identification of which genes enhanced expression.

RIBOSOME EXPRESSION, POST TRANSLATION MODIFICATIONS OF RRNA

A very important part of the minimal cell is the synthesis of the ribosome. Although DNA replication is necessary for evolvability, the ability to produce the ribosome is not only important for the propagation of the minimal cell, but for its intermediate term survival, since if ribosomes are damaged the production of proteins will stop and so will other functions. The *E. coli* ribosome consists of two subunits, the 30s and 50s subunits. The 50s subunit itself consists of the 23s and 5s RNAs and more than 30 proteins. Structural studies of the 50s subunit report more than 31 proteins [25], whereas a study of RNA chaperone activity of the large subunit proteins studied 34 recombinant proteins [26]. The 30s subunit consists of the 16s RNA and more than 20 proteins. According to a structural study the 30s subunit consists of 21 proteins, [27], though active 30s subunits were made from 20 recombinant proteins [28]. The eventual goal would be to be able to synthesize all these components and assemble them in the PURE system. The current state of the art for *in vitro* ribosome assembly is to assemble them from purified proteins and expressed RNAs in *E coli* cell extracts supplemented with a cytoplasmic mimicking buffer [29]. The ribosomal proteins and rRNAs were separated according to established protocols [30]. Active ribosomes which expressed firefly luciferase were assembled from the total protein extract of the 30s and 50s subunits and either purified ribosomal RNAs, or RNAs expressed in *E. coli* cell extracts. All of this was done with cytoplasmic mimicking buffers. The following combinations of proteins and RNA were used to assemble ribosomes: (i) 30s proteins and purified 16s RNA, along with purified intact 50s subunits. (ii) The same as preceding except with 16s RNAs *in vitro* expressed in cell extract. (iii) 50s proteins and purified 23s and 5s RNAs along with purified intact 30s subunits. (iv) The same as preceding except with the 23s and 5s RNAs *in vitro* expressed in cell extract. (v) The combination of both 50s proteins and 30s proteins as well as the the purified 23s, 5s and 16s RNAs. (vi) The same as preceding except with all the RNAs expressed *in vitro* in cell extracts. It was also attempted to assemble ribosomes in the PURExpress system. It was possible to assemble active ribosomes from the proteins of the 50s and 30s subunits, along with purified ribosomal RNAs. It was also possible to use *in vitro* expressed 16s RNA with 30s proteins complemented with purified intact 50s subunits to express luciferase in the PURExpress, though the amount was greatly reduced as compared to when purified 16s RNA was used. When 50s proteins, and in vitro expressed 23s and 5s RNA along with purified intact 30s subunits, were put in the PURE system, luciferase was not expressed at all, whereas with purified 23s and 5s RNA it was. This suggests that modifications of the RNAs by proteins in the cell extract are crucial for ribosomal function. It is the proteins that make these modifications that we propose to search for with a similar screening technique as proposed for enhancing translational activity above.

The 5s RNA lacks nucleoside modifications and is short, so it is unsurprisingly active when transcribed *in vitro* [31]. The 16s RNA has 11 modifications in *E. coli*, though it is possible to assemble the subunit and bind tRNA without the modifications [32]. However, using *in vitro* expressed 16s RNA lacking these modifications to assemble ribosomes yields less active ribosomes than ones assembled with purified 16s RNA [29]. 23s RNA has 23 post translational modifications and ribosomes assembled with *in vitro* expressed RNA are 30 fold less active than when purified RNA is used [33]. Of these 23 post translational modifications, all but 6 have been excluded as being absolutely necessary [34]. Of these 6, two are known to be individually dispensable [35]. 3 of the remaining four genes have recently been identified [36] [37] [38]. This leaves at least one key undiscovered enzyme, and possibly other RNA modifying enzymes that may enhance ribosomal activity.

We would suggest a similar approach as recommended with the amplification of genes enhancing translation above. We propose to encapsulate in an emulsion all or some of the ORFs from *E. coli*, the 5 known key ribosomal modifying enzymes genes, the 50s and 30s ribosomal proteins, the genes for the 5s 16s (specially modified) and 23s RNAs, a specially modified polymerase gene, and primers pairs for the ORF genes. The specially modified 16s RNA has instead of the cognate sequence to the Shine Delgarno sequence a new sequence. It's cognate sequence is then included in the mRNA of the polymerase gene. This is a so called orthogonal ribosome mRNA pair [39]. If the ORF proteins are included at less than one per emulsion droplet, and the other genes for the rRNA as well as the rRNA modifying genes are included so that there is at least one of each gene per droplet. Then when the ORF genes are expressed, if functional ribosomes are assembled, they will express the polymerase gene, which upon temperature cycling will amplify the genes that add functionality to the ribosomes. After several rounds of selection next generation sequencing will identify which of the ORFs had a positive effect. It would also be possible to include the ORF genes at hundreds of copies per compartment in the experiment so that droplets that had combinations of useful genes would express the polymerase effectively. After many rounds of selection the multiple useful genes would comprise most of the population.

6.2. GROWTH AND DIVISION, TOWARDS AUTONOMOUS SELF REPLICATION

We have discussed in the previous section how the replication plays an important role in the minimal cell, and how it can be use to improve the properties of part of the minimal cell through evolution. However for these processes to become entirely autonomous and self regulating i.e. to operate from a completely bottom up approach, it is necessary that the individual cells must replicate and divide their own compartments. Here we will discuss routes to continued growth and division of membranes.

In chapter 2 - 4 of this thesis, we addressed in detail the first steps of growth of membranes from acyl coAs. In short summary we used the *E. coli* lipid biosynthesis genes, *plsB*, *plsC*, *cdsA*, *pgsA*, *pgpA*, *pgpC*, *pssA* and *psd*, to produce the lipids LPA, PA, CDP diacylglycerol, phosphatidylglycerol phosphate, phosphatidylglycerol, phosphatidyl serine and phosphatidylethanolamine. It so far was not possible to increase the membrane

content by more than a 1%. An obstacle that we foresee for the continuous growth is that one of the necessary precursors, acyl coA has a structure very similar to a surfactant, and therefore may be able to disrupt liposomes. It may therefore necessitate the growth of vesicles from shorter more water soluble precursors, as is done in the *E. coli* palmitate biosynthesis pathway [40]. More attractively one could employ the single enzyme complex for palmitate synthesis FAS B of *Brevibacterium ammoniagenes* that has been reconstituted from purified proteins *in vitro* [41] and that requires only NADPH, H+, malonyl coA and acetyl coA to function.

To achieve the division of liposomes, requires a detailed understanding of both the biochemical and biophysical processes involved. In a previous work we discuss how there are two possible and non mutually exclusive routes to division, that of membrane deforming proteins, and that relying only on the physical properties of liposomes and their lipid content, tunable through lipid biosynthesis [1]. Here we focus on the latter due to its relation to membrane synthesis.

There is much work that supports the idea that minimal cell division could occur through the properties of lipids alone. Recent work by Mercier et al. showed that excess membrane synthesis in *Bacillus subtilis* was sufficient to drive the proliferation of so called L-forms, i.e. strains without the ability to synthesize the cell wall [42]. A work by Sakuma et al. [43] showed that the combination of crossing the lipid phase transition temperature of DPPC, and the presence of inverse coned shaped lipid, DLPE, could result in multiple generations of liposome division. The parallels between L-form studies, and those of giant vesicles was reviewed elsewhere [44].

Based on the results with L-forms, an almost naive approach to generate cell division could be the simple synthesis of lipids to create excess membrane area. Mercier et al. described that rod-like filamentous cells obtained by the growth of *Bacillus subtilis* in the presence benzamide, an inhibitor of cell division, upon the digestion of cell wall with lysozyme, formed L-form like shaped protoplasts. This result was attributed simply to excess area of the filamentous cells as compared to their volume. As mentioned above we are able to synthesize many membrane lipids using *E. coli* machinery. If the efficiency of lipid synthesis can be increased, then microscopy studies of GUVs synthesizing lipids are called for, though there may be the obstacle that to create the same increase in area to volume ratio, more lipids must be synthesized per vesicle for the larger sized vesicles visualizable by fluorescence microscopy than for smaller bacteria sized vesicle. If the aforementioned difficulty of surfactant like properties of acyl-coA precursors can be overcome, either through gradual supply of precursors by flow, or by fatty acid synthesis, one might expect a similar result as to the one found for L-form like protoplasts.

Another evidence that increased membrane synthesis could lead to vesicle fission was found theoretically [45]. Using the so called spontaneous curvature model of Helfrich [46], Svetina calculated a shape trajectory for a vesicle whose surface area is increasing due to the addition of lipids and that leads to division. He found that so long as the doubling time for vesicle area growth, the bending modulus, the intrinsic curvature (the curvature of the membrane if it is in a completely relaxed state, determined by the shape and number of lipids in each leaflet) and the hydraulic conductivity of the membrane are interrelated in a specific way, then vesicles can grow and divide.

An alternative approach to achieve division is as opposed to changing the area of

the membrane by adding lipids, is to do so by change in temperature that changes the phase of the lipids. In the work of Sakuma et al. [43] they observed multiple generations of both budding and birthing of vesicles depending on the lipid composition when temperature cycling across the phase transition temperature of one of the lipids. Specifically, they observed that liposomes that contained a fraction of DPPC and a fraction of DLPE underwent budding and birthing when crossing the T_m of DPPC. Budding is when a new vesicle is formed from an outward protrusion of the mother vesicle and birthing is when a new vesicle is formed from and inward protrusion that is eventually expelled from the mother vesicle. For larger amounts of DPPC, outward budding occurs, for lesser amounts of DPPC, inward birthing occurs. The authors explain the shape deformations with the so called area difference elasticity model [47]. Another implementation of that model was made by Svetina [45]. There they give the energy of the vesicle as:

$$w = w_b + w_r = (1/4) \oint da(c_1 + c_2 - c_0)^2 + \frac{k_r}{k_c}(\Delta a - \Delta a_0)^2 \tag{6.1}$$

where w_b is referred to as the local bending energy, and w_r is referred to as the non local bending energy. That is because as we will see, the w_b term depends on the curvature at a single point, whereas the w_r term depends on an integral of the curvatures over the entire vesicle shape. Likewise, the terms k_c and k_r are the local and nonlocal bending modulii. The other variables are defined as follows $c_1 = C_1 R_s$ and $c_2 = C_2 R_s$ are the so called reduced curvatures of the vesicle surface, with C_1 and C_2 the actual vesicle curvatures and $R_s = \sqrt{\frac{A_0}{4\pi}}$ where A_0 is the total surface area of membrane in equilibrium. Similarly the term $c_0 = C_0 R_s$ is the reduced intrinsic curvature, with C_0 the curvature of the membrane in a relaxed state (which can be non-zero due to shape and distribution of lipids). $\Delta a_0 = \frac{\Delta A_0}{8\pi h R_s}$ where $\Delta A_0 = A_2 - A_1$ are the initial area of the outside and inside leaflet of the membrane and h is the thickness of the membrane. $da = \frac{dA}{4\pi R_s^2}$ is the reduced area differential with dA the normal area differential. $\Delta a = \frac{1}{2}\oint c_1 + c_2 da$. If one minimizes the local bending energy w_b subject to constraint on the vesicle volume V and the vesicle surface area $A \approx A_0$ with the spontaneous curvature set to $c_0 = 0$ then one obtains shape equations that can be solved to obtain the following phase diagram with the axis of reduced volume $v = V / \frac{4\pi R_s^3}{3}$ and reduced area difference Δa figure (6.2).

The axes are v and Δa. It can been seen that as one moves along the x axis from right to left corresponding to increased vesicle surface area, one progresses from birthing like shapes to budding like shapes. This corresponds well to the the fraction of DPPC in the work of Sakuma, as for low fraction of DPPC, the birthing or cup like behavior is displayed, and for large fraction of DPPC, budding or pear like behavior can be observed. These sorts of phase diagrams can therefore be used to guide future experiments, and more detailed descriptions of the shapes can be found elsewhere [48] [47].

In the work of Sakuma [43] they also discuss the role that the DLPE plays. They indicate that it can help to destabilize the neck of budded vesicles encouraging complete division [49]. It is also clear by synthesizing new lipids, it is possible to alter both the surface area of the vesicle A_0, and the preferred area difference ΔA_0 by altering the number of lipids in the membrane as well as their distribution between the two leaflets. Finally, though it may be true that the PURE system does not perform well for temperatures

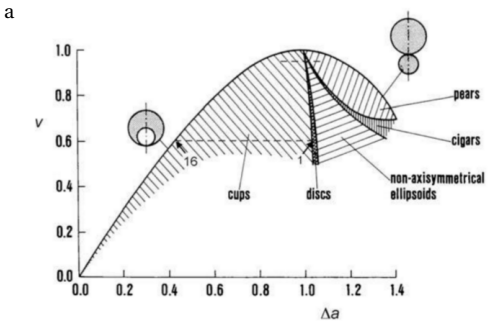

Figure 6.2: | Phase diagram of lipid shapes in the area difference elasticity model.
Axis are v and Δa and it can be seen that moving along the x axis predicts the shapes found in the work of Sakuma [43].

above 37 °C [50] thus making temperature cycling above the phase transition temperature of DPPC problematic, this can be solved by reducing the chain fatty acids of some of the lipids from 16:0 to 14:0 which should decrease the melting temperature. Another obstacle may be that the enzymes for lipids synthesis may not function as well in the gel phase though that remains to be tested.

6.3. MICROCHAMBERS, A COMPARTMENTALIZATION APPROACH

6.3.1. INTRODUCTION

The compartmentalization of biochemical reactions is important for many reasons. For instance, in a PURE*frex* system reaction with many components, one can expect that in volumes of 1 μm the number of molecules per chamber and hence the expression per chamber may vary due to stochastic effects of encapsulation [51]. This can be expected because a single molecule in a 1 μm^3 chamber has a concentration of 1.66 nM and the concentrations of proteins in the PURE*frex* system ranges from 20 nM to 5000 nM. Not only that rate constants of chemical reactions may be increased because of increased effective concentrations [52]. To study in detail the effects of compartment size, it would be useful to fabricate compartments of a controlled size [53], as opposed to the stochastic sizes obtained by encapsulation in emulsions [54] or liposomes [55] [50] [22]. In addition to confinement effects, encapsulation is important for evolution experiments, both to establish the genotype to phenotype linkage [20], [13] [19], as discussed above, and to prevent the error catastrophe from occurring in self replication experiments [56]. Furthermore the uniformity of size decreases the variation between chambers that might otherwise bias the evolution experiments towards larger or smaller chambers. With all these things in mind, we investigated the possibility of making microchambers out of various materials. Polydimethylsiloxane (PDMS) is a widely used material for microfluidics and easy to use, and is thus a good starting point. Agarose and polyacrylamide are hydrogels, and may be more biocompatible than PDMS as well as being able to support diffusion of nutrients from the surrounding gel resulting in a semi-open system.

In detail, PDMS is a polymer that can be purchased as a two part resin system, which

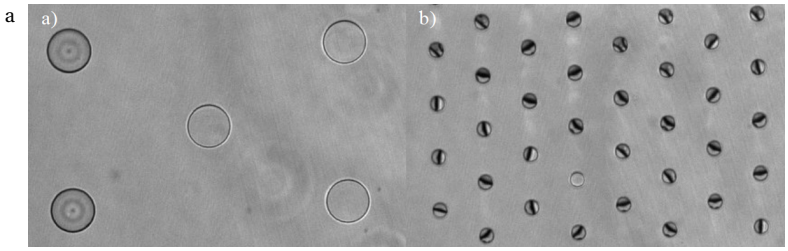

Figure 6.3: | Bright field microscopy of PDMS microchambers.
(a) 30 μm diameter (7pl) microchambers filled with fluoroscein solution, b) 10 μm diameter (0.8 pl) microchambers partially filled with fluoroscein solution. Pretreatment of the chambers with oxygen plasma improved the filling (not shown).

upon mixing polymerizes. The resulting polymer is optically transparent and thermally and chemically stable. The polymerized PDMS is also porous, which can lead to diffusion of small molecules and unwanted drying. In addition to absorption, small molecules can also be adsorbed to the surface, especially polar molecules which can interact via hydrogen bonding to the siloxane group of PDMS. Examples of molecules than can adsorb include fluorescent dyes, organic solvents and proteins [57] [58], though this can be reduced by treating the surface with bovine serum albumin or chemically functionalizing the surface with silanes. In a pilot experiment we made PDMS microchambers and encapsulated the PURE*frex* system in them and monitored obtained expression of a fluorescent protein.

In a parallel approach to the PDMS microchambers, we also experimented with forming microchambers out of agarose and polyacrylamide. The reason for that was to create a semi open system in which small molecules, but not proteins, can diffuse in and out of the chamber. This may extend the lifetime of the PURE reaction, based on results with cell extracts [21]. For evolution experiments it would also allow for competition between chambers. Both agarose and polyacrylamide are hydrogels, which means that they can contain large amounts of water within them, supporting the encapsulation of a feeding buffer for the PURE*frex* system, which among other components contains amino acids and NTPs. Towards this goal we formed agarose and polyacrylamide gels in 96-well plates, which had a smaller well (with gel walls) inside the well. These experiments were made to conduct assays to test whether the gels could retain the protein and tRNA components of the PURE*frex* system, while allowing the diffusion of small molecules in and out of the chambers.

6.3.2. RESULTS AND DISCUSSION

GENE EXPRESSION IN PDMS MICROCHAMBERS

It was possible to successfully form and fill chambers out of PDMS. First the chambers were formed, then cured and then cleaned in ethanol by sonication and exposed to oxygen plasma. The exposure to oxygen plasma made the chambers hydrophilic and activates the surface of the PDMS so that it can covalently bind to glass. The solutions (either a carboxyfluoroscein, solution, or PURE*frex*) were then put in the chambers (5 μl) covered with a cover glass and clamped in a vice. This was sufficient to seal the chambers

insofar as was when a chamber was photobleached, the fluorescence did not recover (not shown). An example brightfield image of formed chambers is shown in figure 6.3. Unfortunately however, after approximately half an hour, the chambers dried out (not shown). When the PURE system was encapsulated in the PDMS microchambers and monitored with the microscope, an increase in the fluorescence was observed, as shown in figure 6.4. The increase in intensity of three hours is more than two standard deviations, implying that the increase was significant. The expression however appears to flatten out at 30 minutes. Normally in a PURE system reaction this does not occur until at least two hours, though there is precedent in the literature for a expression time of approximately 30 min in microchambers of 7 pl volume [53]. The second phase of increase may be due to drying, as that will concentrate the fluorescent protein. Experiments were performed whereby the outer perimeter of the glass PDMS interface were sealed with vacuum grease, two component epoxy or candle wax. However, none of those approaches mitigated the drying, which suggest absorption of the liquid by the PDMS. Altogether the fact that it was possible to express proteins in a microchamber is an encouraging result, both for studying reaction kinetics and volume effects and also for creating compartments for evolution experiments. In the future better passivation of surfaces and a technique to prevent drying will need to be developed to pursue this avenue further.

DIFFUSION ASSAYS IN HYDROGELS

We are interested in making a microchamber that is open to flow of small molecule nutrients and toxins in an out of the chamber, whereas macromolecules such as proteins and tRNA should remain in the chambers. An approach to that would be to make hydrogels containing nutrients and with chambers or microchambers molded into the hydrogels. Alternatively it would be possible to seal PDMS microchambers with a hydrogel pad. To

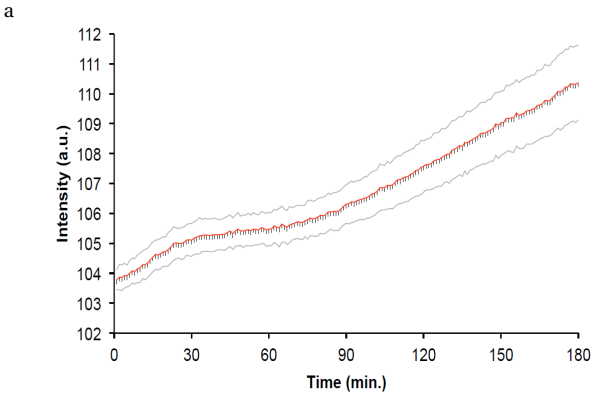

Figure 6.4: | PURE system expression of emGFP in microchambers.
(a) Average intensity of 60 PDMS microchambers (10 μm diameter, 0.8 pl) during emGFP protein synthesis by the PURE system. The standard deviation is shown in grey. The intensity increases for 30 min, then halts for 30 min and subsequently increases again after 60 min. The first increase is likely due to protein expression and the second may be attributed to drying of chambers concentrating the expressed protein

assess the permeability of the agarose and polyacrylamide gels, we measured the diffusion of carboxyfluorescein, YFP and BODIPY-labeled tRNA through them. To do this we made a well in a hydrogel which itself is in a 96-well plate as shown in figure 6.5 a. To make the well, first the unhardened gel solution is put in the 96-well plate, and then a form with the shape of the smaller well is placed into the larger well before the gel hardens. We first studied agarose because of its non-toxicity and ease of use, and its reported ability to immobilize single enzymes [59]. The maximum percentage of agarose we could use well still being able to handle it easily was 2.5 %. Figure 6.5 shows that the agarose gel was not able to prevent diffusion molecules out of the well, neither the carboxyfluoroscein, BODIPY labeled tRNA or purified YFP were retained in the well.

We proceeded to make wells out of polyacrylamide. There is a difficulty with making wells from polyacrylamide in that the polymerization reaction only occurs in the absence of oxygen. Thus the molding form must fit tightly in the well, and even then the gels did not always polymerize. Despite reliability issues it was possible to make gels to test the diffusion of the YFP, bodipy tRNA and carboxyfluoroscein. As can been seen in figure 6.5 c) a 20% polyacrylamide gel effectively retains YFP in the well, partially contains the BODIPY tRNA whereas the carboxyfluroscein is not retained. The molecular weight of tRNA is approximately 26 kDa and though YFP is similar (26 kDa) it also forms dimers. This can explain why the YFP is retained in the well but not the tRNA. Alternatively it may be that the ester bond binding the BODIPY to the tRNA is partially hydrolysed, allowing the BODIPY to diffuse out of the well. An attempt was made with a 26%

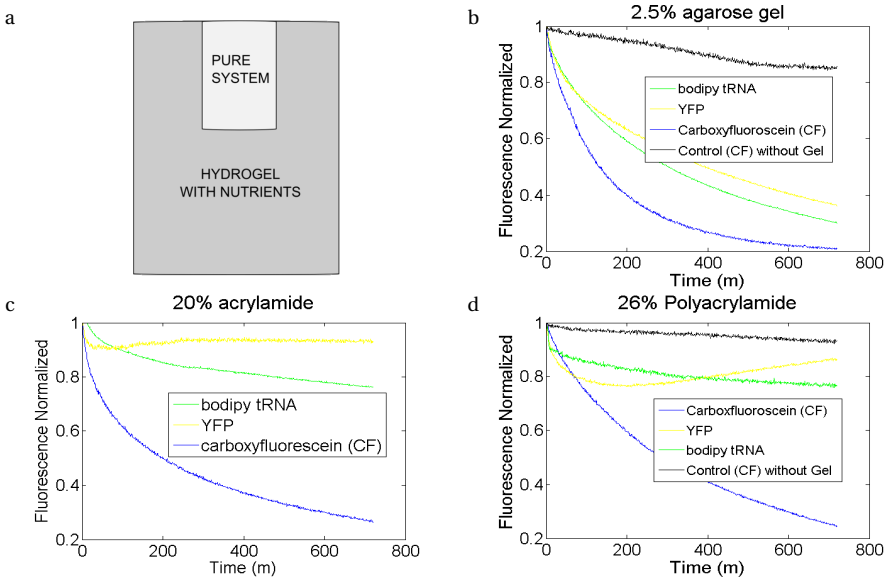

Figure 6.5: | Diffusion assay to asses permeability of hydrogels
(a) a schematic of a well within a well. A well is formed in a hydrogel which itself is in a 96 well plate. (b) Diffusion of YFP, bodipy tRNA and carboxyfluoroscein through a 2.5 % agarose well. (c) Diffusion of YFP, bodipy tRNA and carboxyfluoroscein through a 20% polyacrylamide well. (d) Diffusion of YFP, bodipy tRNA and carboxyfluoroscein through a 26% polyacrylamide well.

polyacrylamide gel, again the YFP was mostly retained and the BODIPY tRNA was slightly better retained than with the 20% gel. As for carboxyfluoroscein, it was not retained. Although the results with the acrylamide were promising in terms of the retention of larger molecules compared to smaller molecules, we could not further increase the gel percentage due to the concentration of acrylamide stock. The optimum ratio of crosslinker for minimum pore size was used, that is to say 19:1[60]. We do not recommend continuing with acrylamide, partly due to the messiness of the gels and their toxicity, and partly due to the polymerization problems. An alternative would be crosslinked dextran, which can be cross linked with the relatively harmless glutaraldehyde [61], and the pore size can potentially be tuned by the molecular weight of the dextran and the cross linker percentage.

6.3.3. METHODS

FABRICATING AND FILLING PDMS MICROCHAMBERS

For the fabrication of PDMS microchambers, a positive pattern of the microchambers was etched on a silicon wafer. PDMS was then made using the Sylgard 184 silicone elastomer kit (Dow Corning). The base and the curing agent were mixed at a ratio of 10:1 and subsequently degassed. A negative mold was made by covering the original positive mold with PDMS and allowing it to harden. This negative mold was then used to produce multiple sets of microchambers, by covering the mold with PDMS and by letting it harden. The PDMS was cured by placing it in an oven at 70 °C for one to two hours. Both the silicon wafer and the mold were silanized with a hydrophobic silane compound before covering with PDMS to make the separation easier. The 10-μm deep microchambers had a cylindrical shape with diameters of 10 μm or 30 μm. This corresponds approximately to volumes of 0.8 pl and 7 pl, respectively.

To make simultaneous measurements of multiple microchambers possible, the chambers must be completely sealed and filled. A sealed chamber should not have any exchange of molecules with its surroundings. To achieve that, chambers were sonicated in ethanol for 5 min, and then exposed to oxygen plasma to make the surfaces hydrophilic. PDMS and glass can be bound covalently when they are brought in contact right after plasma treatment. To encourage the contact between the microscope cover glass and the PDMS, the slide and chamber assembly was squeezed in a vice.

PROTEIN EXPRESSION

The PURE*frex* system was assembled in the standard way with the template being EmGFP in a 5-μl volume. The DNA was added to the PURE system immediately before applying the oxygen plasma to the chambers. The time between adding the DNA to the PURE system and the first images in the microscope was approximately 15 min. Expression was done at 37°C in a microscope

IMAGE ANALYSIS

A MATLAB algorithm which relied on a threshold intensity value was used to localize chambers. A centroid for the resulting round shapes was found and an area around this centroid with the known radius was drawn. The average values of the intensity were then calculated for each circular region and then the average value across all chambers as well as the standard deviation across the chambers were calculated.

HYDROGEL DIFFUSION ASSSAYS

For agarose hydrogel, 2.5% weight by volume of agarose was put in PURE buffer solution (20 mM HEPES pH 7.6, 180 mM potassium glutamate, 14 mM magnesium acetate) and heated in the microwave. The material was put into a black 96-well plate followed by the insertion of a form and the gel was allowed to harden. Three wells were formed, solutions of BODIPY labeled tRNA, YFP and carboxyfluoroscein (250 μM) respectively were put in each well. An additional well of the 96 well plate was filled with carboxyfluoroscein. Fluorescence was measured at 477/525 nm for BODIPY tRNA, 505/528nm for YFP, and 483/530 nm for carboxyfluoroscein. For acrylamide gels 180 μl of 10 × PURE buffer solution was mixed with 416.4 μl MQ and 1200 μl of 40% acrylamide solution with 19:1 acrylamide to crosslinker ratio. To improve polymerization degassing was performed by piercing the tube containing the acrylamide solution with a syringe needle, and leaving it in to have a very narrow opening. The solution was then put under vacuum for 10 min. Then 499 μl of this solution was then mixed with 0.5 μl of 25% APS and 0.5 μl of TEMED and placed in a black 96-well plate. The well was sealed with a form and polymerized for 25 min. Three wells were formed, solutions of bodipy labeled tRNA, YFP and carboxyfluoroscein (250 μM) respectively were put in each well. Fluorescence measurement was the same as for the agarose gel. For the 26% acrylamide gel a similar procedure was followed as for the 20% gel except that 180 μl of 10 × PURE buffer was mixed with 1600 μl of the acrylamide stock solution as well as 16.4 μl of MQ. The solution was degassed and then 499 μl of the solution was mixed with 0.5 μl of 25 % APS and 0.5 μl of TEMED. Three wells were formed, solutions of BODIPY labeled tRNA, YFP and carboxyfluoroscein (250 μM) respectively were put in each well. An additional well of the 96 well plate was filled with carboxyfluoroscein.

REFERENCES

[1] Z. Nourian, A. Scott, and C. Danelon, "Toward the assembly of a minimal divisome," *Systems and synthetic biology*, vol. 8, no. 3, pp. 237–247, 2014.

[2] E. J. Stewart, R. Madden, G. Paul, F. Taddei *et al.*, "Aging and death in an organism that reproduces by morphologically symmetric division," *PLoS Biol*, vol. 3, no. 2, p. e45, 2005.

[3] F. Crick *et al.*, "Central dogma of molecular biology," *Nature*, vol. 227, no. 5258, pp. 561–563, 1970.

[4] J. E. Cronan and R. M. Bell, "Mutants of escherichia coli defective in membrane phospholipid synthesis: mapping of sn-glycerol 3-phosphate acyltransferase km mutants," *Journal of Bacteriology*, vol. 120, no. 1, pp. 227–233, 1974.

[5] G. P. Smith, "Filamentous fusion phage: novel expression vectors that display cloned antigens on the virion surface," *Science*, vol. 228, no. 4705, pp. 1315–1317, 1985.

[6] H. R. Hoogenboom, A. P. de Bruine, S. E. Hufton, R. M. Hoet, J.-W. Arends, and R. C. Roovers, "Antibody phage display technology and its applications," *Immunotechnology*, vol. 4, no. 1, pp. 1–20, 1998.

[7] T. Schirrmann, "Affinity maturation by phage display," *Therapeutic Antibodies*, p. 309, 2009.

[8] N. E. Biolabs, "Phage display faq," https://www.neb.com/applications/protein-analysis-and-tools/ /media/1231BB0939D54AAA96E04FE0C8EA7437.ashx, 2015, 2015-11-12.

[9] C. Zahnd, P. Amstutz, and A. Plückthun, "Ribosome display: selecting and evolving proteins in vitro that specifically bind to a target," *Nature Methods*, vol. 4, no. 3, pp. 269–279, 2007.

[10] E. Miyamoto-Sato and H. Yanagawa, "Puromycin technology for in vitro evolution and proteome exploration," *Viva Origino*, vol. 3, no. 34, pp. 148–154, 2006.

[11] N. Doi and H. Yanagawa, "Stable: protein-dna fusion system for screening of combinatorial protein libraries in vitro," *FEBS letters*, vol. 457, no. 2, pp. 227–230, 1999.

[12] A. Sepp, D. S. Tawfik, and A. D. Griffiths, "Microbead display by in vitro compartmentalisation: selection for binding using flow cytometry," *FEBS letters*, vol. 532, no. 3, pp. 455–458, 2002.

[13] F. J. Ghadessy, J. L. Ong, and P. Holliger, "Directed evolution of polymerase function by compartmentalized self-replication," *Proceedings of the National Academy of Sciences*, vol. 98, no. 8, pp. 4552–4557, 2001.

[14] D. S. Tavvfik and A. D. Griffiths, "Man-made cell-like compartments for," *Nature biotechnology*, vol. 16, 1998.

[15] Y.-F. Lee, D. S. Tawfik, and A. D. Griffiths, "Investigating the target recognition of dna cytosine-5 methyltransferase hhai by library selection using in vitro compartmentalisation," *Nucleic acids research*, vol. 30, no. 22, pp. 4937–4944, 2002.

[16] H. M. Cohen, D. S. Tawfik, and A. D. Griffiths, "Altering the sequence specificity of haeiii methyltransferase by directed evolution using in vitro compartmentalization," *Protein Engineering Design and Selection*, vol. 17, no. 1, pp. 3–11, 2004.

[17] A. D. Griffiths and D. S. Tawfik, "Directed evolution of an extremely fast phosphotriesterase by in vitro compartmentalization," *The EMBO journal*, vol. 22, no. 1, pp. 24–35, 2003.

[18] E. Mastrobattista, V. Taly, E. Chanudet, P. Treacy, B. T. Kelly, and A. D. Griffiths, "High-throughput screening of enzyme libraries: in vitro evolution of a β-galactosidase by fluorescence-activated sorting of double emulsions," *Chemistry & biology*, vol. 12, no. 12, pp. 1291–1300, 2005.

[19] T. Nishikawa, T. Sunami, T. Matsuura, and T. Yomo, "Directed evolution of proteins through in vitro protein synthesis in liposomes," *Journal of nucleic acids*, vol. 2012, 2012.

[20] N. Ichihashi, K. Usui, Y. Kazuta, T. Sunami, T. Matsuura, and T. Yomo, "Darwinian evolution in a translation-coupled rna replication system within a cell-like compartment," *Nature communications*, vol. 4, 2013.

[21] A. S. Spirin, V. I. Baranov, L. A. Ryabova, S. Y. Ovodov, and Y. B. Alakhov, "A continuous cell-free translation system capable of producing polypeptides in high yield," *Science*, vol. 242, no. 4882, p. 1162, 1988.

[22] V. Noireaux and A. Libchaber, "A vesicle bioreactor as a step toward an artificial cell assembly," *Proceedings of the national academy of sciences of the United States of America*, vol. 101, no. 51, pp. 17 669–17 674, 2004.

[23] W. Aoki, M. Saito, R.-i. Manabe, H. Mori, Y. Yamaguchi, and E. Tamiya, "Integrating reductive and synthetic approaches in biology using man-made cell-like compartments," *Scientific reports*, vol. 4, 2014.

[24] J. Shendure and H. Ji, "Next-generation dna sequencing," *Nature biotechnology*, vol. 26, no. 10, pp. 1135–1145, 2008.

[25] N. Ban, P. Nissen, J. Hansen, P. B. Moore, and T. A. Steitz, "The complete atomic structure of the large ribosomal subunit at 2.4 å resolution," *Science*, vol. 289, no. 5481, pp. 905–920, 2000.

[26] K. SEMRAD, R. GREEN, and R. SCHROEDER, "Rna chaperone activity of large ribosomal subunit proteins from escherichia coli," *Rna*, vol. 10, no. 12, pp. 1855–1860, 2004.

[27] W. M. Clemons, J. L. May, B. T. Wimberly, J. P. McCutcheon, M. S. Capel, and V. Ramakrishnan, "Structure of a bacterial 30s ribosomal subunit at 5.5 å resolution," *Nature*, vol. 400, no. 6747, pp. 833–840, 1999.

[28] G. M. Culver and H. F. Noller, "Efficient reconstitution of functional escherichia coli 30s ribosomal subunits from a complete set of recombinant small subunit ribosomal proteins." *Rna*, vol. 5, no. 6, pp. 832–843, 1999.

[29] M. C. Jewett, B. R. Fritz, L. E. Timmerman, and G. M. Church, "In vitro integration of ribosomal rna synthesis, ribosome assembly, and translation," *Molecular systems biology*, vol. 9, no. 1, p. 678, 2013.

[30] K. H. Nierhaus, "Reconstitution of ribosomes," *Ribosomes and protein synthesis: A practical approach*, pp. 161–189, 1990.

[31] M. I. Zvereva, O. V. Shpanchenko, O. A. Dontsova, K. H. Nierhaus, and A. A. Bogdanov, "Effect of point mutations at position 89 of the e. coli 5s rrna on the assembly and activity of the large ribosomal subunit," *FEBS letters*, vol. 421, no. 3, pp. 249–251, 1998.

[32] W. Krzyzosiak, R. Denman, K. Nurse, W. Hellmann, M. Boublik, C. Gehrke, P. Agris, and J. Ofengand, "In vitro synthesis of 16s ribosomal rna containing single base changes and assembly into a functional 30s ribosome," *Biochemistry*, vol. 26, no. 8, pp. 2353–2364, 1987.

[33] K. Semrad and R. Green, "Osmolytes stimulate the reconstitution of functional 50s ribosomes from in vitro transcripts of escherichia coli 23s rrna," *Rna*, vol. 8, no. 04, pp. 401–411, 2002.

[34] R. Green and H. F. Noller, "In vitro complementation analysis localizes 23s rrna posttranscriptional modifications that are required for escherichia coli 50s ribosomal subunit assembly and function." *Rna*, vol. 2, no. 10, p. 1011, 1996.

[35] M. Del Campo, Y. Kaya, and J. Ofengand, "Identification and site of action of the remaining four putative pseudouridine synthases in escherichia coli." *Rna*, vol. 7, no. 11, pp. 1603–1615, 2001.

[36] E. Purta, M. O'Connor, J. M. Bujnicki, and S. Douthwaite, "Ygde is the 2-o-ribose methyltransferase rlmm specific for nucleotide c2498 in bacterial 23s rrna," *Molecular microbiology*, vol. 72, no. 5, pp. 1147–1158, 2009.

[37] D. V. Lesnyak, P. V. Sergiev, A. A. Bogdanov, and O. A. Dontsova, "Identification of escherichia coli m 2 g methyltransferases: I. the ycby gene encodes a methyltransferase specific for g2445 of the 23 s rrna," *Journal of molecular biology*, vol. 364, no. 1, pp. 20–25, 2006.

[38] S.-M. Toh, L. Xiong, T. Bae, and A. S. Mankin, "The methyltransferase yfgb/rlmn is responsible for modification of adenosine 2503 in 23s rrna," *Rna*, vol. 14, no. 1, pp. 98–106, 2008.

[39] W. An and J. W. Chin, "Synthesis of orthogonal transcription-translation networks," *Proceedings of the National Academy of Sciences*, vol. 106, no. 21, pp. 8477–8482, 2009.

[40] D. Chan and H. Vogel, "Current understanding of fatty acid biosynthesis and the acyl carrier protein," *Biochem. J*, vol. 430, pp. 1–19, 2010.

[41] G. Murtas, "Internal lipid synthesis and vesicle growth as a step toward self-reproduction of the minimal cell," *Systems and synthetic biology*, vol. 4, no. 2, pp. 85–93, 2010.

[42] E. Allan, C. Hoischen, and J. Gumpert, "Bacterial l-forms," *Advances in applied microbiology*, vol. 68, pp. 1–39, 2009.

[43] Y. Sakuma and M. Imai, "Model system of self-reproducing vesicles," *Physical review letters*, vol. 107, no. 19, p. 198101, 2011.

[44] Y. Briers, P. Walde, M. Schuppler, and M. J. Loessner, "How did bacterial ancestors reproduce? lessons from l-form cells and giant lipid vesicles," *Bioessays*, vol. 34, no. 12, pp. 1078–1084, 2012.

[45] S. Svetina, "Vesicle budding and the origin of cellular life," *ChemPhysChem*, vol. 10, no. 16, pp. 2769–2776, 2009.

[46] W. Helfrich, "Elastic properties of lipid bilayers: theory and possible experiments," *Zeitschrift für Naturforschung C*, vol. 28, no. 11-12, pp. 693–703, 1973.

[47] L. Miao, U. Seifert, M. Wortis, and H.-G. Döbereiner, "Budding transitions of fluid-bilayer vesicles: the effect of area-difference elasticity," *Physical Review E*, vol. 49, no. 6, p. 5389, 1994.

[48] U. Seifert and R. Lipowsky, "Morphology of vesicles," 1995.

[49] C.-M. Chen, P. Higgs, and F. MacKintosh, "Theory of fission for two-component lipid vesicles," *Physical Review Letters*, vol. 79, no. 8, p. 1579, 1997.

[50] Z. Nourian, W. Roelofsen, and C. Danelon, "Triggered gene expression in fed-vesicle microreactors with a multifunctional membrane," *Angewandte Chemie*, vol. 124, no. 13, pp. 3168–3172, 2012.

[51] D. K. Karig, S.-Y. Jung, B. Srijanto, C. P. Collier, and M. L. Simpson, "Probing cell-free gene expression noise in femtoliter volumes," *ACS synthetic biology*, vol. 2, no. 9, pp. 497–505, 2013.

[52] R. Grima, "An effective rate equation approach to reaction kinetics in small volumes: Theory and application to biochemical reactions in nonequilibrium steady-state conditions," *The Journal of chemical physics*, vol. 133, no. 3, p. 035101, 2010.

[53] T. Okano, T. Matsuura, Y. Kazuta, H. Suzuki, and T. Yomo, "Cell-free protein synthesis from a single copy of dna in a glass microchamber," *Lab on a Chip*, vol. 12, no. 15, pp. 2704–2711, 2012.

[54] A. D. Griffiths and D. S. Tawfik, "Miniaturising the laboratory in emulsion droplets," *Trends in biotechnology*, vol. 24, no. 9, pp. 395–402, 2006.

[55] P. Walde, K. Cosentino, H. Engel, and P. Stano, "Giant vesicles: preparations and applications," *ChemBioChem*, vol. 11, no. 7, pp. 848–865, 2010.

[56] T. Matsuura, M. Yamaguchi, E. P. Ko-Mitamura, Y. Shima, I. Urabe, and T. Yomo, "Importance of compartment formation for a self-encoding system," *Proceedings of the National Academy of Sciences*, vol. 99, no. 11, pp. 7514–7517, 2002.

[57] S. Hemmilä, J. V. Cauich-Rodríguez, J. Kreutzer, and P. Kallio, "Rapid, simple, and cost-effective treatments to achieve long-term hydrophilic pdms surfaces," *Applied Surface Science*, vol. 258, no. 24, pp. 9864–9875, 2012.

[58] M. W. Toepke and D. J. Beebe, "Pdms absorption of small molecules and consequences in microfluidic applications," *Lab Chip*, vol. 6, no. 12, pp. 1484–1486, 2006.

[59] H. P. Lu, L. Xun, and X. S. Xie, "Single-molecule enzymatic dynamics," *Science*, vol. 282, no. 5395, pp. 1877–1882, 1998.

[60] R. Rüchel, R. L. Steere, and E. F. Erbe, "Transmission-electron microscopic observations of freeze-etched polyacrylamide gels," *Journal of Chromatography A*, vol. 166, no. 2, pp. 563–575, 1978.

[61] D. Imren, M. Gümüşderelioğlu, and A. Güner, "Synthesis and characterization of dextran hydrogels prepared with chlor-and nitrogen-containing crosslinkers," *Journal of applied polymer science*, vol. 102, no. 5, pp. 4213–4221, 2006.

7

CONCLUSION

In this thesis we performed a small part of the construction of a minimal cell. At the outset we asked: what do we hope to learn and gain by building a minimal cell? We answered: Firstly the design principles of life, i.e. what chemical and biophysical processes are necessary to sustain life. We also stand to learn a great deal about the individual components which may provide new biotechnologies. It will also be possible to make new kind of sensing technologies, smart medicine, and eventually the production of chemicals with a specialized semi-synthetic cell. Did we achieve these goals, or a part of them?

In this thesis the principal work was the *in vitro* synthesis of 8 proteins for lipid biosynthesis and their characterization. These enzymes were able to synthesize seven phospholipids. This is a new development insofar as it is the first coupling of membrane metabolic pathway and flow of genetic information *in vitro*. We believe it will be a fairly straightfoward process to diversify the lipid structures to other lipids including phosphatidylcholine and cardiolipin two important bacterial lipids.

To study the pathways implemented, we developed an LC-MS method for lipids, this is not unique [1] [2] though represents an important tool for our laboratory for continued quantitative studies of lipid metabolism *in vitro*. We were able to characterize *E. coli* GPAT and LPAAT extensively including time course synthesis of LPA and DPPA. We found that *in vitro* GPAT and LPAAT were liposome-associated and we found that liposomes greatly enhanced the activity of GPAT and LPAAT. We further showed that we could use fatty acid substrates of different carbon length and saturation, as well as we were able to make minor changes in the lipid composition without disrupting enzyme activity. We also showed that the GPAT and LPAAT enzymes could be studied using fluorescence-based approaches, through detecting the reaction by-product CoA, and by the incorporation of NBD-labeled fatty acid in the phospholipid products. As a corollary we found that at least one of the enzymes can use NBD-labeled fatty acyl CoAs, which showed potential for microscopy studies of GPAT and LPAAT activity.

Within the context of minimal cells, we made significant advances. In addition to showing the *in vitro* synthesis and activity of eight lipid synthesizing enzymes, we were able to encapsulate two of those enzymes in liposomes and perform lipid synthesis from

the inside of the liposomes. From the kinetics and a study of DPPA incorporated into the membrane we found that for the substantial growth of minimal cells, the efficiency of enzymes will need to be increased. We think that it is important to mention that fatty acyl CoAs can act as surfactants potentially disrupting liposomes [3], which may necessitate incorporating fatty acid synthesis starting from the more hydrophilic components acetyl CoA and malonyl CoA and NADPH and H+ [4].

Besides volume expansion, we postulate that *in vesiculo* lipid biosynthesis could be exploited to change the equilibrium state of the membrane and trigger asymmetric division. First, in light of the recently unveiled mechanism of L form cell reproduction [5], we predict that internal synthesis of phospholipids could be sufficient to induce shape deformation as a manifestation of the excess surface area of membrane. Alternatively synthesis of saturated lipids and the crossing of the phase transition temperature to increase vesicle surface area may also induce membrane division [6]. We view division as a key step in the construction of the minimal cell and it is crucial for autonomous evolution.

Insofar as actually identifying and studying the biochemical and biophysical properties of life, we did not yet discover something new. We did prove that we could reconstitute some of the biochemical processes in an *in vitro* environment. As alluded to, we also set the stage for studying the biophysical process of division as implemented through lipid synthesis, that promises to be a fruitful avenue of research.

A possible application of our lipid synthesizing technique is to be able to synthesize specific lipids *in vitro* that might not otherwise be possible *in vivo* or chemically. For instance we envision synthesizing isomerically specific lipids, i.e. controlling the saturation and position of the fatty acid at both the sn-1 and sn-2 position of the lipids, something not easily done *in vivo*. This would be an interesting approach to make liquid chromatography standards for LC-MS and would have applications in lipidomics. Otherwise it can be interesting to synthesize lipids labeled with fluorophores, though it is expected to only make sense in a few specialized instances when specificity is required.

How far away are we from actually being able to construct a minimal cell? That is difficult to assess, though a very optimistic metric would be if we expect a minimal cell to require about 150 genes, and it took us four years to achieve eight functional genes, then perhaps it would take 75 person-years. Taking an arbitrary but useful rule of thumb, that it takes a least a factor of π longer than expected to do anything then it would take 235-person years. We can safely say that it will take at least 59 PhDs to achieve a minimal cell. If there would be 20 labs collaborating each with 3 dedicated PhDs it could be done in four years. Though this calculation is far from exact though it is not such a daunting number. What about cost? If each PhD person-year with salary and consumables costs about 60 000 €[7] then the estimated cost is approximately 14 million € which is approximately 1% of the annual EU research council budget [8]. Furthermore the industrial microbiology market is 6.5 billion dollars [9]. If an engineered minimal cell would replace natural and engineered organisms only 1.5% of the industrial microbiology market it would have paid for itself in a year. With these somewhat naive calculations as a guideline, we would conclude that it is a worthwhile goal.

Altogether, this thesis represents a minimal dent in the work required to construct a minimal cell though that alone was gratifying and offers promise of future successes in

our lab or others.

REFERENCES

[1] G. Astarita, J. H. McKenzie, B. Wang, K. Strassburg, A. Doneanu, J. Johnson, A. Baker, T. Hankemeier, J. Murphy, R. J. Vreeken, *et al.*, "A protective lipidomic biosignature associated with a balanced omega-6/omega-3 ratio in fat-1 transgenic mice," *PloS one*, vol. 9, no. 4, p. e96221, 2014.

[2] V. Gonzalez-Covarrubias, M. Beekman, H.-W. Uh, A. Dane, J. Troost, I. Paliukhovich, F. M. Kloet, J. Houwing-Duistermaat, R. J. Vreeken, T. Hankemeier, *et al.*, "Lipidomics of familial longevity," *Aging Cell*, vol. 12, no. 3, pp. 426–434, 2013.

[3] D. Deamer and G. Victor, "Lysophosphatidylcholine acyltransferase purification and applications in membrane studies," *Biomembranes and Cell Function*, vol. 414, pp. 90–96, 1983.

[4] G. Murtas, "Internal lipid synthesis and vesicle growth as a step toward self-reproduction of the minimal cell," *Systems Synthetic Biology*, vol. 4, pp. 85–93, 2010.

[5] R. Mercier, Y. Kawai, and J. Errington, "Excess membrane synthesis drives a primitive mode of cell proliferation," *Cell*, vol. 152, no. 5, pp. 997–1007, 2013.

[6] Y. Sakuma and M. Imai, "Model system of self-reproducing vesicles," *Physical review letters*, vol. 107, no. 19, p. 198101, 2011.

[7] J. C. Ltd, "Costs of training and supervising postgraduate research students," 2005.

[8] E. R. Council, "Facts and figures european research council," 2016.

[9] M. Hawkings, "Insight into the $6.5 billion global industrial biology market," 2016.

SUMMARY

Natural life is extraordinarily complex, which by definition means that it has many interconnected and functioning parts. The goal of synthetic biology is to engineer living systems, though due to their very complexity they remain recalcitrant to engineering. What if it were possible to reduce the complexity to a finite amount of parts that are well understood and therefore possible to manipulate. That is the motivation for constructing a so called minimal cell.

How complex, and what functions should something have to be considered alive? A definition that we find fundamental is an entity, that can take chemicals from its environment and be able to maintain itself in spite of the fact that globally entropy is increasing. To maintain its survival over the long term a living entity must be able to metabolize, have a container which specifies a boundary that can grow and be replicated, have genes which encode the above functions, and the genes themselves should be able to be replicated with the possibility for mutation, which is necessary for evolution.

What is meant by minimal? A simple way of quantifying the complexity of an organism is by simply counting the number of genes it has. That implies that the organism is based on DNA, which is read by an RNA polymerase. It also implies that at least some of the RNA is translated into protein. If we accept the number of genes as a metric of complexity for an organism, then one can approach finding the minimal genome in two ways: the top down and bottom up approaches. The top down approach is to eliminate as many genes as possible from existing organisms. In our lab, we apply the bottom up approach, whereby cellular functions are reconstituted from purified components with an emphasis on the process being under controlled conditions. Specifically we use the so-called semi-synthetic approach whereby DNA, RNA and protein are the core functioning elements. To get from DNA to RNA a process known as transcription is necessary and from RNA to protein a process known as translation must take place. To perform these core functions we make use of the PURE system. The PURE system's main function is to metabolize RNA and proteins from small molecules, though it also has the ability to regenerate some of its chemical components and degrade others. Encapsulation of purified proteins into cellular units is also necessary for making a minimal cell and we do that with glycerophospholipids. *Furthermore we aim to grow and divide those compartments which is the main focus of this thesis.*

Using glycerophospholipid liposomes (volumes enclosed by a bilayer of phospholipids), as scaffolds, we synthesized the *E. coli* proteins GPAT and LPAAT, responsible for the synthesis of lysophosphatidic acid and phosphatidic acid, respectively. First, by synthesizing the proteins from outside of liposomes and then purifying the liposomes we showed that the proteins are associated with liposomal membranes. Second, we developed a liquid chromatography mass spectrometry (LC-MS) method for the detection of enzyme products. We then used the LC-MS method to study the activity of GPAT (*plsB* gene) and LPAAT (*plsC* gene) from proteins expressed outside of liposomes. Our find-

ings include that proteins are active in various buffers, even when the proteins were co-expressed with the activity step. Next we found that it was crucial to have liposome supports to have efficient protein activity. We further observed that it was possible to use at least two types of fatty acyl CoA substrates and that the composition of the liposomal supports can be at least slightly varied. We also showed that at least some (~30%) of the synthesized lipids are incorporated into liposomal membranes, i.e the liposomes are growing. We also calculated the expected volume expansion of the liposomes from the synthesized lipids and found it to be ~1%. For future growth of minimal cells the efficiency of the enzymes or their synthesis will need to be increased. Finally we found that it was possible to express the proteins and perform lipid synthesis from inside liposomes, which is an important step in making a minimal cell.

We continued the study of lipid biosynthesis in the PURE system by expressing six phospholipid headgroup-modifying enzymes. We expressed the *E. coli* proteins phosphatidate cytidylyltransferase (*cdsA* gene), phosphatidylserine synthase (*pssA* gene), phosphatidylserine decarboxylase (*psd* gene), which are responsible for converting phosphatidic acid to diacyl-phosphatidylethanolamine. We also expressed phosphatidylglycerophosphate synthase (*pgsA* gene), and two phosphatidylglycerolphosphatases (*pgpA* gene, and *pgpC* gene) which along with phosphatidate cytidylyltransferase (*cdsA* gene) are responsible for converting phosphatidic acid to diacyl-phosphatidylglycerol. We were able to detect the end products of the two enzymatic pathways indicating that all enzymes were active.

We further studied the activity of the GPAT and LPAAT enzymes using light. We found that it was possible to detect the by-product of the GPAT and LPAAT reactions, co-enzyme A, with a fluorogenic assay. To use the assay we developed multiple methods for removing DTT, which otherwise interferes with the measurements. We studied the enzymes under various conditions using the CoA assay and found that it is in particular useful for studying LPAAT, which appeared to be active in the non-reducing conditions required for the assay. We also developed methods to study GPAT and LPAAT based upon an NBD (nitrobenzoxadiazole)-labeled fatty acyl CoA which changes its fluorescence properties when moved from a polar to a non polar environment. We studied this molecule with and without the presence of enzymes, by spectrofluorometry, mass spectrometry and microscopy. We found that it was particularly useful for studying LPAAT, and the combination of GPAT and LPAAT, which gave a signal in the NBD assays over their respective controls.

We also delved into the meaning of evolution and then focused on *in vitro* implementations of evolution as a bridge to a minimal cell, examining ways that genome replication and screening of large numbers of genes can be applied to the minimal cell project. We then discussed division, in particular how lipid biosynthesis and the biophysical properties of membranes may provide a route to division of liposomes. We predict that internal synthesis of phospholipids could be sufficient to induce shape deformation as a manifestation of the excess surface area of membrane. Alternatively synthesis of saturated lipids and the crossing of the phase transition temperature to increase vesicle surface area may also induce membrane division. We view division as a key step in the construction of the minimal cell and believe it is crucial for autonomous evolution. Finally we presented a few results from a project to build chambers and microchambers to

compartmentalize reactions, that we believe would be useful for *in vitro* evolution and studying the effects of small volumes on biochemical reactions.

In summary, we made significant advances in reconstituting lipid synthesis from *in vitro* synthesized proteins, making 7 classes (LPAs, PAs, PGs, PEs, PSs, CDP diacylglycerols, and PGPs) from 8 *in vitro* synthesized membrane proteins (from genes: *plsB*, *plsC*, *cdsA*, *pgsA*, *pgpA*, *pgpC*, *pssA*, *psd*). We studied the proteins and their activity via various laboratory techniques including mass spectrometry and fluorescence. In the near term the process will be improved to try to achieve greater volume expansion of liposomes, as well as implementing new enzymes to synthesize a wider variety of lipids. Besides expanding in these directions, in the future the lab will investigate altering the biophysical properties of liposomes via lipid synthesis in an attempt to achieve vesicle division.

Altogether, this thesis represents a minimal dent in the work required to construct a minimal cell though that alone was gratifying and offers promise of future successes in our lab or others.

SAMENVATTING

Het natuurlijke leven is extreem complex, wat per definitie betekent dat het veel onderdelen heeft die met elkaar verbonden zijn en verschillende functies hebben. Het doel van de synthetische biologie is om levende systemen te manipuleren, ondanks dat dit erg lastig is wegens de enorme complexiteit van de systemen zelf. Wat nu als het mogelijk was om deze complexiteit te reduceren tot een eindig aantal onderdelen, onderdelen waarvan hun werking goed begrepen is, en daarom ook manipulatie ervan mogelijk zal zijn? Dit is de motivatie om een zogenoemde minimale cel te creëren.

Hoe complex, en aan welke functies moet iets voldoen om levend te zijn? In onze mening is een fundamentele definitie hiervoor een entiteit, die moleculen vanuit zijn omgeving op kan nemen en zichzelf kan onderhouden, ondanks het feit dat de globale entropie toeneemt. Om het voortbestaan van deze entiteit over langere termijn te garanderen moet een levende entiteit kunnen metaboliseren, een container hebben die een begrenzing aangeeft en kan groeien en repliceren, genen hebben die coderen voor deze genoemde functies, en de genen zelf moeten in staat zijn gerepliceerd te kunnen worden met de mogelijkheid voor mutaties - noodzakelijk voor evolutie.

Wat wordt bedoeld met een minimale cel? Een eenvoudige manier om de complexiteit van een organisme te kwantificeren is door simpelweg het aantal genen te tellen. Dit impliceert dat het organisme is gebaseerd op DNA, dat uitgelezen wordt door een RNA polymerase. Het impliceert ook dat in ieder geval een deel van het RNA vertaald wordt in eiwitten. Als we accepteren dat het aantal genen een matrix is voor de complexiteit van het organisme, kan men twee verschillende manieren bedenken om een minimaal genoom te herleiden: de top-down en bottom-up aanpak. De top-down aanpak is gebaseerd op het elimineren van zoveel mogelijk genen van een huidig organisme. In ons lab gebruiken we de bottom-up aanpak, waarin cellulaire functies gereconstrueerd worden met nadruk op gecontroleerde condities van het proces. We gebruiken hoofdzakelijk de zogenoemde semi-synthetische cel aanpak, waarbij DNA, RNA en eiwit de elementen zijn met de kernfuncties. Transcriptie is het vereiste proces om van de informatie in DNA, RNA te produceren en om vervolgens eiwit te maken vindt het translatieproces van het RNA plaats. We maken gebruik van het “PURE system” dat deze kerntaken uitvoert. De hoofdfunctie van het “PURE system” is om RNA en eiwitten te metaboliseren beginnende met kleine moleculen. Daarnaast heeft het de mogelijkheid om sommige moleculen te regenereren. De inkapseling van gezuiverde eiwitten in celachtige units is ook een noodzakelijk stap voor het maken van een minimale cel. Dit doen we met glycerolfosfolipiden.

Bovendien hebben we als doel om deze compartimenten te laten groeien en te laten delen en dat is de belangrijkste focus van dit proefschrift.

We hebben de *E. coli* eiwitten GPAT en LPAAT, verantwoordelijk voor de synthese van lysofosfatidezuur en fosfatidezuur, gesynthetiseerd gebruikmakende van glycerolfosfolipide liposomen (volumes omringd door een dubbele fosfolipide laag) als platform. We

hebben eerst laten zien dat de eiwitten zich associëren met het membraan van de liposomen, door de eiwitten buiten de liposomen te synthetiseren en daarna de liposomen te zuiveren. Ten tweede hebben we een "liquid chromatography mass spectrometry" (LC-MS) methode ontwikkeld voor de detectie van enzymproducten. We hebben vervolgens de LC-MS methode gebruikt om de activiteit van GPAT (*plsB* gen) en LPAAT (*plsC* gen), van eiwitten die tot expressie zijn gebracht buiten de liposomen, te bestuderen. Onze bevindingen zijn dat de eiwitten actief zijn in verscheidene buffers en zelfs wanneer de eiwiten to co-expressie zijn gebracht tijdens de activiteit fase. We hebben ook gevonden dat de aanwezigheid van liposomen cruciaal is voor efficiënte eiwitactiviteit. We hebben verder geobserveerd dat het mogelijk is om minstens twee types vet acyl CoA substraten te gebruiken en dat de compositie van het liposoom platform lichtelijk gevarieerd kan worden. We hebben ook laten zien dat in ieder geval zo'n 30% van de gesynthetiseerde lipiden in het membraan van de liposomen wordt opgenomen, m.a.w. de liposomen groeien. De verwachte expansie van het volume van de liposomen door de incorporatie van de nieuwe lipiden hebben we berekend als zijnde 1%. Voor de toekomstige groei van minimale cellen zal de efficiëntie van de enzymen of de synthese ervan verhoogd moeten worden. Tot slot hebben we aangetoond dat het mogelijk is om de eiwitten binnen de liposomen tot expressie te brengen die vervolgens lipide synthese uitvoeren, een belangrijke stap voor het construeren van een minimale cel.

We hebben de studie van biosynthese van lipiden in het PURE systeem voortgezet door zes enzymen tot expressie te brengen die de hoofdgroep van fosfolipiden kunnen modificeren. We hebben de *E. coli* eiwitten fosfatide cytidil transferase (*cdsA* gen) en fosfatidylserine synthase (*pssA* gene), fosfatidylserine decarboxylase (*psd* gen), die verantwoordelijk zijn voor het omzetten van fosfatidezuur in diacylfosfatidylethanolamine, tot expressie gebracht. We hebben eveneens fosfatidylglycerolfosfaat synthase (*pgsA* gen) en twee fosfatidylglycerol fosfatases (*pgpA* gen en *pgpC* gen), die samen met fosfatide cytidyl transferase (*cdsA* gen) verantwoordelijk zijn voor de omzetting van fosfatidezuur naar diacylfosfatidylglycerol, tot expressie gebracht. We waren in staat om de eindproducten van de twee enzymatische routes te detecteren, een indicatie dat alle enzymen actief zijn.

We hebben vervolgens de activiteit van de GPAT en LPAAT enzymen bestudeerd met licht. We hebben aangetoond dat het mogelijk is om het bijproduct van de GPAT en LPAAT reacties, co-enzym A, met een fluorogeen assay van Enzo Life Sciences te detecteren. Om dit assay te gebruiken hebben we meerdere methodes ontwikkeld om DTT te verwijderen, dat anders interfereert met de metingen. We hebben de enzymen bestudeerd onder verschillende condities met het CoA essay en kwamen erachter dat het uitermate geschikt is om LPAAT, dat actief schijnt te zijn in de niet gereduceerde condities noodzakelijk voor het assay, te bestuderen. We hebben tevens methodes ontwikkeld om GPAT en LPAAT te bestuderen die gebaseerd zijn op een NBD (nitrobenzoxadiazole) gelabeld vetzuur CoA dat zijn fluorescente eigenschappen verandert als deze van een polaire naar een apolaire omgeving gaat. We hebben de moleculen met en zonder de aanwezigheid van enzymen bestudeerd met spectrofluorometrie, massa spectometrie en microscopie. Deze methode was voornamelijk nuttig voor het bestuderen van LPAAT en de combinatie van GPAT en LPAAT, waarbij het signaal in de NBD assay duidelijk hoger was ten opzichte van de controle reacties.

We hebben tevens het belang van evolutie uitgelicht en hebben ons daarbij gefocust op *in vitro* implementaties van evolutie die een brug kunnen vormen naar een minimale cel. We bekijken hoe manieren voor genoom replicatie en het screenen van grote aantallen genen toegepast kunnen worden voor het minimale cel project. We bespreken vervolgens deling, met name hoe de biosynthese van lipiden en de biofysische eigenschappen van het membraan een mogelijke route kunnen verschaffen voor het delen van liposomen. We voorspellen dat interne synthese van fosfolipiden genoeg kan zijn om een vormverandering te induceren, een gevolg van de overmaat aan membraanoppervlakte. Andere manieren om membraandeling te induceren zijn synthese van verzadigde lipiden en het passeren van de fase transitie temperatuur die de liposoom oppervlakte ook doen toenemen. We zien deling als een belangrijke step in het construeren van een minimale cel en zijn van mening dat het cruciaal is voor autonome evolutie. Tot slot presenteren we enkele resultaten van een project waarin we microkamers bouwen om reacties op een alternatieve manier te compartimentaliseren. Deze aanpak kan wellicht bruikbaar zijn om in vitro evolutie te bestuderen alsmede het effect van kleine volumes op biochemische reacties.

Samenvattend hebben we significante vooruitgang geboekt in het reconstrueren van lipide synthese door in vitro gesynthetiseerde eiwitten, waarin we zeven klasses (LPAs, PAs, PGs, PEs, PSs, CDP diacylglycerols, en PGPs) van acht in vitro gesynthetiseerde membraaneiwitten (van de genen: *plsB*, *plsC*, *cdsA*, *pgsA*, *pgpA*, *pgpC*, *pssA*, *psd*) gemaakt hebben. We hebben de eiwitten en hun activiteit bestudeerd met verschillende technieken, inclusief massa spectrometrie en fluorescentie. In de nabije toekomst zal het proces verbeterd worden met als doel een grotere volume-expansie van liposomen tot stand te brengen, alsmede het implementeren van nieuwe enzymen om een grotere variatie van lipiden te kunnen synthetiseren. Naast het uitbreiden in deze richtingen zal het lab in de toekomst ook onderzoek doen naar het veranderen van de biofysische eigenschappen van liposomen door lipide synthese als poging voor het bereiken van celdeling.

Alles bij elkaar genomen beschrijft dit proefschrift enkel een kleine stap in het werk dat nodig is om uiteindelijk een minimale cel te construeren, niettemin was dit alleen al bevredigend en brengt het beloften voor toekomstige successen in ons lab of in andere labs.

ACKNOWLEDGEMENTS

First and foremost I would like to thank Christophe Danelon. I cannot think of a better role model to have spent four years studying with. Your commitment to research and people is inspiring and I thank you for everything. I would also like to thank Pauline and Fabai for always being there for me, in the good times and the bad times. I could not ask for better friends and you are both amazing people. F060, Maarten, Bojk, Mahipal, I have utmost respect for you guys. Thanks for your great professionalism, and of course your equally great unprofessionalism. To Jelmer and thanks for the support, the squash, and the conversations about crazy ideas. To Alicia I very much enjoyed playing in the band with you, thanks for being a great friend.

To the rest of the Danelon lab, Fabrizio, Jonas, Johannes, Zohreh, Anne, and Huong, Essie and Ilja, thanks for the great support, the ideas, and collaborations, lab trips and dinners. Thanks to Paul and Ivo and Margreet for being great students. I think I got better throughout the years, and hope that you found our exchanges as fruitful as I did. To all the other students throughout the years, thanks for being great people.

To the Nieuwelaan, that was an amazing two and half years. I really felt supported and integrated as part of Dutch society, and more importantly our own woenvereniging. To Tim, you are a great friend and person, as you said so aptly there will be a hole in my heart, lets visit in the future. To Wessel, thanks for being a great friend, and for challenging me to be a better person. To Jurrian and Aafke, thanks for always letting me be a third wheel. Both of you are great people. Jurrian you are natural leader and a very kind person. Aafke your energy is relentless, and you are fascinating person. To Remy and Leslie, the rock solid pair, thanks for being great people and a bit scary, but in a good way. To Isa, I will always remember hoisting a cabinet into your window, thank you for your kindness and uniqueness. Friends for life. To Jacqueline, thank you for being kind and caring, and for being an amazing baker. To Bart, I also respect you immensely, I enjoyed connecting with you, over normal and weird things, and I appreciate that you always had something for me to do, if I needed a job. To Milan, thank you for the chats and being you, and of course for the uitje for twee. To Sabrin, you are wise beyond your years, and a great friend, thanks! To the other former nerds, Erik, and Cleo and Peter, and Mathilde I enjoyed living with you. Hope their is a visit soon. To Koen thanks for the walks and life chats. To Alex, thanks for the inspiration. To Pietro, that goes for you too. To Eelco, thanks for a great attitude and a fun eetcafe, I really remember it. To Ben and Maryse, thanks for being a stalwart pair, and always being positive. To Jasper and Merel, thanks for being nice people, and being examples of real world idealism. To Jule, thanks for the chats, and for organizing Nieuwelaanfeest. To Rowan, the same to you. To Pierre, you are awesome, come visit me in Canada! To Michiel, thanks for organizing huiskamerconcerts, and being the coolest dude at the Nieuwelaan. To Ilonka, you rock, cookies and cakes and a great attitude and spirit.

Back to BN. Helena, thank you for being awesome, for Mexican food, mass spec sym-

pathy and being a great friend. Marek, without you, my project may have never succeeded, thank you for being a great mentor. Louis, what can I say, you rock. To Cees, thank you for starting me off at BN and supporting me through a difficult year. To Adi, Daniel, Kuba, Joones, Sergei, Calin thanks for being a driving force in the department. Jorine, Yaron, Laura thanks for the scientific chats and friendships. Jakob Kersemakkers, perhaps before I die, I will have figured you out, thanks for the dry humor and cynicism. To the old guard, David, Iwijn, and Jan, and Juan, and Peter, Francesco, Gary, Michiel and many others for the early years, thanks for being role models well I was growing (well hopefully that will continue). To Adam, thanks for everything. To Felix, you are awesome, I was touched by your comments in the Klooster, and hope to visit with you in the future. To Elise, thanks for always being positive and the inspiration. To Anne and Mark and Sumit thank you for being genuinely interested in my farming plans. I appreciate our chats. To Nicole, thanks for being a new friend and always smiling. To Jelle and Dimitri, thanks for the support with all projects and for being consistently in a good mood. To the Chirlminites, and Meyers, Luuk, and Mohammed, Stanley Jetty, Malwina, Michaela and Mattia, couldn't ask for better BN relatives. To the rest of the faculty, thanks for steering the ship.

To Franz and Gillian, thanks for being great roomates and introducing me to the Canadian community in Delft. Thanks to Dominika for the colorful comments. To Andrew Saffery, thanks for being, awesome and kind. To Kapo, thanks for being Kapo. To Finn, thanks for eating my books, and my shoes and my pizzas, and running around a lot. To Amelie, thanks for being calm and for the delicious food (and awesome fireworks). To Maria, thanks for being honest, and weird.

To Joop and Doreen thanks for always supporting me. I will remember you both for years. Doreen I hope that I would have made you proud. To Dave, thanks for understanding. To Roxanne and Yvonne and Ivo, thanks for supporting me.

To Linda Boekestijn, dankjewel voor de support van mijn nieuwe ideeën, I will really miss you. Marijn, dankjewel voor jouu positiviteit. Benno en Danny en Anthony en Rose en Rebecca, dankjewel voor de goede tijden.

To Simone and Emmie, thank you for the epic friendship, from a great beginning and through the years. To Milou, thanks for all the fun. To Halima, thanks for opening my mind in these final days.

To Tomas, Esteban and Filipe, thank you for making what could have been an awful year back into a great year. To Tom and Lajko, thanks for the fun. To Mattia and to Mark Ruemmeli, thanks for the great start in Europe.

Finally to Mom, and Dad, thanks for everything and our Sunday evening chats. To the sibs, Darcy, Jenny, Ian and Jolanta, thanks for always being supportive.

To anybody that I might have missed. Thank you very much for making these 8 years of European life a treasure that I will remember forever. I invite you all to visit me in Canada.

CURRICULUM VITÆ

Andrew SCOTT

01-06-1984 Born in St. John New Brunswick, Canada.

EDUCATION

1997-2002 High School
Esquimalt Community School, Victoria

2003–2007 Undergraduate in Physics
McGill University, Montreal

2008–2009 M.Sc. Molecular Bioengineering
TU Dresden, Dresden

2009–2010 M.Sc. Nanoscience
TU Delft, Delft
Thesis: A hybrid solid state and biological nanopore
Supervisor: Prof dr. C. Dekker

2011–2016 PhD. Bionanoscience
TU Delft, Delft
Thesis: In vitro phospholipid synthesis for growing and dividing minimal cells
Supervisor: Dr. C.J.A. Danelon
Promotor: Prof. Marileen Dogterom

LIST OF PUBLICATIONS

1. **Nourian, Z., Scott, A., and C. Danelon**, *Towards the Assembly of a minimal Divisome*, Systems and Synthetic Biology **Volume 8, Issue 3**, 237-247 (2014).

2. **Scott, A., De Graaf, P., Noga, M.J., Yilidrim, E,. Westerlaken, I., and C. Danelon**, *Cell-free phospholipid biosynthesis by gene-encoded enzymes reconstituted in liposomes*, Nature Chemical Biology, **submitted** (2016).